Postural control mechanism of human bipedal standing

Hiroko TANABE

CONTENTS

ABSTRACT

Bipedal standing is one of the fundamental behaviors in human being, and the understanding of its control mechanism and stability is essential for the quality of life of the elderly and the improvement of sport performances. The understanding of the relationship between body fluctuations and muscle activities during quiet standing will enhance the knowledge of the human body controller in the central nervous system, and yet it has not fully understood due to the aperiodicity and nonlinearity of the body sway and small muscle activities. In this dissertation, I investigated the postural control mechanism and postural stability from the aspect of biomechanics (in vivo) and bioengineering (in silico).

In Study 1, 2, and 3, I investigated the coordinative structure of kinematics and muscle activities during tiptoe standing. In Study 1, I compared joint coordination during tiptoe standing between ballet dancers and non-dancers to investigate the change in kinematic coordinative structure through balance training. Joint coordination was calculated by using principle component analysis and the ankle-knee coordination in the sagittal plane showed in-phase coordination for ballet dancers while non-dancers showed its anti-phase coordination. This study indicated the plasticity of joint coordination through training and the possibility that joint coordination reflects balance stability during standing. Then I investigated the relationship between joint coordination patterns and muscle co-activation in Study 2. The surface electromyograms (EMG) over 13 leg muscles were recorded together with kinematic data, which was used for

the calculation of joint coordination in the same way as Study 1. I found that in-phase coordination, which was the feature of joint coordination in ballet dancers in Study 1, was associated with EMG-EMG coherence (muscle co-activation) up to 50 Hz, while anti-phase coordination was not associated with muscle co-activation in such a high frequency band. The relationship between kinematics and kinetics coordination was proved for the first time in this study. Moreover, I investigated the relationship between joint phase transition in a short period and muscle activations in Study 3. The joint phase transition (joint coordination) was computed by using the Hilbert transformation in this study. I observed the cross correlation between phase transitions and EMG signals, suggesting that short periods of phase transitions is controlled via muscle activities.

In Study 4 and 5, I investigated the function of intermittent feedback control for human bipedal standing in silico (Study 4) and in vivo (Study 5). In Study 4, I implemented computer simulation of a quadruple inverted pendulum as a model of human tiptoe standing. I set an intermittent feedback PD controller with joint viscoelasticity and joint control strategy (intermittent, continuous, or passive) as simulation parameters. First, I confirmed that the joint fluctuations of the pendulum showed similar properties as the actual human body oscillations during tiptoe standing. Among the 480 pairs of simulation parameters, I found only 30 pairs that can stabilize the pendulum for more than 60 seconds, in which the hip must always be controlled intermittently. Also, postural robustness of the pendulum varied with different joint control strategies, which accompanied with the change in kinematic joint coordination. This study

showed the necessity of intermittent feedback controller for the postural control during quiet standing of multi-segment human body. However, the function of intermittent control regarding muscle activities has not yet been understood at all. So in Study 5, I investigated intermittent muscle activity during quiet standing in vivo. Kinematic and kinetics (EMG) data were recorded to analyze the EMG on/off switch timing in the phase plane and the contribution of EMG on/off switching to control output (that is, joint torque). Both EMG on and off periods were distributed in the first and third quadrant of the phase plane where unstable manifolds of the system are considered to exist. In addition, the EMG on/off switching was associated with joint torque fluctuations along with anatomical direction of action for each muscle. This is the first study to demonstrate the function of intermittent muscle activations towards the control output.

In summary, I found various evidences regarding postural control mechanism from the viewpoint of the structure at musculoskeletal level, its function, and expertise (or plasticity). This dissertation deepened the understanding of postural control mechanism in which the control system selects suboptimal control strategy among the redundant system for stabilizing the body in a constantly changing environment.

General Introduction

Balance stability of quiet standing

In our daily life, we humans must stabilize our bodies in a variety of postures. Human body during quiet standing is inherently unstable, which is because the passive stiffness of the muscle-tendon-ligament is insufficient to compete with the gravitational toppling torque (Loram and Lakie 2002a; Casadio et al. 2005). Because of this, human upright posture should make an "unstable equilibrium" of saddle type in multi-dimensional state space consisted of multi-joint angular positions and velocities. That is, the state of the postural control system moves in a phase space converging towards the equilibrium along stable manifolds but diverging away from the equilibrium along unstable manifolds as time elapses. Therefore, the state of the system must be controlled actively in the vicinity of the equilibrium to maintain upright posture.

Sensory systems respond to afferent signals of body fluctuations and transmit sensory signals to the controller in the central nervous system (CNS) to achieve postural stability. Then the CNS sends out efferent signals to muscles and tendons as motor commands. The fluctuation of the center of pressure (CoP) is the final control output, the displacement of which results from the coordinative interaction of various sensory components such as visual, vestibular, proprioceptive, and cutaneous systems. Because the CoP is fluctuating with a restriction of its behavioral range (that is, the base of support), the time series of the CoP has been often

used for the analysis of postural stability during quiet standing.

Many researchers have focused on ballet dancer's movement or cognition process because dancing movements involves embodied cognition about themselves and environment. Many studies have investigated their postural control mechanism, which may reflect the expertise of balance control, by using CoP analysis. CoP path length, sway amplitude, and sway area (rectangular or 95% confidence level of ellipse) are traditional linear analysis for measuring postural stability (Gerbino et al. 2007; Stins et al. 2009; Kilby and Newell 2012). Non-linear method is useful to focus more on postural controller such as open-loop and closed-loop of the feedback control system, and this method has been used for detecting unstable posture in the elderly (Collins and De Luca 1995), Parkinson's disease patients (Mitchell et al. 1995), and during muscle fatigue (Gimmon et al. 2011). However, these results are not always consistent both in linear and non-linear CoP analysis (Tanabe et al. 2014).

CoP analysis is useful to easily estimate the whole body oscillation because the CoP is coherent with the whole body center of mass (CoM). However, the CoP is just the outcome of the control, which is via motor command, muscular activities, and multi-joint oscillations. Therefore, it is essential to comprehensively understand the whole postural control mechanism from the aspect of motor behavior (expertise, motor plasticity, and associating motor learning and learning environment; Study 1), musculoskeletal coordinative structure (multi-joint oscillation and muscle co-activation; Study 2 and 3), modeling (internal model and function of control input and output; Study 4), and system (comprehensive sys-

tem dynamics; Study 5). In this dissertation, I examined all of those components of postural control mechanism with five studies (Fig 1).

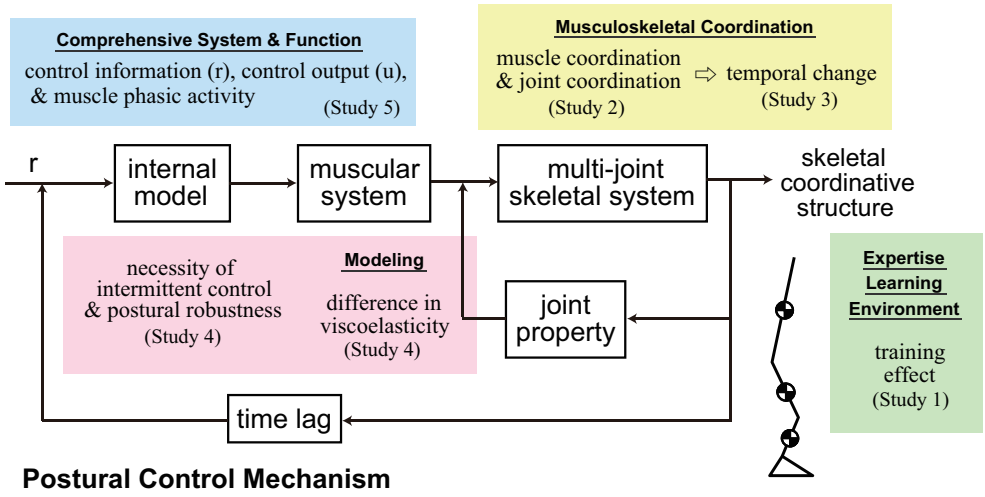

Figure 1: Comprehensive postural control mechanism of human bipedal standing. Multi-joint body segments oscillate during standing with coordinative structure as an outcome of motor control. In Study 1, I investigated the ballet training effect on such skeletal behavior, reflecting postural expertise, learning, and social demand (environment) to postural control strategy. Then, I demonstrated the relationship between joint coordination and muscle coordination in Study 2 and the temporal change in such relationship in Study 3. These two studies revealed the direct contribution of muscle coordinative structure to generate joint coordination. Then I implemented computer simulations of human bipedal standing in Study 4 for examining the relationship between control strategy in the internal model, joint properties, and skeletal behavior (motor output). It was suggested in Study 4 that intermittency in the postural control mechanism is necessary to stabilize the body under unstable conditions. Lastly, I extracted such intermittent (phasic) component of muscle activities from experimentally recorded surface electromyography data in Study 5. This allowed me to investigate the direct relationship between joint oscillations as control information in a feedback loop, individual muscle activities, and torque output during aperiodic human quiet standing, leading to a comprehensive understanding of postural control mechanism and its function.

Coordinative structure in kinematics and kinetics

Many studies have focused on joint coordination during quiet standing as a simple motor output among an infinite number of neural-muscular-

skeletal control strategies (Kuo et al. 1998; Aramaki et al. 2001; Pinter et al. 2008; Hsu et al. 2013; Kato et al. 2014; Tanabe et al. 2014). Some of them focused on aging effect on joint coordination during quiet standing (Hsu et al. 2013; Kato et al. 2014) and balance training effect of ballet dancers during tiptoe standing (Tanabe et al. 2014). These studies indicate the plasticity of postural control mechanism through aging or training is reflected in joint coordination. In addition, it was found that joint coordination has relationship between the center of mass (CoM) acceleration (Sasagawa et al. 2014) and the mutual relationship between CoP and CoM (Wang et al. 2014), indicating that joint coordination has some function for the postural stabilization during quiet standing.

Joint coordination represents the coupling patterns of two adjacent joints involving three segments' oscillations, which may be controlled by muscle activities associated with the fluctuations of the two joints. Regarding the synchronous muscle activities during quiet standing, the coherence between two electromyography (EMG) signals, which represents muscle co-activations in the frequency domain, has been demonstrated (Boonstra et al. 2008; Saffer et al. 2008). EMG signals can be divided into the frequency domain of alpha, beta, and gamma bands, and these bands are associated with different neural commands of the CNS (Ushiyama 2013). Thus, EMG-EMG coherence is useful to speculate the kinetic strategy of postural control via motor cortex.

Skilled postural control of ballet dancers

Many researchers have focused on their movement or cognition process because dancing movements involves embodied cognition about themselves and environment, so investigating dancers' performance is beneficial for studying motor control, expertise, and action-perception links. Dance training enhances sensorimotor functions for postural control. For instance, dancers maintain given postures for longer durations (Crotts et al. 1996) and can keep more vertical alignment during stepping (Chatfield et al. 2007). Many studies showed "better balance skills" in dancers (Golomer et al. 1997a,b; Golomer et al. 1999; Bruyneel et al. 2010), however, many of them focused on only time series of center of pressure (CoP) and center of mass (CoM) during standing and did not directly reveal "why the body oscillations of dancers is better". That is, definition of postural stability and the neural-muscular-skeletal mechanism underlying dancers postural control is still unclear.

Frank and Earl (1990) state that muscle synergies for postural control is associated with the selection of specific motor programs occurring in various areas of the central nervous system (CNS) including the motor cortex, the brainstem motor regions, and the spinal cord. Afferent feedback from the environment via somatosensory neurons in the proprioceptive, visual, and vestibular systems contributes to the postural maintenance. Dancers' postural control expertise may be based on improved somatosensory functions associated with changed multimodal processing, and enhanced proprioceptive skills, such as the balance abil-

ity with sensory interference, may contribute to the expertise (Jola et al. 2011). Dance training shifts the relative sensorimotor dominance from vision to proprioception, suggesting that dancers have more accurate position sense based on proprioceptive information (e.g., Golomer and Dupui 2000). Position-matching tasks involving hand location in space have empirically revealed dancers' accurate position sense (Jola et al. 2011).

One of the dance specific postures is tiptoe standing (called *relevé* in ballet) and there are some biomechanical research regarding tiptoe standing. For example, Albers et al. (1992/1993) investigated foot plantar pressures during tiptoe standing with pointe shoes. Muscle activities have also been recorded during tiptoe standing and their amplitudes were found to be different with changing in leg positions such as turn-out (Kadel et al. 2004; Mass et al. 2004). There are some other researches dealing with tiptoe standing, however, most of them are conference abstract level and hard to share. We have to struggle to understand dancers postural control expertise with sharing more research database.

Modeling of human bipedal standing

Inverted pendulum model has been used as a linearized way of describing human bipedal standing (Peterka 2002; Lakie et al. 2003; Bottaro et al. 2005; Asai et al. 2009; Suzuki et al. 2012). The system of the pendulum is linearized at the vicinity of the equilibrium because joint fluctuations are small enough to approximate the colioris force to be zero because the sway amplitude and velocity are very small during

quiet standing even during tiptoe standing. Modeling the human bipedal standing allows us to understand the internal model of human postural control and the dynamics of the state point and to investigate necessary and sufficient conditions for the postural stability and robustness constitutively.

The inverted pendulum model for human quiet standing has been conventionally with a continuous feedback controller based on proportional and derivative feedback (PD control) model (Peterka 2000; Masani et al. 2003; Maurer and Peterka 2005). The model segment(s) are actuated by passive and active joint torque(s). Passive torque is generated by stiffness or damping properties of muscle tonus and surrounding tissues such as ligaments and tendons without time lag. Active feedback torque is produced via neural closed-loop associated with a feedback of the state point about 200 ms ago, which represents the modulation of muscle contractions based on the body kinematics and dynamics of spontaneous body oscillations (Morasso and Schieppati 1999; Winter 1990; Winter et al. 1996). This time lag for the active control includes sensory transduction, neural processing, transmission, and muscle activation delays as reported in Peterka (2000). However, the biggest problem of this time-continuous feedback control is such large feedback time delay in the sensorimotor loop, which is a source of instability. Possible candidate for avoiding this time-delayed instability could be the non-reactive, preprogrammed impedance control, because this does not require reacting to the falling motions of the pendulum. However, muscle co-contractions increase metabolic cost as a trade-off.

On the contrary, many studies have recently advocated the computational theory of the intermittent feedback control as a model of human quiet standing (Bottaro et al. 2005; 2008; Asai et al. 2009; Gawthrop et al. 2011; 2014; Suzuki et al. 2012) and there are a number of versions of the intermittent control have been proposed. The first version exploits the fact that the state point of the pendulum transiently approaches the equilibrium along stable manifolds of the unstable saddle-type system, which I used in my model (Study 4). The transient conversion along the stable manifold without active control by muscle activations is responsible for the stabilization of the pendulum. The second version assumes anticipatory ballistic bias control (Loram and Lakie 2002b; Lakie et al. 2003; Loram et al. 2005; Loram et al. 2011) with a mathematical model of predictor for compensating a feedback delay (Gawthrop et al. 2011). This model considers the intermittency as the computational time for the anticipation (Loram et al. 2012; van de Kamp et al. 2013). The third one includes open-loop periods in the model which represents a sensory dead-zone (Collins and De Luca 1993; Eurich and Milton 1996; Milton et al. 2009; Insperger et al. 2013). The forth version is called "act-and-wait control", in which a delay-induced unstable system is stabilized by setting finite number of poles at appropriate locations (Insperger 2006; Stpn and Insperger 2006; Insperger and Stpn 2010). The fifth one is the noise-induced stabilization in which the system tuned in the vicinity of the edge of stability by using noise (Cabrera and Milton 2002; Bormann et al. 2004). Only the first version considers intermittent controller for the stability purpose.

Postural control: control input/output and internal model

Human bipedal standing is controlled by using integrated sensory cues from the visual, vestibular, and somatosensory systems, each contribution of which changes (rewaighting) depending on postural tasks (Peterka 2002). Such postural control feedback loop is suffered from time-delayed instability due to transmission from somatosensory system to brain of about 35 40 ms (Applegate et al. 1988), the neural transmission from the brain to muscles of about 27 37 ms (Ackermann et al. 1991; Lavoie et al. 1995), electromechanical delay (Muro and Nagata 1985; Moritani et al. 1987; Moss 1991; Mora et al. 2003), and psychological refractory period (Telford 1931; Vince 1948; Navas and Stark 1968). Together with this time delay of the feedback loop, the passive stiffness caused by joint viscoelasticity of the muscle-tendon-ligament is insufficient to compete with the gravitational toppling torque during quiet standing (Loram and Lakie 2002a; Casadio et al. 2005). Therefore, human upright posture is an unstable equilibrium of saddle type in multi-dimensional state space, in which the state point converges to the equilibrium along stable manifolds and diverges away from the equilibrium along unstable manifolds as time elapses.

Regarding the control mechanism of such unstable postural system, impedance control, which resists destabilizing motion by regulating co-activation levels of antagonist muscles, has been proposed in the field of neuroscience (Hogan 1984; 1985). The CNS stabilizes unstable dynamics

by learning optimal impedance, in which antagonist muscles co-activate in a preprogrammed manner (Burded et al. 2001; Franklin et al. 2007). Such a feed-forward, non-reactive control decreases a risk of delay-induced instability and enhances the robustness to external perturbations, however, this strategy has a trade-off that increasing impedance causes high metabolic cost consumed by muscle co-activations. This is very critical for maintaining postural stability as a fundamental activity of human being (Weyand et al. 2009).

Internal models associated with motor command-output relationship may be capable of optimizing such a trade-off during automatic movements such as quiet standing (Gomi and Kawato 1993; Morasso et al. 1999). Generally, human motor control systems must include continuous and intermittent processes incorporating discrete switching. Continuous systems integrate visual, vestibular, and somatosensory information, and this is represented by the spinal and transcortical reflexive pathways and provide high-bandwidth feedback at short latency (Brookes 1986; Rothwell 1994; Pruszynski and Scott 2012). Intermittent systems exist within the basal ganglia, prefrontal cortex, and premotor cortex and provide low-bandwidth feedback at longer frequency (Redgrave et al. 1999; Cisek and Kalaska 2005; Dux et al. 2006). In the context of human bipedal standing, continuous system, involving muscle spindle and Golgi tendon organ feedback, provide tonic equilibrium joint moments via tonic stretch reflexes (Sherrington 1947) and partial dynamic stabilization in the unstable state space (Marsden et al. 1981; Fitzpatrick et al. 1996; Loram et al. 2002a,b). However, the continuous control strategy itself is insufficient

to regulate the dynamics of the postural system (Marsden et al. 1981), and intermittency of the postural control mechanism plays an important role to the stabilization dynamics in the vicinity of the equilibrium.

STUDY1

Inter- and intra- lower limb joint coordination of non-expert classical ballet dancers during tiptoe standing

Abstract

The main objective of this study was to compare ballet dancers' and non-dancers' joint coordination during tiptoe standing. Nine female non-expert ballet dancers and nine female non-dancers were asked to perform heel-toe and tiptoe standing for approximately 30 s, during which the center of pressure (COP) and kinematic data from the metatarsophalangeal, ankle, knee, and hip joints were measured. Principal component analysis was performed on the angular displacements to determine joint coordination. The weighting vectors suggested that dancers' ankle and knee joints fluctuated in-phase in the anteroposterior direction, whereas all combinations of adjacent joints had anti-phase coordination for non-dancers. In addition, there was a significant difference in the intra-joint coordination pattern between groups. In particular, dancers' metatarsophalangeal (MP) and ankle joints tended to sway to the left-front or right-rear. However, there were no differences between the groups in the path length or rectangular COP. These results suggest that dancers maintained quiet postures via a decrease in the mechanical degree of freedom and that postural expertise may not be determined from a traditional COP analysis, even during unstable tiptoe standing. This in-phase coor-

dination, which has an arch-like configuration, could be characteristic of dancers' lithe legs.

Introduction

One of the fundamental aesthetic elements of a dancer is his or her slim, lithe, and strong legs. Although most of the aesthetical components of ballet may exist during dancing and largely depend on upper body posture, it is possible that even when standing, dancers have different postural control compared to non-dancers, which may be partially because of leg joint movements. By investigating dancers' leg joint coordination during standing, we can observe leg joint fluctuations at the micro-level for an aesthetical discussion, namely, we will be able to obtain insight into whether subtle fluctuations of this joint coordination could lead observers to describe a dancer's posture as beautiful.

Tiptoe standing (relev or demi-pointe) is one of the fundamental postures in ballet dancing and is referred to as three-quarter pointe, during which the ankle is located directly above the metatarsophalangeal (MP) joint. In ballet training, controlling the dancer's position in relev has obvious benefits for learning all pirouettes (turns) and making a dancer's legs appear slimmer (Warren 1989). Therefore, ballet students in beginner courses dedicate themselves to acquiring accurate standing while in relev. Because ballet dancers exhibit better postural control as a result of their ballet training (Rein et al. 2011), many studies have focused on ballet dancers' balance expertise (Blsing et al. 2012). Dancers have a lower power of body oscillations (Golomer et al. 1997) and are less

dependent on vision for postural control with increased accuracy of their proprioceptive inputs (Golomer et al. 1999). However, these results have only been reported during ordinary heel-toe standing. Despite the importance of relev for classical ballet, no current studies have focused on ballet dancers' joint coordination in this position. Because of its difficulty compared to heel-toe standing, researching relev could be an appropriate task to determine postural control differences between dancers and non-dancers. We have previously observed that non-dancers performed tiptoe standing with a different neurophysiological mechanism compared to heel-toe standing (Tanabe et al. 2012). Understanding how dancers stand on tiptoe will provide more insight into ballet dancers' skills. Therefore, in this study, we investigated postural expertise during tiptoe standing in ballet dancers and compared it with that of non-dancers.

Many studies have investigated dancers' postural control during static posture by using a center of pressure (COP) analysis; however, these results are not always consistent in linear (Gerbino et al. 2007; Kilby and Newell 2012; Stins et al. 2009) and non-linear (Kilby and Newell 2012; Stins et al. 2009) analyses. The joint movements involved in maintaining a standing position result in a fluctuation of the COP. Thus, if we suppose that postural maintenance strategies of dancers and non-dancers are different, it is difficult or impossible for a COP analysis to discriminate postural control between dancers and non-dancers. However, investigating a joint's oscillations and its relationships to other joints (inter-joint coordination) could elucidate the postural control process from a mechanical perspective. This knowledge could also lead the argument of postural

control to the discussion regarding the visible portion because it is easier to perceive joint fluctuations compared to a COP movement, so this could lead to research with tangible benefits for ballet pedagogy with regard to balance control. Therefore, in this study, we measured joint movements in the MP, ankle, knee, and hip joints during both heel-toe and tiptoe standing.

In the present study, both inter- and intra-joint coordination were investigated using principal component analysis (PCA) during heel-toe and tiptoe standing. PCA is useful to detect invariant coordinative structure of the system (Daffertshofer et al. 2004) and has been applied to studies of posture (Aramaki et al. 2001; Kuo et al. 1998; Pinter et al. 2008), gait (Delzio et al. 1997; Hubley-Kozey et al. 2006; Ivanenko et al. 2005; Troje 2002), and rhythmic movements (Toiviainen et al. 2010) because of its potential for data reduction and explanation (Jolliffe 1986). The central objective of PCA is to reduce the dimensionality of a data set while retaining the variation and to summarize the most important information in the data set (Jolliffe 1986). This summation of the information in the data set can be described in the following manner:

$$Z = \sum W_i C_i + residural$$

where W_i is weighting coefficient and C_i is the matrix of the original data set. By comparing the weighting coefficients for each time series of kinematic data, we can determine the contribution of each kinematic data and the relationship between them within the entire data set. This approach is reasonable because we were interested in inter-joint coordination among

lower joint fluctuations. Thus, we hypothesized that dancers' inter-joint coordination as a process to maintain posture is different from that of non-dancers and that the differences resulting from postural expertise might not appear in traditional outcomes of postural control (namely, a COP fluctuation or body sway) but rather in the process of postural control (i.e., joint fluctuations).

Moreover, coordination between anteroposterior and mediolateral fluctuations (namely, intra-joint coordination) can be investigated by focusing on the weighting vectors for the time series of both directions of each joint. This intra-joint coordination during unstable tiptoe standing might also provide insight into ballet-specific joint control during an ordinary upright posture. Anteropoeterior and mediolateral coordination in COP dynamics has been examined during normal heel-toe standing (King et al. 2012); however, whether each joint's oscillations in either direction exhibit coupling during unstable tiptoe standing requires investigation.

The first objective of this study was to determine the inter- and intra-joint coordination acquired by ballet training by initially executing PCA on kinematic data during both tiptoe and heel-toe standing and then comparing the results with those from non-dancers. The second objective was to demonstrate that it could be difficult to extract the postural expertise of dancers by some of traditional COP analysis even during unstable postural tasks.

Materials and methods

All procedures used in this study were consistent with the Declaration of Helsinki and approved by the Ethics Committee of the Graduate School of Human and Environmental Studies at Kyoto University. Approval was based on an appropriate risk/benefit ratio and a study design with minimal risk. All procedures were conducted in accordance with the approved protocol. Written informed consent was obtained from the participants following a written and verbal description of the study to ensure the participants' understanding of the procedure. Informed consent continued throughout the study via dialogue between the researcher and participants.

Participants

Nine female non-professional classical ballet dancers (age = 22.78 ± 4.68 yr, height = 160.28 ± 4.49 cm, body mass = 51.83 ± 7.65 kg) and nine healthy female participants with no formal dance experience (age = 21.78 ± 2.33 yr, height = 157.72 ± 5.96 cm, body mass = 48.32 ± 6.38 kg) participated in this study. We recruited dancers with sufficient ballet training to perform tiptoe standing; the average number of years of classical ballet training for the 9 trained participants was 11.56 ± 4.80 yr. Three of the non-dancers participated in sports training or exercising, such as jogging, basketball, and canoeing, whereas the other six did not exercise regularly. None of the participants had a significant medical history or signs of gait, postural, or neurological disorders, and none had vision problems.

Experimental protocol and measurement

The basic setup and postural sway measurements during bipedal standing have been described in our previous studies (Kouzaki and Masani 2012; Kouzaki and Shinohara 2010). Each participant was instructed to stand quietly on a force platform (EFP-A-1.5kNSA13B, Kyowa, Tokyo, Japan) with her eyes open. The participants looked at a fixed point on a plain wall in front of them. The participants stood barefoot with their arms resting comfortably at their sides and their feet together and parallel. The participants' head-neck-trunk movements were restricted by a stiff wooden splint strapped to their back (Fig 1a). This splint restricted entire body motions to the metatarsopharangeal (MP), ankle, knee, and hip joints. We excluded the balancing movement of the head and spine with the splint according to a previous study (Aramaki et al. 2001), which measured the angular displacements of ankle and hip joints using splints attached for fixing participants' upper bodies and knees. The participants performed the following two types of standing for 30 s: (1) standing quietly with their heels on the platform, which is henceforth referred to as heel-toe standing, and (2) tiptoe standing. Ten trials were conducted for each condition, and a rest period of at least 3 min was allowed between the trials. All participants were asked to initially perform ten heel-toe standing trials, followed by ten tiptoe standing trials. A 30-s period was selected because it provided an appropriate timeframe in terms of practical, experimental, and analytical length; the period needed to be short enough to allow participants to complete the task and be similar to the

actual length of tiptoe standing during ballet training or dancing, and the period also needed to be long enough to make frequency analysis feasible.

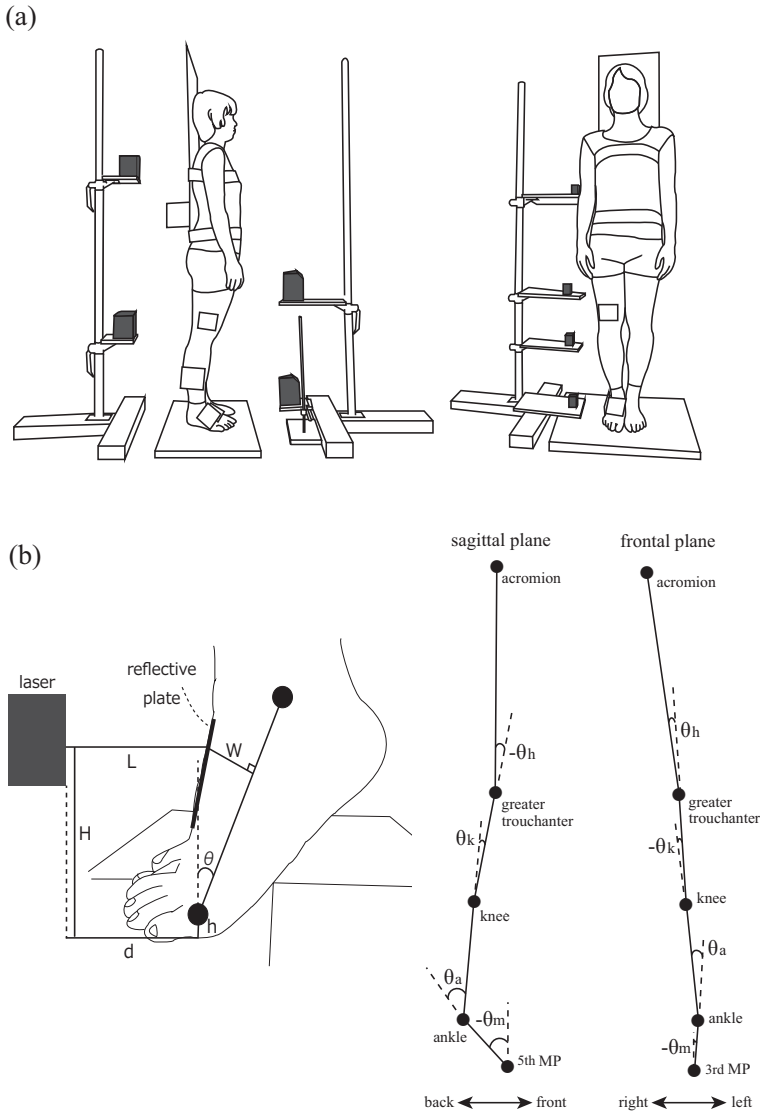

Figure 1: Experimental set up and parameters for the analysis. (a) Experimental setup. Each joint ' s displacement was measured by eight laser sensors. (b) Parameters for the data analysis. The left and right figures show the parameters for the calculation of angular displacement and joint angles in the sagittal and frontal planes, respectively.

Kinematic data from the MP, ankle, knee, and hip joints in the sagittal and frontal planes were obtained with eight laser sensors (four sensors

for the sagittal plane: a resolution of 10 m, LK-500, Keyence, Japan; and four additional sensors for the frontal plane: a resolution of 4 m, IL-S100, Keyence, Japan). All signals were stored with a sampling frequency of 100 Hz on the hard disk of a personal computer using a 16-bit analog-to-digital converter (PowerLab/16SP, ADInstruments, Sydney, Australia). Data processing was performed using Matlab 6.5 (The MathWorks, Natick, MA).

Data analysis

By using the 30-s signals from the force platform, we calculated the center of pressure (COP). A COP time series was passed through a 15 Hz-Butterworth low-pass filter (Kouzaki et al. 2007; Kouzaki and Masani 2012). We then calculated the COP path length in a two-dimensional plane and rectangular area (Tanabe et al. 2012).

A time series of the kinematic data was passed through a 10-Hz Butterworth low-pass filter. Changes in the position of the MP, ankle, knee, and hip, as measured with the laser sensors, were then converted to angular displacements in the anteroposterior and mediolateral directions as follows (all θ s are shown in Fig 1b-right):

$$tan\theta = \frac{L - d + \dfrac{W}{cos\theta}}{H - h}$$

where θ is an angle between a line connecting the two joints and the vertical direction, L is the horizontal distance between lasers for each joint in the sagittal and frontal planes and a reflective plate of the laser

attached to the skin, d is the horizontal distance between the laser and MP joint, W is the distance between the line connecting two joints and the reflective plate, H is the height of the laser from the force platform, and h is the height of the MP joint from the force platform. Each parameter is shown in Figure 1b-left. The relative angle positions were then calculated for each joint. We measured the length of W from the middle of the reflective plate before its attachment and then lased to the middle of the plate during the tasks. Thus, the potential error between the reflection point of the laser and the point for the measurement of W was negligible.

The coordination of oscillations in the MP, ankle, and hip joints was computed in both the anteroposterior and mediolateral directions using principal component analysis (PCA) (Hubley-Kozey et al. 2006; Jolliffe 1986; Kuo et al. 1998; Pinter et al. 2008). In this analysis, the original data set is transformed to a new set of variables (Zk (k = 1,2,$\cdots$,n); n is the number of variables in the data set) that are uncorrelated:

$$Z_k = \sum_k \sum_i W_{ki} C_i(t)$$

where Z_k is defined as the kth principal component (PC) as a linear combination of the ith variable in the data set $C_i(t)$ and the weighting coefficients W_{ki}. The initial few PCs retain most of the variation present in the original variables. In this study, seven variables were used in PCA for tiptoe standing, while five variables were used for heel-toe standing; the time series of angular movements from the MP to the hip joints for tiptoe standing and from the ankle to the hip joints for heel-toe standing were used for PCA. We excluded mediolateral kinematic data of the

knee because it is anatomically impossible for the knee to move in this direction. All of the variables were initially standardized with a mean of zero and a variance of one.

These variables formed a matrix A:

$$A(m,n) = [X_1, X_2, ..., X_n]$$

where X_i is the normalized time series for each joint, m is the length of variables, and n is the number of variables included in the analysis (i.e., n = 5 and 7 for heel-toe and tiptoe standing, respectively). The covariance matrix C was calculated in the following manner:

$$C(n,n) = \frac{1}{m-1} \cdot A^T A$$

A matrix of orthogonal eigenvectors T(n,n) and a diagonal matrix of eigenvalues were then calculated using an eigenvector decomposition of matrix C:

$$C = T\Lambda T^{-1}$$

The first principal component (PC) explains the largest possible fraction of the total variance in all joints' angular movements. Similarly, the descending PCs represent the remaining possible fraction of all variables. According to the definition of PCA, the number of PCs is identical to the number of variables, and all PCs are orthogonal. The proportion of the diagonal elements of $\Lambda[\lambda_1, \lambda_2, \cdots, \lambda_n(\lambda_1 > lambda_2 > \cdots > \lambda_n)]$ is defined as the ratio in which $PC_i(i = 1, 2, \cdots, n)$ describes the fluctuations of all of the variables. The ratio of λ_i (%Variance(i)) is calculated in the following manner:

$$\%Variance(i) = \frac{\lambda_i}{\sum_{k=1}^{n} \lambda_k}$$

If the %Variance calculated using a shuffled data set (i.e., an unrelated kinematic data set) is smaller than that of non-shuffled data set, the %Variance of the kth principal component (PC_k) can be interpreted as how much PC_k contains information from the entire variable matrix and the configuration of the cumulative %Variance reflects the dimensionality or complexity of the information from all variables. The greater the %Variance or the faster the cumulative %Variance saturates, the smaller the dimensionality of the leg joint fluctuation information. The 1st to kth PCs (the possible number of k is from 2 to n; n is the number of variables), whose cumulative %Variance was above 0.8, were used to investigate joint coordination (the value of 0.8 was arbitrary because the cumulative %Variance tended to saturate at the PC, which initially exceeded 0.8). When a greater number of PCs was required for a cumulative %Variance of ¿ 0.8 (namely, the larger number of k), the overall joint movement was more complex.

Each weighting coefficient in the kth PC ($W_{ki}; k, i = \{1, 2, \cdots, n\}$) is calculated between -1 and 1 and represents the correlation between each variable (in this study, kinematic time series) and the PC. Therefore, the distribution of the weighting coefficients across kinematic variables reflects two types of joint coordination: inter and intra-joint. Inter-joint coordination was determined by comparing two weight values of adjacent joints in the anteroposterior or mediolateral directions and was classified

into three coordination patterns: anti-phase

$$W_{1,1} \cdot W_{1,2} < 0 \text{ and } |W_{1,1}| \gg 0 \text{ and } |W_{1,2}| \gg 0$$

in-phase

$$W_{1,1} \cdot W_{1,2} > 0 \text{ and } |W_{1,1}| \gg 0 \text{ and } |W_{1,2}| \gg 0$$

and middle (i.e., other patterns except for anti- or in-phase). On the other hand, intra-joint coordination was determined by comparing two weight values for the identical joint in the anteroposterior and mediolateral directions.

We analyzed the squared coherence spectrum (Tanabe et al. 2012) and calculated the phase between the angular displacements to examine the relationship between the angular displacements of two joints in the frequency domain. The time series of joint angular displacements without low-pass filtering was used to analyze the coherence spectrum. Data signals were segmented into epochs of 128 ms with no overlap. The data segments that corresponded to each 128-ms epoch were Hanning-windowed to reduce spectral leakage. We used a 95% confidence level (CL) of the coherence (Ushiyama et al. 2010).

$$CL(\alpha) = 1 - (1 - \frac{\alpha}{100})^{\frac{1}{n-1}}$$

Statistical analysis

The data are presented as the means ± SD in the text, tables and figures. The statistical significance of the path length, rectangular area of the COP, and SD of each joint's fluctuation were analyzed using a t-test.

Effect size was estimated using Cohen's d. A Chi-squared test was used to describe group differences in the number of trials that required a PC3 and the joint coordination patterns. Effect size was estimated using Cramr's V for the Chi-squared test (Cramr 1999). For all statistical calculations, p¡.05 was accepted as significant. All statistical analyses were conducted using Matlab 6.5 (The MathWorks, Natick, MA).

Results

Path length and the rectangular area of COP

The path length in a two-dimensional plane and the rectangular area of the COP are shown in Table 1. There was no significant difference in the path length of the COP between groups for either heel-toe (p = 0.98, t(16) = -0.028, and d = -0.013) or tiptoe standing (p = 0.90, t(16) = 0.11, and d = 0.051). In addition, there was no significant difference in the rectangular area of the COP between groups for either heel-toe (p = 0.18, t(16) = 1.2, and d = 0.57) or tiptoe standing (p = 0.15, t(16) = -1.2, and d = -0.56).

	Path length			Recutangular area		
	untrained	trained	p	untrained	trained	p
HS	29.27±5.37	29.17±9.29	0.98	2.59±1.05	3.98±3.28	0.18
TS	66.54±9.70	67.35±19.94	0.9	5.05±1.44	4.29±1.31	0.15

Table 1: Mean value of path length and rectangular area of COP during heel-toe and tiptoe standing. HS and TS represent heel-toe standing and tiptoe standing, respectively.

The validity of the interpretation of %Variance

To determine that the calculated %Variance represented the amount of information that each PC shared and that the saturation of cumulative %Variance denoted the dimensionality or complexity of joint fluctuations, we conducted PCA for a data set of unrelated kinematic signals (shuffled data), which included variables from the identical participant and different trials of standing conditions. Figure 2 represents one example of cumulative %Variance of PC1 using a shuffled (dashed line) and non-shuffled data set (solid line) during heel-toe standing. The plot of the shuffled data set was always below the plot of the non-shuffled data set for both heel-toe and tiptoe standing.

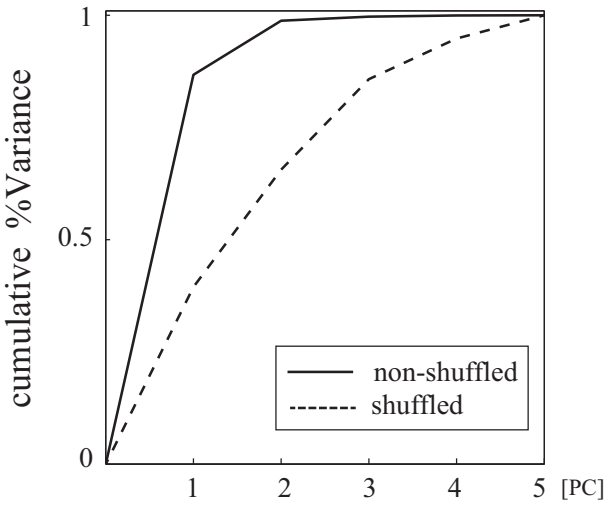

Figure 2: An example of the cumulative %Variance during heel-toe standing (i.e., five variables were used for PCA). The solid and dashed lines are the plots of non-shuffled (original) and shuffled data set, respectively. The shuffled data set consisted of five kinematic variables from the identical participant, but in different trials.

Inter- and intra- joint coordination during tiptoe standing

To examine the complexity of overall joint sway during tiptoe standing, we implemented principal component analysis (PCA) and computed the %Variance for each trial. Regardless of ballet training, the cumulative %Variance exceeded 0.8 from PC1 to PC2 or PC3 among seven variables. In addition, there was no significant difference in the number of trials whose cumulative %Variance required a PC3 to saturate at 0.8 between groups ($\chi^2(1) = 1.31, p > 0.05, V = .086$).

We also calculated the weights for each joint and PC and examined the relationship between each joint's weights to investigate the joint coordination of the leg during tiptoe standing. The definition of inter-joint coordination patterns (i.e., anti-phase, in-phase, and middle) is shown in Figure 3a. Figure 3b depicts the weighting coefficients of PC1 during tiptoe standing for all participants and trials. The most apparent difference between the groups was that ankle and knee sways were in-phase for the dancers (i.e., more horizontally plotted lines between the ankle and knee in the anteroposterior direction) but every adjacent joint swayed anti-phase for non-dancers. In addition, regarding the anteroposterior coordination between the ankle and knee, the dancers had more trials that we could not classify as either in- or anti- phase (namely, middle pattern) compared with non-dancers. The numbers of trials in which the ankle-knee patterns were anti-phase, middle, and in-phase were 35, 32, and 23, respectively for dancers, and 76, 6, and 8, respectively, for non-dancers. There were significant differences in the numbers of trials between these

three patterns ($\chi^2(2) = 40.19, p < 0.01, V = .47$). However, the residual joint coordination (from PC2 and PC3) showed no notable differences between the groups (figure not shown) relative to the relationships between joints (anti-phase, in-phase, or middle).

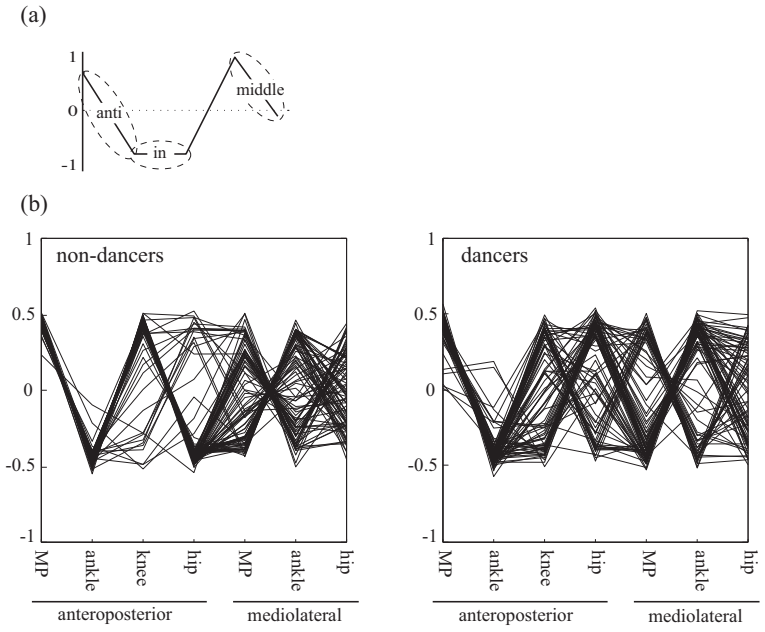

Figure 3: (a) The definition of joint coordination patterns (anti-phase, in-phase, and middle) and (b) the plots of the weighting vectors during tiptoe standing of non-dancers (left) and dancers (right). All of the weighting vector plots for all trials are stacked for each group. Thus, a bolder line consists of overlapping single plots of similar weighting vector patterns. The initial four weight values are anteroposterior joint fluctuations, and the remaining three values are mediolateral joint fluctuations. The positive values represent the fluctuations towards the front and the right in the anteroposterior and mediolateral directions, respectively.

Furthermore, we computed the coherence spectrum and its phase between angular displacements of ankle and knee in the anteroposterior direction to prove the interpretation of the results of PCA (anti- or in-phase) and examine its frequency characteristics. Figure 4 shows the

phase in the frequency domain when the coherence spectrum between the ankle and knee joint displacements was significant. The value of the coherence spectrum was high (approximately 0.5 to 0.8) when it exceeded the significance level (figure not shown). All trial phases were plotted when their PCA results were anti-phase (left figure: 76 trials from non-dacers; middle figure: 35 trials from dancers) and in-phase (right figure: 23 trials from dancers). There were many phases at zero when the joints swayed in-phase (Fig 4-right), which were along a relatively high frequency domain (10 20 Hz). Moreover, the dancers' inter-joint coherence, in which the joints swayed both anti- and in-phase (Fig 4 middle and right), was significant until the higher frequency domain (20 Hz), whereas the coherence of the non-dancers was significant only in the lower frequency domain (less than 10 Hz).

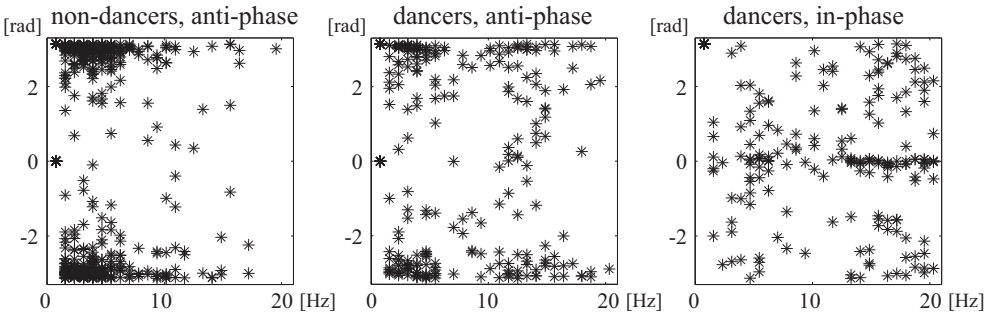

Figure 4: The anteroposterior phase between the ankle and knee. The left, middle, and right figures illustrate the phase in the frequency domain of all trials, in which PCA results were anti-phase in the untrained group (left, 76 trials), anti-phase for dancers (middle, 35 trials), and in-phase for dancers (right, 23 trials).

In addition, intra-joint coordination (i.e., the coordination of the identical joint in the sagittal and frontal planes) was investigated by

comparing the weights of the identical joint in the anteroposterior and mediolateral planes (Fig 3b). The intra-joint coupling pattern between the sagittal and frontal sways of each joint is shown in Table 2. There was a significant difference between groups in regard to the numbers of coupling patterns for all three joints ($MP : \chi^2(2) = 37.67, p < 0.05, V = .46; ankle : \chi^2(2) = 32.27, p < 0.05, V = .42; andknee : \chi^2(2) = 10.93, p < 0.05, V = .25$). In particular, dancers had a significantly greater number of trials of anti-phase intra-joint coupling between the MP and ankle compared with non-dancers. The anteroposterior and mediolateral sways of the MP and ankle in the dancers tended to fluctuate with the anti-phase (toward the left-front or right-rear).

		anti-phase	middle	in-phase	χ^2	p
MP	untrained	38	19	33	37.7	$< 10^{-3}$
	dancers	54	12	24		
Ankle	untrained	35	24	31	32.3	$< 10^{-3}$
	dancers	53	11	26		
Hip	untrained	28	41	21	10.9	0.004
	dancers	25	39	26		

Table 2: The numbers of trials for each coupling pattern during tiptoe standing. Top, middle, and bottom tables show the numbers for the MP, ankle, and hip joints, respectively. The value of the chi-squared tests and the p values are shown on the right side. The value for the degree of freedom was 2 for all joints.

Inter- and intra- joint coordination during heel-toe standing

We also performed PCA for joint coordination during heel-toe standing. For all participants and trials, the cumulative %Variances from PC1

to PC2 or PC3 exceeded 0.8 regardless of ballet experience (five variables were used). Similar to the case of tiptoe standing, there were no significant differences in the number of trials in which the cumulative %Variance required a PC3 to exceed 0.8 between the groups ($\chi^2(1) = 1.05, p > 0.05, V = .077$).

The plot of the weights of each joint's anteroposterior and mediolateral displacement for PC1 is depicted in Figure 5. In contrast to tiptoe standing, there was no notable difference in inter-joint coordination (anti-phase, in-phase, or the middle) between groups. Additionally, there was no significant difference between groups in the intra-joint coupling of anteroposterior and mediolateral sways; namely, the number of trials for each intra-joint coordination in the dancers was similar to that of the non-dancers ($ankle; \chi^2(2) = 1.28, p > 0.05, V = .085; and hip; \chi^2(1) = 5.38, p > 0.05, V = .17$). However, there were more coupling trials in which anteroposterior and mediolateral fluctuations swayed with anti- or in-phase coordination than with middle pattern trials, regardless of ballet training, for both the ankle (dancers: 72/90 trials; and untrained: 67/90 trials) and hip (dancers: 68/90 trials; and untrained: 76/90 trials). The residual joint coordination (from PC2 and PC3) also showed no noteworthy difference between groups (figure not shown) in regard to the relationships between joints (anti-phase, in-phase, or the middle).

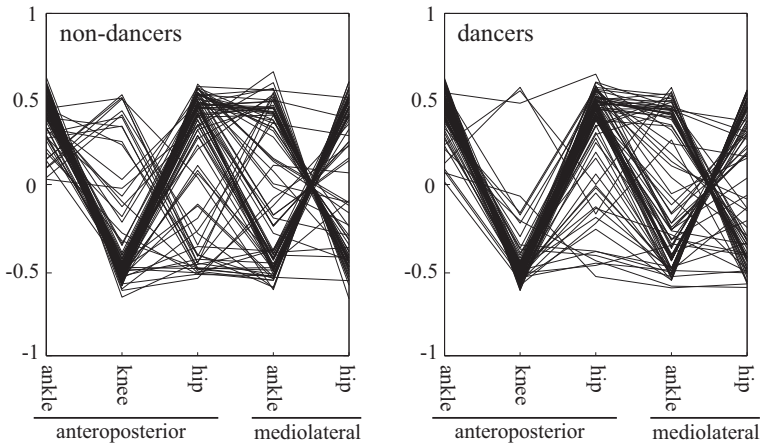

Figure 5: The weighting vector plots during heel-toe standing of non-dancers (left) and dancers (right). All of the weighting vector plots for all trials are stacked for each group. Thus, a bolder line consists of overlapping single plots of similar weighting vector patterns. The initial three weight values are anteroposterior joint fluctuations, and the remaining two values are mediolateral joint fluctuations. The positive values represent the fluctuations toward the front and the right for the anteroposterior and mediolateral directions, respectively.

Fluctuations of joints' angular displacements

The SDs of the angular displacements of the MP, ankle, knee, and hip joints during both standing conditions are shown in Table 3. The anteroposterior fluctuations of the knee and hip joints in the dancers were significantly smaller than those of the non-dancers during tiptoe standing ($p = 0.025$ and 0.027, $t(16) = -3.1$ and -2.8, and $d = -1.5$ and -1.3, respectively). In addition, the mediolateral SD of the ankle in the dancers was significantly greater than that in the non-dancers during heel-toe standing ($p = 0.020$, $t(16) = 2.1$, and $d = 0.99$). No other significant differences were observed for other joints.

(a)	Anteroposterior			Mediolateral		
	untrained	trained	p	untrained	trained	p
MP	32.0±8.7	27.9±11.3	0.11	19.9±9.4	21.5±8.4	0.64
Ankle	39.6±10.6	31.9±13.0	0.17	11.5±4.5	11.7±5.8	0.90
Knee	25.5±12.7	11.7±3.9	0.025	-	-	-
Hip	29.1±20.7	9.3±3.4	0.027	6.1±1.1	7.1±3.4	0.23
(b)	Anteroposterior			Mediolateral		
	untrained	trained	p	untrained	trained	p
Ankle	3.5±0.79	5.4±3.7	0.15	4.7±1.2	6.5±2.3	0.02
Knee	4.0±2.4	6.7±4.7	0.13	-	-	-
Hip	3.2±1.6	3.6±1.5	0.47	12.5±7.4	13.7±9.5	0.75

Table 3: Mean values of SD for angular displacements of the MP, ankle, knee, and hip joints. (a) and (b) indicate tiptoe and heel-toe standing, respectively.

Discussion

Inter-joint coordination

During tiptoe standing, dancers had a significantly larger number of trials in which their ankles and knees swayed in-phase in the anteroposterior direction. However, in most of the trials of the non-dancers, these joints swayed in anti-phase (Fig 3b). In addition, the SD of the knee joint fluctuations in the anteroposterior direction in the dancers was significantly smaller than that in the non-dancers (Table 3). This smaller SD could be because of ballet training, in which one of the fundamental instructions is to maintain locked knees (namely, the anterior cruciate stops the movement of the outer femoral condyle and holds the quadriceps, which is pulled onto the kneecap), which is known as closure rotation (Grieg 1994). Although we cannot definitively conclude that this result is the effect of ballet training specifically, the possibility

that this result can be attributed to general training is low because the three non-dancers with such experience displayed similar results to the other non-dancers. However, these results suggested that dancers have relatively small degrees of freedom in their joints when standing on tip-toe, although it remains unclear whether locking the knees, which forces the agonist and antagonist muscles around the knee to sway in a phasic way, stabilizes posture or dancers are forced to perform in-phase joint coordination. However, this result raises the question of whether or not in-phase joint coordination stabilizes the posture.

What makes the ankle and knee fluctuate in-phase during tiptoe standing? Figure 4 indicates that the joint movements of dancers are synchronized up to higher frequency domain and that the results of the PCA in dancers are a reflection of the phase in a higher frequency domain (10-20 Hz). One possible explanation for this coherence is control from the motor cortex. Oscillations derived from the motor cortex are coherent with EMG signals, and this corticomuscular coherency appears in the 15-35 Hz frequency range (beta-band) (Ushiyama 2013). Additionally, significant coherency between EMG and MMG (Mechanomyogram) signals has been demonstrated previously (Kouzaki and Fukunaga 2008). Therefore, because the coherence between the angular displacements of the ankle and knee observed in this study emerged in this beta-band, the motor cortex is possibly involved in the generation of the observed ankle-knee coupling. Moreover, Boonstra et al. (2008) have proposed that the 13-18 Hz synchronization of EMGs in the femur could be because of a physiological subsystem involved in balance-related postural

responses and that this synchronization does not relate to fatigue. They hypothesized that relatively distant muscles which work at different joints fluctuate in a synchronized manner as well as muscles work at the one joint followed by the coupling of angular displacements at a higher frequency. Additionally, this coupling could be independent of muscle fatigue. The 13-18 Hz synchronization may be different from the coherence in the beta-band; however, we could not distinguish between the beta-band and the 13-18 Hz frequency band. The motor cortex, which has a large role in muscle activation, could be networked with other areas of the brain, such as the premotor and supplementary motor areas, in challenging postural conditions (Byblow et al. 2007). Dancers might be able to tap into considerable flexibility in their neural system, thus leading to a higher frequency of in-phase fluctuation between the ankle and knee, followed by the muscle activations around these joints, via this neural network. Moreover, it is possible that heightened input from the basal ganglia and cerebellum also contribute to these higher frequency oscillations. To understand dancers' postural control in more detail, further analysis is necessary to clarify the precise neurophysiological properties of muscle activity, joint movements, and the activation in the areas of the brain associated with motor control.

In contrast to tiptoe standing, there were no obvious differences in inter-joint coordination between the groups during heel-toe standing. Regardless of ballet training, the adjacent joints tended to sway anti-phase with one another in the anteroposterior direction, and the ankles and hips fluctuated anti-phase in the mediolateral direction. Anteroposterior re-

ciprocal angular acceleration of the ankle and hip joints has been demonstrated during ordinary heel-toe standing with the knees fixed by splints (Aramaki et al. 2001). Considering this result, mechanically adjacent joints might fluctuate anti-phase during more stable heel-toe standing. The only difference between the groups during heel-toe standing was observed in the amplitude of the ankle joint's mediolateral sway. This larger ankle fluctuation in the dancers was only observed during heel-toe standing, thus emphasizing the dancers' expertise at locking the anatomically flexible ankle joint during tiptoe standing to achieve a stable posture.

In this study, the anteroposterior inter-joint coordination patterns of dancers during tiptoe standing tended to be more variable, particularly between the ankle and knee and between the knee and hip. This result suggested that dancers appear to have more flexible strategies for joint coordination. However, the coordination between the MP and ankle joints in the mediolateral direction for dancers was predominantly prone to anti-phase fluctuation, whereas the coordination of non-dancers appeared to be more variable. The following question arose: Does this diversity in the coordination pattern represent the ability to address unstable posture or unpredictability of joint fluctuations in difficult postural conditions? Although the dancers who participated in this study were mature enough to performing tiptoe standing, the flexibility in applying different tactics for coordination might be different at the professional level. Future experiments using professional dancers will be able to address this question.

Intra-joint coordination

By comparing the values of the weights between the identical joints in the anteroposterior and mediolateral directions, we were also able to investigate the coupling of intra-joint coordination. During heel-toe standing, there was a coupling of intra-joint fluctuations. This result was consistent with the results of a previous study (King et al. 2012), which showed the coupling of the COP sways in the anteroposterior and mediolateral directions during various types of quiet standing. Anteroposterior and mediolateral postural controls have been treated as relatively independent strategies (Winter et al. 1996). Our results indicated that although the anatomical mechanisms for the COP fluctuations in each direction might be independent, the neuromuscular intra-joint control of fluctuation in both directions might be coupled.

For tiptoe standing, we also observed that there was intra-joint synchronization between anteroposterior and mediolateral fluctuations. In particular, dancers' MP and ankle joints of their right leg had a more anteroposterior and mediolateral anti-phase pattern between their sways, thus indicating that dancers' right MPs and ankles have a tendency to move left-front or right-rear. In this study, all participants were instructed to keep their toes facing forward. Dancers have learned to tiptoe-stand with their weight distributed along three points of the foot: the thumb, thenar, and digital pad of the middle toe (Warren 1989), namely, the side of the big toe. Therefore, dancers' right MPs and ankles are considered to actively move in the left-front or right-rear direction. Although we only

investigated joint coordination of the right leg in this study, the left leg might be prone to an identical coordination pattern (i.e., right-front/left-rear pattern of the MP and ankle).

This is the first study to demonstrate anteroposterior and mediolateral intra-joint sway coupling during tiptoe standing for dancers and non-dancers. Dancers showed a robust tendency toward anti-phase intra-joint coordination of the MP and ankle joints, whereas non-dancers did not have a fixed pattern. If the body sways more and more variably, then a compensatory strategy may simplify the sway pattern, thus making the body sway regular and predictable (Riley and Clark 2003). Therefore, dancers might have learned a regular and predictable sway pattern to maintain unstable tiptoe posture, namely, fixed anteroposterior and mediolateral intra-joint fluctuations.

Ballet dancer's joint coordination

Learning movement skills is a process through which the neural control system achieves movement coordination by mastering redundant degrees of freedom of the body or limb system (Bernstein 1967). Many studies have demonstrated a small joint angular amplitude or decreasing joint amplitude during learning that has been interpreted as a sign of "joint freezing" (Chow et al. 2007; Higuchi et al. 2002; Hodges et al. 2005; Steenbergen et al. 1995), which was interpreted as a reduction of the degrees of freedom in a multi-joint movement (Chow et al. 2007; Higuchi et al. 2002; Hodges et al. 2005; Steenbergen et al. 1995). In-phase joint coordination between the ankle and knee in dancers during tiptoe stand-

ing observed in this study could make joint configuration smoother and more arch-like compared with anti-phase coordination, which makes a notched leg configuration. Thus, inter-joint in-phase coordination might be a new type of reduction in the degrees of freedom of multi-joint fluctuations. However, as Bernstein noted, redundancy in the degrees of freedom is likely to only occur in the initial stages of motor learning (Bernstein 1967; Hodges et al. 2005). Thus, further investigations involving simulations with a musculoskeletal model are necessary to determine whether the in-phase joint coordination we observed in this study leads a quieter posture. In addition, an investigation of joint coordination in more skillful participants, such as professional dancers, can corroborate the features of ballet-specific joint movements, which may clarify whether the joint movements of dancers are aesthetically pleasing to the audience.

Dancers exhibited in-phase coordination between the ankle and knee joints in the sagittal plane. In-phase coordination indicates that two joints fluctuate in the same direction synchronously. We suggest that this micro-level of in-phase coordination configures the joints in an arch. Thus, this arch-like configuration due to in-phase coordination might be a product of dancers' lithe legs during standing. Our results suggested that the micro-level of joint coordination could be related to the beauty of dancers' standing postures. Further investigation is necessary to understand the relationship between the kinematic indices and the beauty of motion.

Regarding the dimensionality of joint fluctuations, we observed that there was no difference between the groups for either tiptoe or heel-toe standing in the number of trials with a cumulative %Variance that re-

quired a PC3 for a 0.8 saturation. This result suggested that the complexity of the leg joint fluctuations of dancers did not differ from that of non-dancers. The total number of variables (i.e., the number of kinematic data) used in PCA was 7 for tiptoe standing and 5 for heel-toe standing (see methods). This study is the first to investigate the dimensionality of joint fluctuations using PCA, and the results indicated that the complexity of leg joint fluctuations during standing might not differ, regardless of postural expertise, and that the dimensionality might be approximately 2 or 3 regardless of postural instability. Exploring this concept in more detail will be essential to clarify the relationship between the dimensionality of joint fluctuations and postural expertise.

COP fluctuation

The path length and rectangular area are traditional analyses of the COP used to estimate postural stability. These methods typically assume that the larger the body fluctuation, the more unstable the posture. However in this study, no significant differences in path length or rectangular area of the COP were observed between dancers and non-dancers during heel-toe or tiptoe standing. In previous studies comparing dancers and non-dancers, such inconsistent results have also been reported in the COP analysis. For instance, there have been reports both of significant differences in the parameters of the COP analysis between groups (Stins et al. 2009) and no significant differences in these parameters (Gerbino et al. 2007). Balance training may have an effect on body fluctuation only during challenging balance conditions and may not transfer to less

challenging balance conditions, which are more representative of daily life (Schmit et al. 2005). In addition, the SDs of path length for heel-toe and tiptoe standing and of rectangular area for heel-toe standing were high in the trained group. Considering that the dancers had a variety of joint coordination patterns, whereas non-dancers only had an anti-phase pattern, these results might imply that dancers can modulate their joint fluctuations and corresponding COP movements in a more flexible manner. This larger variability in the motor outputs of dancers might be derived from a larger source of sensory information or multiple control strategies for postural stability compared with that of non-dancers. Our results are examples that show a simple linear COP analysis cannot extract the balance ability of dancers, even during unstable tiptoe standing. By contrast, in this study PCA was successfully used to examine skill level and postural control, thus providing insight into the skillful control of joint fluctuations.

Participants, Experimental tasks, and PCA

The ballet dancers recruited in this study were non-professionals. Because tiptoe standing is an elementary skill of classical ballet, the dancers (with more than ten years of ballet experience) were considered mature enough to perfectly perform tiptoe standing. However, the joint coordination of professional ballet dancers could be different from that of non-professional dancers. Thus, further investigation using professional dancers is necessary to clarify ballet dancers' postural control strategy and the relationship between kinematics indices and the beauty of pos-

ture.

We attached the splint to the back of the participants and fixed their upper body to restrict the entire body motion to the MP, ankle, knee, and hip joints. Aramaki et al. (2001) obtained notable results regarding lower limb joint coordination during heel-toe standing using a splint attached to the participants' backs. Additionally, by using the splint, we could control the movement of the participants' upper bodies. However, this method might result in an unnatural standing posture. Moreover, we did not fixed the participants' arms because they could hold on to the barre in case they lost their balance during unstable tiptoe standing; thus, we instructed the participants not to move their arms while standing. Therefore, in future studies, more practical tasks should be used to understand the postural control of more pragmatic stances.

By using PCA, we demonstrated the contribution of and relationships between the kinematic data by comparing each weighting coefficient for each time series. We focused mainly on PC1 in this study because PC2 and PC3 contained much less information than PC1 (see Fig 2), although PC2 and PC3 were necessary to saturate the cumulative %Variance. However, there might be differences in the postural control strategies between the groups in these smaller principal components. Further assessment is necessary to clarify the slight differences in postural control that significantly affect balance control abilities.

Conclusion

There were three main results of this study: (1) during tiptoe standing, dancers exhibited an anteroposterior in-phase coordination of ankle-knee sway, whereas non-dancers predominantly showed an anti-phase coordination of the adjacent joints; (2) there was intra-joint coordination during heel-toe and tiptoe standing, particularly for dancers, in which the MP and ankle joints tended to sway left-front or right-rear during tiptoe standing; and (3) some traditional COP analysis could not completely determine postural expertise, even during unstable tiptoe standing.

STUDY2

Joint coordination and muscle activities of ballet dancers during tiptoe standing

Abstract

We aimed to investigate lower limb joint coordination in dancers during tiptoe standing and the relationship between joint coordination and muscle co-activation. Seven female ballet dancers performed tiptoe standing with six kinds of leg positions (the first five positions are from classical dance and the 6th position is from modern dance) for 10 s. The kinematic data of the metatarsophalangeal, ankle, knee, and hip joints and surface electromyograms (EMG) over 13 lower limb muscles were recorded. Principal component analysis was performed to determine joint coordination. Metatarsophalangeal-ankle and ankle-knee had in-phase coordination while knee-hip showed anti-phase in the sagittal plane. In addition, most EMG-EMG coherence around metatarsophalangeal and ankle joints was significant up to 50 Hz when these two joints swayed with in-phase. In conclusion, ballet dancers had in-phase coordination from metatarsophalangeal to knee joints, which was associated with muscle co-activation to a higher frequency domain (50 Hz) in comparison with anti-phase coordination.

Introduction

Many studies have investigated dancers' superb equilibrium control and posture by comparing dancers and non-dancers or dancers with a variety of skill levels (see review Blsing et al. 2012). Joint coordination, which is a synergistic structure underlying the mechanically redundant human body segments, is an important topic of human motor control. Many studies have focused on joint coordination with a variety of motor tasks: standing posture (e.g. Kuo et al. 1998; Aramaki et al. 2001; Pinter et al. 2008), gait (e.g. Deluzio et al. 1997; Hubley-Kozey et al. 2006; Ivanenko et al. 2005; Troje 2002), and rhythmic movements (Toiviainen et al. 2010). We have also examined ballet dancers' lower-limb kinematic coordination during tiptoe standing with bare feet (Tanabe et al. 2014), which is "en demi-pointe" and not "en pointe" (we refer to demi-pointe as tiptoe standing throughout this study), suggesting that dancers' key coordinative pattern for lower limb joints was in-phase coordination between adjacent joints. However, we have examined ballet dancers' postural control only with the 6th position used in modern/contemporary dance. The first five positions are used in classical dance, in which the legs are turned out (external rotation) might affect or constrain the skeletal and muscular coordinative structures during standing. Thus, it is necessary to examine joint coordination under a variety of leg configurations to understand ballet dancers' postural stability and its control strategy. A dynamical systems approach, which uses a mathematical compression analysis such as principal component analysis (PCA), is one approach to capture the

kinematic organization, and this approach proposes combining extremely redundant kinematic components with multiple body segments into functional units called coordinative structures or synergies (e.g., Turvey et al. 1988; Mitra et al. 1998). Ballet dancers' superb postural control ability might derive from a neural-muscular-skeletal system that efficiently controls the mechanical structure; however, the postural control strategy specific to ballet dancers has not been clarified at the level of skeletal system coordinative structures such as joint-to-joint coordination (i.e., in-phase or anti-phase coordination). Based on this dynamical systems approach, we aimed to investigate the joint coordination of ballet dancers during tiptoe standing (demi-point) in a variety of postures.

Joint coordination represents the coupling patterns of two adjacent joints involving three segments' oscillations. Thus, two muscles associated with the fluctuations of the two adjacent joints might activate synchronously for the sake of kinematic coupling. As for the synchronous muscle activities during human standing, the coherence between two electromyography (EMG) signals, which reveals the muscle co-activation in the frequency domain, has been demonstrated during quiet standing (Boonstra et al. 2008; Saffer et al. 2008). EMG signals can be divided in the frequency domain into alpha, beta, and gamma bands, which represent different neural commands of the central nervous system (CNS) (Ushiyama 2013). It is possible that different joint coordination patterns are caused by different coupling patterns of muscle activities. Thus, we also aimed to examine the EMG-EMG coherence between joint coordination patterns for inspecting the musculo-skeletal relationship regarding

joint coordination and speculating on the control of joint coordination via motor cortex.

The purpose of this study was to investigate the joint coordination for a variety of foot positions (six kinds of leg positions; the first five from classical dance and the 6th from modern dance). Furthermore, we aimed to examine the differences in muscle co-activations between joint coordination patterns as a first step to understand the postural control mechanism underlying the generation of joint coordination.

Materials and methods

All procedures used in this study were in accordance with the Declaration of Helsinki and were approved by the Ethics Committee of the Graduate School of Human and Environmental Studies at Kyoto University. Approval was based on an appropriate risk/benefit ratio and a study design wherein the risks were minimized. All procedures were conducted in accordance with the approved protocol. Informed consent is a process beginning with both written and verbal description of the study and insurance of participant understanding followed by a signed consent form. Informed consent continued throughout the study via a dialogue between the researcher and participants.

Participants

Seven female non-professional classical ballet dancers (age = 24.1 ± 5.0 yr, height = 160.8 ± 5.1 cm, body mass = 53.0 ± 7.9 kg) participated in this study. All of them were right-handed and right leg dominant: hand

and leg dominance was tested by asking participants the hand used for writing and utensils and the leg used to kick balls, put in front when starting running, and put forward first when suddenly falling down, respectively. They had enough experience with ballet training to perform tiptoe standing; the average number of years of their training was 14.4 ± 3.6 yr. None of the participants had a significant medical history or signs of gait, postural, or neurological disorders, and no one had vision problems. One of the participants had genu recurvatum (her heels were off the floor when she sat with her legs extended forward), however, there was no obvious differences in the results of this study relevant to genu recurvatum.

Experimental protocol and measurement

Participants stood barefoot (without wearing any shoes) with their eyes open and arms crossed in front of their chest and performed demi-point, which is tiptoe standing on the ball of the foot. They performed the six leg positions used in dance, from 1st to 6th position, while facing forward (en face). The 1st to 5th positions are defined in classical ballet as positions with the legs turned out, and the 6th position is used in modern/contemporary dance. These leg configurations are shown in Figure 1: the distance between both feet for 2nd and 4th positions were one-and-a half times the length of the foot and the length of one foot, respectively, according to Warren (1989, p13). In this study, we referred to those standing positions as T1 to T6. For the 3rd to 5th positions, participants performed two kinds of leg configurations; right-front (referred to as T3f,

T4f, and T5f) and right-rear (referred to as T3b, T4b, and T5b). For 1st through 5th positions, participants' legs were turned out with maximal external rotation at the hip and they were in parallel and closed during the 6th position. Each of a total of nine conditions lasted for 10 s and five trials were conducted for each standing condition. A sufficient rest period of at least 5 min was allowed between the conditions. All participants were asked to perform each kind of tiptoe standing in random order.

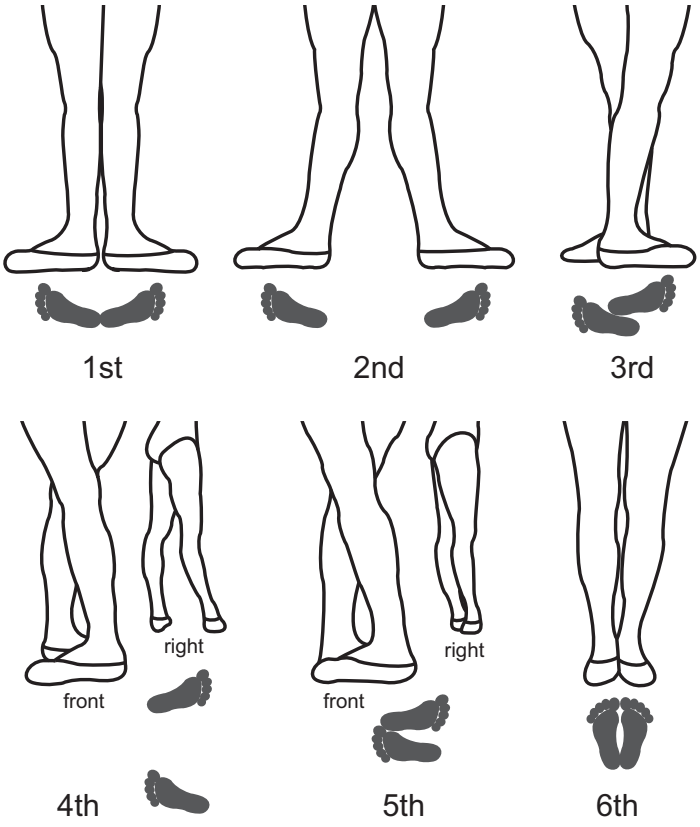

Figure 1: Six leg positions. Front view and footprint are shown for all positions. In addition, right side view (right top) is shown for the 4th and 5th positions. All of these positions were performed with facing front (en face) in this study

For calculating joint angles of metatarsophalangeal (MP), ankle, knee, and hip (greater trochanter) joints subsequently, we measured the anteroposterior/mediolateral displacements of the ankle, knee, hip, and anterior superior iliac spine (ASIS). We attached reflective boards (8cm × 8cm white plastic boards) to the front and the right sides (at the level of lateral malleolus, region genu anterior, greater trochanter, and ASIS) of their right legs using double-sided tape for most of the leg positions except for the rear leg of 3rd, 4th, and 5th positions. For these three positions, the boards were replaced from the anterior to the posterior surface of the knee and hip. The two boards attached to the front and right sides of the body for each joint were connected and fixed to be 90 degrees. Then we applied lasers to the middle of the boards. Eight laser sensors were used (four sensors in front of the participants: 10 m resolution, LK-500, Keyence, Japan, and four additional sensors on the right side of the participants: 4 m resolution, IL-S100, Keyence, Japan) to obtain kinematic data of ankle, knee, hip, and ASIS in anteroposterior and mediolateral directions with a sampling frequency of 2 kHz. During calibration, we checked that a constant value of 1V was outputted for a constant slide of the board (1cm for LK-500 and 0.6cm for IL-S100). The arrangement of the eight laser sensors is illustrated in Figure 2a. EMG signals from the gluteus medius (GM), rectus femoris (RF), sartorius (SR), vastus lateralis (VL), long head of biceps femoris (BFL), semimembranosus (SM), medial gastrocnemius (MG), lateral gastrocnemius (LG), soleus (SOL), peroneus longus (PL), tibialis anterior (TA), extensor digitorum longus (EDL), and flexor hallucis brevis (FHB) mus-

cles were recorded from participants' right legs with Ag-AgCl electrodes with an interelectrode distance of 12 mm (DL-141, S&ME, Japan) (EMG locations are shown in Figure 2b). To minimize the cross talk between adjacent muscles, we first ascertained the location of the belly of each muscle by using an ultrasound B-mode image, and then we placed the electrodes over the belly. The reference electrode for the EMGs was placed over the lateral malleolus of left leg. The electrodes were connected to a preamplifier with a bandwidth of 5.2500 Hz (DL-741, S&ME, Japan). All signals were stored with a sampling frequency of 2 kHz on the hard disk of a personal computer using a 16-bit analog-to-digital converter (PowerLab/16SP, ADInstruments, Sydney, Australia). Data processing was performed with Matlab 6.5 (The MathWorks, Natick, MA).

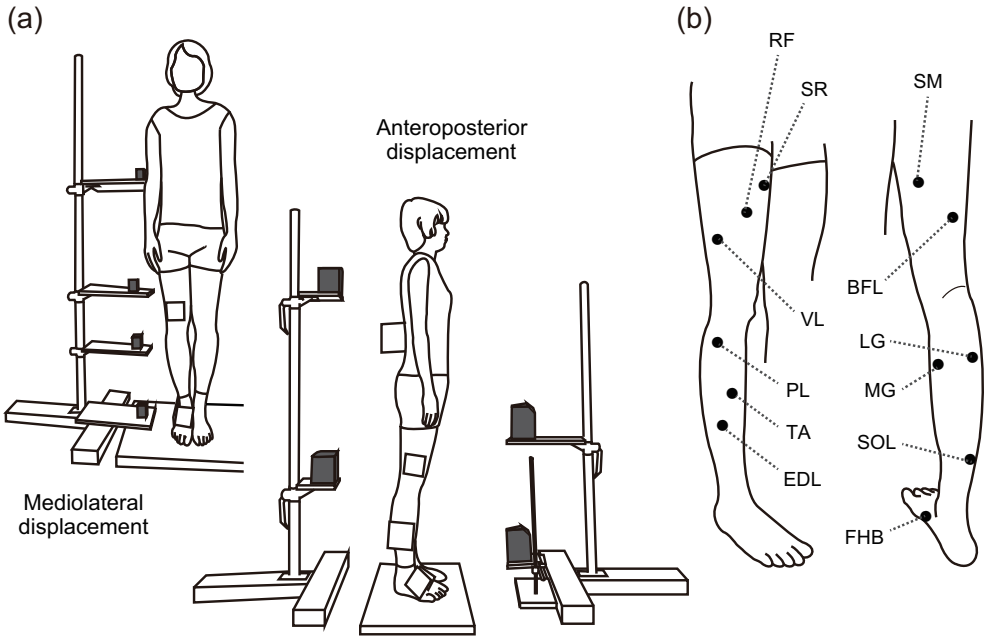

Figure 2: Experimental set-up and EMG location. (a) The displacements of the ankle, knee, hip, and ASIS were measured by eight laser sensors (small black equipment in front/side of participants). Laser lights were reflected at

the square reflective boards attached to participants' body. Participants were always facing front (en face) with their eyes open. When legs were turned out, we re-attached the reflective boards so that they are facing front or right depending on the degree of turn out of the subjects' legs. (b) EMG location for twelve leg muscles. The belly of each muscle was detected by using an ultrasound B-mode image before attaching electrodes to the participants' skin surface.

Data analysis

A time series of kinematics data of 10 s was passed through a 20 Hz Butterworth low-pass filter. With the assumption that the vertical displacement of the body is small compared to those in the sagittal and frontal planes, the displacements of ankle, knee, hip, and ASIS measured by the laser sensors were then converted to position coordinates (X_i, Y_i, Z_i) (i=1,2,$\cdots$,5, corresponding to metatarsophalangeal (MP), ankle, knee, hip, and ASIS, respectively) of the center of the individual joints as follows:

$$X_i = Ls_i + R_i$$

$$Y_i = Lf_i + R_i$$

$$Z_i = \sqrt{A_i^2 - (X_i - X_{i-1})^2 - (Y_i - Y_{i-1})^2} + Z_{i-1}$$

where Ls_i and Lf_i are the displacements of ith joint (for $i > 2$) from z axes to the reflective board attached to the front and right side of the ith joint, respectively, R_i is the ith joint's radius (for $i > 2$), the definition of which is shown in Fig 3a, and A_i is the segment length between ith joint and $(i-1)$th joint (an example is shown in Fig 3b). The coordinate of the MP (i = 1) was set to be the origin: $(X_1, Y_1, Z_1) = (0, 0, 0)$.

Because participants' lower limbs were held in external rotation at the hip in 1st to 5th positions, we defined the segment-specific sagittal

and frontal planes of each segment for every trial, which means that the orientation of x-y-z axis is different for each pair of the sagittal and frontal planes. This segment-specific sagittal plane of the ith joint was defined as the plane which crosses the initial locations of the center of rotations for the $(i-1)$th, ith, and $(i+1)$th joints. The frontal plane crosses the initial location of the ith joint, runs parallel to the vertical direction, and crosses at right angles with the sagittal plane (Fig 3c, both planes for MP joint). Then we calculated the joint angles along the defined sagittal and frontal planes.

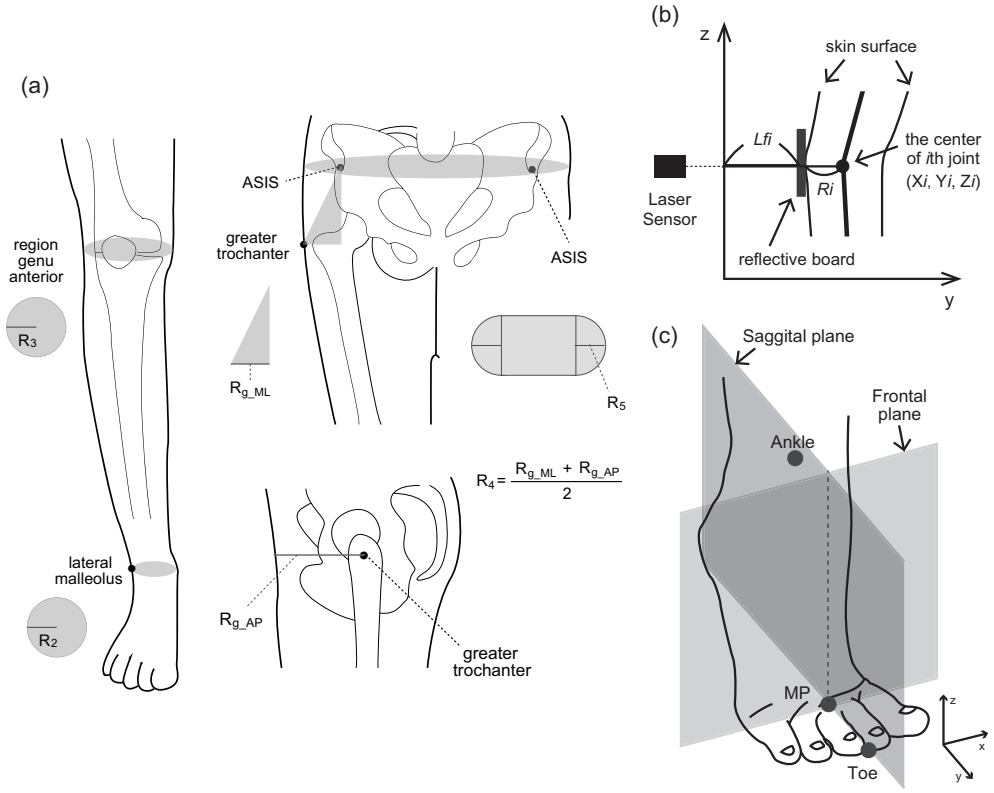

Figure 3: The coordinates of the center of joints and segment-specific sagittal and frontal planes. (a) Radii of the ankle, knee, and hip (greater trochanter) and the depth of the anterior superior iliac spine (ASIS). The ankle and knee were approximated to circles, whose radii were R_2 and R_3, respectively. The radius of hip (R_4) was defined to be the mean of its anterior depth and the horizontal distance between greater trochanter and ASIS. The horizontal plane

including both ASIS was approximated to a rectangle with two semicircles in both sides, and its depth (R_5) was defined as the radius of the semicircle. (b) The definitions of Lf_i and R_i for the calculation of the coordinate in sagittal plane of ith joint (that is, Y_i). (c) The sagittal and frontal planes used for the calculation of MP joint angles. The sagittal plane is a plane through the initial locations of the adjacent three joints (toe, MP, and ankle in this case) and the frontal plane is a plane that includes the initial location of MP joint and is orthogonal with the sagittal plane. These two planes were made for each joint (MP, ankle, knee, and hip) in the same way, and only the orientation of x-y-z axis is different for each pair of the sagittal and frontal plane whatever the degree of turn out is.

PCA (Jolliffe 1986) enables us not only to compress or remove redundant information in kinematic data, but also to examine the covariance between kinematic variables existing in the assembled information. In this study, we investigated the coordination between MP, ankle, knee, and hip joint angles in sagittal and frontal planes by using PCA (medio-lateral kinematic data of the knee was excluded because it is anatomically impossible for the knee to move in this direction). With these seven variables, we first formed a matrix A as follows:

$$A = [X_1, X_2, ..., X_7]$$

where the first four rows represent joint angles of MP, ankle, knee, and hip in the sagittal plane, and the last three rows represent joint angles of MP, ankle, and hip in the frontal plane. The percentage of variance accounted for (VAF) was calculated as follows:

$$VAF(i) = \frac{\lambda_i}{\sum_{k=1}^{7} \lambda_k}$$

where λ_i is the ith eigenvalue of the matrix A.

Joint coordination was assessed by the eigenvectors of A (see Tanabe et al. 2014 for more details). We investigated joint coordination by using

the first eigenvector of A (that is of the first principal component (PC1)) because PC1 possesses the largest tendency of the correlation between the variables (that is, seven time series of joint angles in this study). Using the first eigenvector of A (the weighting vector of PC1), we categorized the joint coordination into three patterns: in-phase, anti-phase, and middle as follows:

$$\text{anti-phase: } W_k \cdot W_{k+1} < 0 \text{ and } |W_k| > 0.4 \text{ and } |W_{k+1}| > 0.4$$
$$\text{in-phase: } W_k \cdot W_{k+1} > 0 \text{ and } |W_k| > 0.4 \text{ and } |W_{k+1}| > 0.4$$

where W_k represent the kth component of the first eigenvector of A, which is associated with the kth joint angle. Otherwise, the coordination was regarded to be the middle pattern. We used the value of 0.4 because the maximum value of weight in our previous study was approximately 0.5 and a similar value of weight was also shown in this study. Although this threshold of 0.4 was arbitrarily selected, this threshold was able to categorize the joint coordination into the three patterns quite evenly. Also, even if this threshold was larger or smaller than 0.4, the in/anti coordination would not be determined as the opposite (anti/in) coordination because in/anti coordination patterns differ based on the relationship of signs between two components of PC1, or rather, there would be more/less middle pattern. In this context, at least the preference of in-phase or anti-phase will be preserved with any value of threshold unless it ' s between 0 and 0.5. Also, to show the dominant coordination pattern for each leg position, the number of trials of each coordination pattern among all five trials was given as the means ± SD.

We also calculated the coherence spectrum between EMG signals to examine the co-activation of muscles. The pairs of EMG signals were selected so that each of the muscles was associated with the movement of an adjacent joint, and we computed coherence spectrum for all of the EMG pairs. EMG time series were rectified because rectification of the surface EMG signal and its power spectrum is useful to reveal the temporal pattern of grouped motor unit discharge (Halliday et al. 1995; Myers al. 2003) and the activation strategy of the muscles (Yoshitake et al. 2002), and were segmented into epochs of 512 ms (1024 points) duration with no overlap (19 epochs). The data set corresponding to each 512-ms epoch was Hanning-windowed to reduce the spectral leakage. As the window size of 512 ms would only provide a single estimate of coherence of the 2 Hz signal (whose period is 500 ms) in each window, we focused on higher frequency domain than 2 Hz in the present study. After that, we separated the EMG-EMG coherence spectrum by joint coordination patterns for each participant and then computed the mean EMG-EMG coherence spectrum of all dancers for each joint coordination pattern. We then compared mean EMG-EMG coherence spectrum between joint coordination patterns.

Statistical analysis

Statistically significant differences in the number of trials for each coordination pattern were tested with a one-factor (joint coordination) ANOVA if the hypothesis of homogeneity of variance between groups was accepted with Levene's test for every standing position and adja-

cent joints' pairs, i.e., MP-ankle, ankle-knee, and knee-hip in the sagittal plane, and MP-ankle, and ankle-hip in the frontal plane. If rejected with Levene's test, Kruskal-Wallis non-parametric test was performed to compare these variables. One-factor ANOVA (factor of frequency occurrence of each joint coordination pattern) was used because we focused on the difference in dominance between joint coordination patterns and not on the difference in the dominance of each coordination pattern between leg positions or between pairs of adjacent joints. Subsequently, the Tukey's post hoc analysis and Mann-Whitney U-test were conducted for detecting the difference in the preference of joint coordination pattern between leg positions for ANOVA and Kruskal-Wallis test, respectively. For the statistical calculations, p ¡ 0.05 was accepted as significant. All statistical analyses were conducted with Matlab 6.5 (The MathWorks, Natick, MA). Also, the 95% confidence level (CL) of coherence was given by (Rosenberg et al. 1989):

$$CL(\alpha) = 1 - (1 - \frac{\alpha}{100})^{\frac{1}{n-1}}$$

where n is the number of epochs and alpha is the confidence interval (in %). In this study, alpha of 95% was chosen and n was 19, resulting in the CL of 0.1533.

Results

Percentage of variance accounted for (VAF)

We calculated VAF for each participant, trial, and standing condition to assess the dimensionality or complexity of joint fluctuations (total

number of PCs were seven). Irrespective of standing conditions, cumulative VAF was almost saturated at the third PC at the value of more than 90%. Mean values of VAF for each standing position are shown in Table 1. VAF of PC1 were ranging from 52.8 60.7%, which means that PC1 contains more than half of the information of all joints' fluctuations for all of the leg positions.

	PC1	**PC2**	**PC3**	**PC4**	**PC5**	**PC6**	**PC7**
T1	55.59 (10.05)	24.70 (5.72)	12.81 (4.53)	4.91 (2.72)	1.84 (1.16)	0.13 (0.13)	0.02 (0.02)
T2	56.41 (8.97)	25.78 (6.43)	12.49 (5.18)	4.14 (1.99)	1.11 (0.75)	0.06 (0.05)	0.01 (0.01)
T3f	60.43 (12.60)	23.99 (7.94)	10.53 (4.97)	3.60 (2.39)	1.36 (1.15)	0.08 (0.06)	0.02 (0.02)
T4f	60.14 (11.63)	25.95 (9.29)	8.96 (4.73)	3.50 (2.45)	1.37 (0.98)	0.07 (0.07)	0.01 (0.01)
T5f	57.38 (9.58)	26.97 (6.92)	10.66 (4.78)	3.63 (2.20)	1.25 (0.58)	0.09 (0.07)	0.02 (0.02)
T6	52.81 (8.40)	26.51 (5.79)	12.90 (5.29)	5.50 (2.19)	2.11 (1.58)	0.14 (0.10)	0.03 (0.03)
T3b	54.02 (9.40)	25.81 (6.18)	12.43 (4.24)	5.48 (3.00)	2.01 (1.54)	0.21 (0.25)	0.03 (0.02)
T4b	55.71 (9.72)	24.97 (5.18)	11.44 (4.30)	5.61 (2.77)	2.06 (1.16)	0.17 (0.21)	0.04 (0.04)
T5b	60.68 (10.92)	22.52 (6.73)	10.29 (4.56)	4.54 (2.39)	1.83 (1.29)	0.12 (0.12)	0.01 (0.01)

Table 1: VAF for each standing position. Mean (± SD) value of VAF[%] for every principal components (from PC1 to PC7) are shown.

Inter-joint coordination

Joint coordination patterns were obtained by comparing the weight values between adjacent joints in sagittal and frontal planes. Figure 4

shows the mean number of trials for each coordination patterns assessed by PC1's weighting vectors for each standing condition.

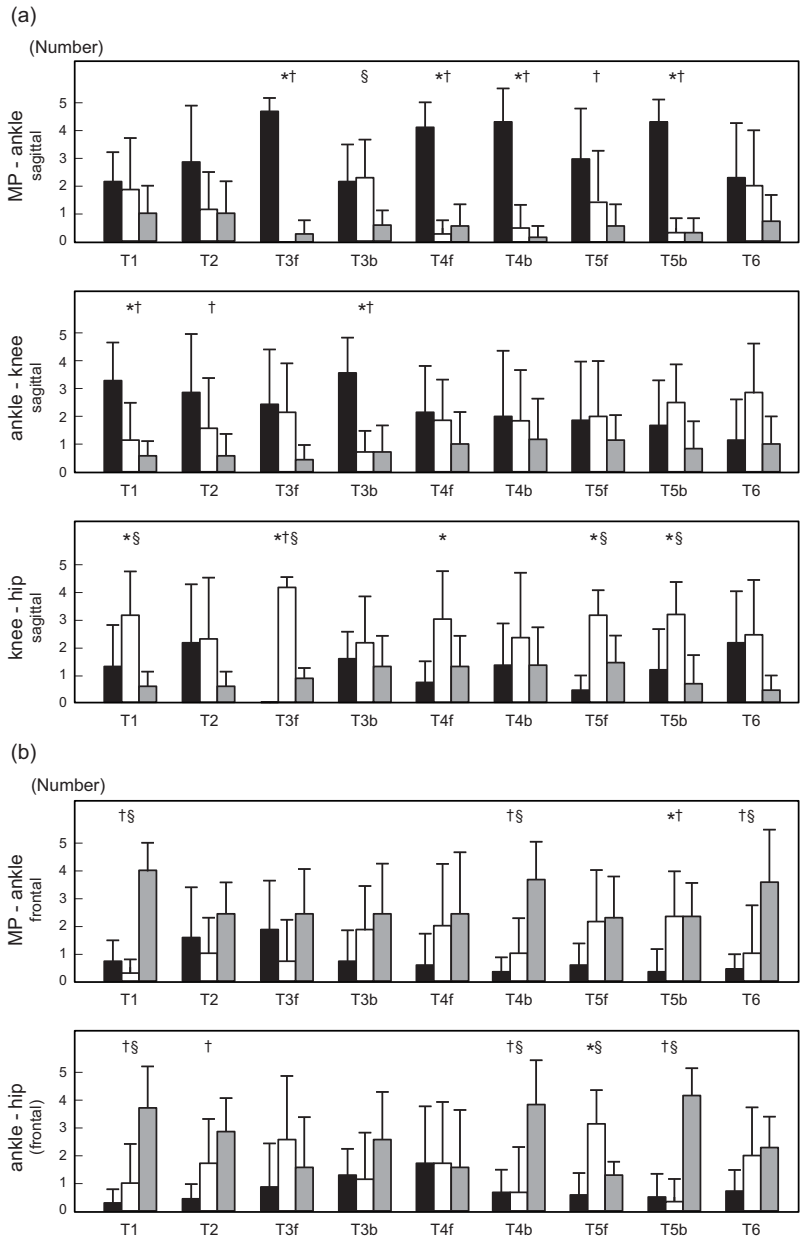

Figure 4: The number of trials of each coordination pattern during tiptoe standing. Black, white, and gray bars represent the mean number of trials with in-phase, anti-phase, and middle, respectively, for each leg position among all participants (maximum of five because each participant performed five trials for each leg position). (a) The top, middle, and bottom lines are of MP-ankle, ankle-knee, and knee- hip coordination in sagittal plane, respectively.

(b) The top and bottom lines are of MP-ankle, and ankle-hip coordination in frontal plane, respectively. *, †, and § : significant difference with $p < 0.05$ between in- and anti- phase, in-phase and middle, and anti-phase and middle, respectively.

For MP-ankle coordination in the sagittal plane (Fig 4a top), in-phase was statistically more common than the other patterns for T3f, T4f, T4b, and T5b ($p < 0.01$ for these four positions) or than middle for T5f ($p = 0.028$). There were more anti-phase trials than middle trials for T3b ($p = 0.022$). Moreover, regarding ankle-knee coordination in the sagittal plane, in-phase was more common than the other patterns for T1 and T3b ($p < 0.01$ for both) or than middle for T2 ($p = 0.061$) (Fig 4a middle). Finally, anti-phase was statistically more common than the other for T1, T3f, T5f, and T5b ($p < 0.01$ for all of these positions) or than in-phase for T4f ($p < 0.01$) for knee-hip coordination in the sagittal plane (Fig 4a bottom). Also, in-phase was much less common than the others for T3f ($p < 0.01$).

Regarding the joint coordination in the frontal plane (Fig 4b), middle pattern was statistically more common than the other for T1, and T4b ($p < 0.01$), and in-phase was less common than the other during T5b ($p = 0.022$) for MP-ankle coordination (Fig 4b, top). Also, there were a larger number of middle trials than the other for T1, T4b, and T5b ($p < 0.01$) and than in-phase for T2 ($p < 0.01$) for ankle-hip coordination (Fig 3b bottom). For T5b condition, anti-phase was more common than the other patterns ($p < 0.01$).

Regarding the difference between front and rear legs, there were obvious differences between the legs for the 3rd position in the sagittal plane

(Fig 4a): in-phase was dominant for MP-ankle coordination of front leg (T3f) and for ankle-knee coordination of rear leg (T3b), and anti-phase was dominant for knee-hip coordination of front leg (T3f).

The relationship between muscle co-activation and joint coordination

To investigate the differences in the muscle co-activation patterns in the frequency domain between the trials with in-phase, anti-phase, and middle coordination patterns, we first calculated the EMG-EMG coherence for all trials and divided the spectrum into classes depending on the joint coordination patterns, and then computed the mean value of coherence for each joint coordination pattern. Figure 5 shows the examples of EMG-EMG coherence associated with MP-ankle joints (left column) and other features of EMG-EMG coherence especially for ankle-knee and knee-hip coordination (right column). Black, gray, and dashed lines represent the mean value of coherence when their joint coordination was in-phase, anti-phase, and middle pattern, respectively. The three figures in the left column were chosen as examples that showed MP-ankle in-phase coordination was associated with higher coherency between lower limb muscles. The right column represents other features of coherency: the top, middle, and bottom figures are examples that show ankle-knee coordination was associated with LG and other lower limb muscles, knee-hip coordination was associated with specific pairs of muscles (in this case RF and SR), and there was no coherency for most of the other muscle pairs, respectively.

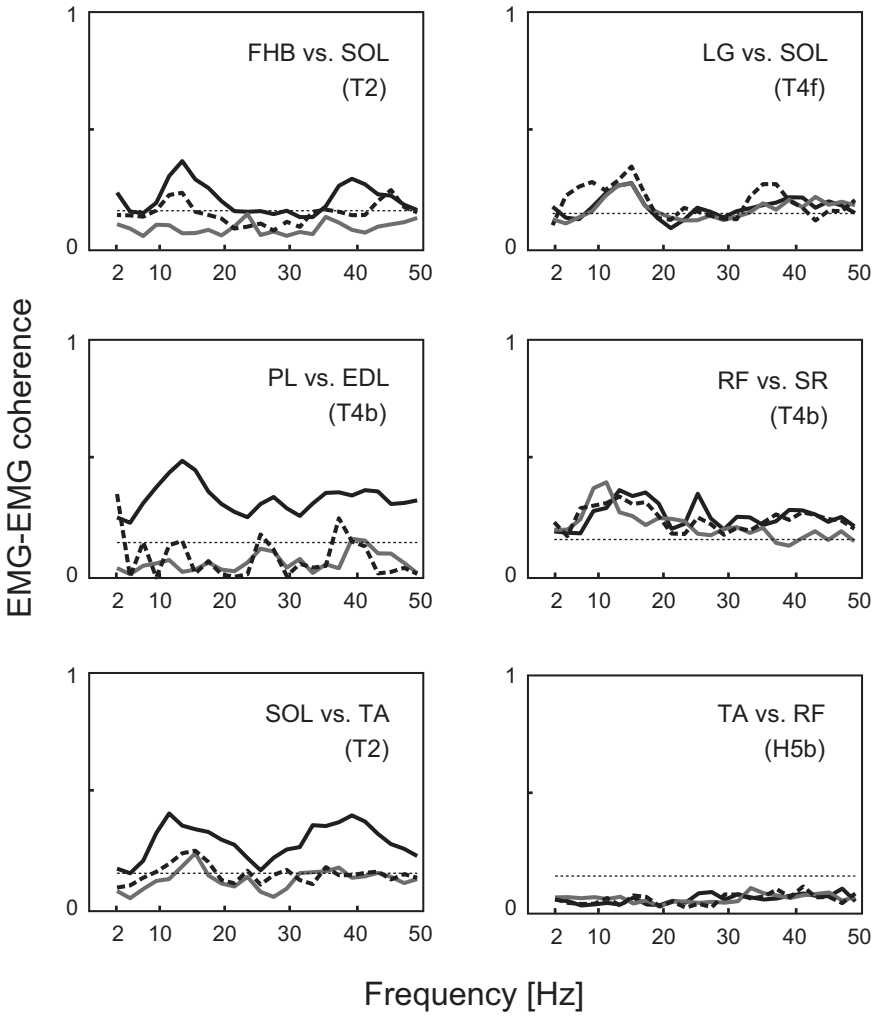

Figure 5: Examples of EMG-EMG coherence spectrum for each joint coordination pattern. Black, gray, and dashed lines represent the mean value of EMG-EMG coherence spectrum of all the trials when the coordination was in-phase, anti-phase, and middle, respectively, from all of the participants for each leg position. Figures of left column are examples of EMG-EMG coherence associated with MP-ankle coordination for showing that MP-ankle in-phase coordination was associated with higher coherency between lower limb muscles: FHB vs. SOL during T2 condition (top), PL vs. EDL during T4b condition (middle), and SOL vs. TA during T2 condition (bottom). Figures of right column are example of the other features of EMG-EMG coherence: LG vs. SOL during T4f condition associated with ankle-knee coordination (top) as an example of ankle-knee coordination associated with LG and other lower limb muscles, RF vs. SR during T4b condition associated with knee-hip coordination (middle) as an example of knee-hip coordination associated with specific pairs of muscles, and TA vs. RF during H5b condition for ankle-knee coordination as an example of no EMG-EMG coherence (bottom). Horizontal dashed lines represent the level of significance (that is, CL = 0.1533, see Methods).

The left column of Figure 5 shows the examples of EMG-EMG coherence spectrum around MP and ankle joints: FHB vs. SOL during T2 condition (top), PL vs. EDL during T4b condition (middle), and SOL vs. TA during T2 condition (bottom). For these three examples, the mean coherence spectrum of in-phase coordination showed a significant level up to 50 Hz and was the highest coherence among the three coordination patterns. On the other hand, the coherence spectrums of anti-phase and middle trials were below the in-phase coherence or the significant level. Similar results, that is, higher values of coherence for in-phase trials, were obtained for all the other combinations of EMG signals around MP and ankle joints, including the pairs of FHB and lower limb muscles and also the pairs of antagonist muscles of lower limb such as a pair of SOL and TA. These results were consistent through all leg positions especially non-crossed leg positions (T1, T2, and T6) and front-leg positions (T3f, T4f, and T5f).

There was almost no difference in the EMG-EMG coherence between ankle-knee and knee-hip joint coordination patterns for all leg positions. The coherence between the pairs of LG (which is knee flexor) and lower limb muscles such as SOL, PL, TA, and EDL, which includes the pairs of antagonist muscles, were significant up to 50 Hz with most of the leg positions (examples are shown in Fig 5 right top: LG vs. SOL during T4f condition). In addition, RF-SR coherence exceeded the significant level up to 50 Hz only for crossed rear leg of tiptoe standing (during T3b, T4b, and T5b conditions). An example is shown in the right-middle of Figure 5. The rest of the EMG-EMG coherence spectrums were not significant

(an example is shown in the right-bottom of Figure 5).

Discussion

Joint coordination

In this study, MP-ankle coordination in the sagittal plane showed a statistical preference for in-phase for more than half of the leg positions (T3f, T4f, T5f, T4b, and T5b). In addition, most of the other positions (T1, T2, and T6) also showed the tendency of in-phase (Fig 4a, top). Also, in-phase was statistically more common for ankle-knee coordination of some positions (T1, T2, and T3b) in the sagittal plane. The in-phase joint coordination was a feature of ballet dancers' joint fluctuations during tiptoe standing (Tanabe et al. 2014). Therefore, the in-phase joint coordination observed frequently in this study may be a possible feature of joint coordination specific to ballet dancers with many years of training.

There were more trials with the middle pattern in the frontal plane (Fig 4). Postural control in the frontal plane might be more difficult than that in sagittal plane because most leg muscles are attached to the front/back side of the segments and this anatomical architecture makes it easier to control the anteroposterior fluctuations compared with mediolateral fluctuation, and as a result, coordination patterns may vary within trials in the frontal plane. We should note that the variability in joint coordination patterns was seen both in different dancers and within the same dancer. The cause of the preference in joint coordination patterns deserves further clarification.

There was a difference in joint coordination preferences between front and rear legs, especially for the 3rd position in the sagittal plane (Fig 4a). All of the dancers that participated in this study were right-leg dominant. Thus, this difference between front and rear legs might be due to body laterality. However, all of the participants said there was no difference between legs in the manageability of tiptoe standing. Therefore, the difference between T3f/T3b conditions may not be due to laterality in dominant legs at least the conscious level, or rather, it might be because of the mechanical asymmetry in the leg configurations.

Regarding the difference between leg positions, crossed-leg positions (3rd, 4th, and 5th positions) tended to be in-phase for MP-ankle coordination and anti-phase for knee-hip coordination both in the sagittal plane (Fig 4a top and bottom). Both legs are stuck together, especially for 3rd and 5th positions, therefore, this mechanical constraint due to crossing legs may force the foot and shank segments to move synchronously, and in-phase coordination was dominant as a result. In-phase coordination makes body segments more susceptible to gravitational toppling torque compared with anti-phase oscillation, because the two segments fluctuate in the same direction. Therefore, to compensate for this destabilizing torque due to in-phase oscillation for the foot-shank segment during leg-crossed positions, the knee and hip may fluctuate in anti-phase in many cases. In addition, there was less bias in joint coordination pattern in the T6 position. The 6th position is the only position in which legs were not turned-out in this study. There was no constraint in the joint fluctuations in the anteroposterior direction during the 6th position, and this may be

the reason that dancers were able to adopt a variety of joint coordination patterns and there was less deviation between them.

Muscle co-activations

We compared joint coordination patterns in EMG-EMG coherence as a coupling of muscles. Although pooled coherence (Amjad et al. 1997) would be a better representation of the coherence spectrum for each coordination pattern, the number of trials were different between coordination patterns for each participant and thus the significance levels of the coherence spectrum were different between both participants and coordination patterns; thus, the coherence spectrum was not comparable between joint coordination patterns. Therefore, in this study, we used the mean coherence spectrum to compare joint coordination patterns. The EMG-EMG coherence around MP and ankle joints showed higher coherence up to 50 Hz for in-phase coordination than the other two patterns (Fig 5). This result suggests that the in-phase joint coordination between MP and ankle was associated with muscle co-activations around these two joints, which is FHB vs. lower limb muscles and antagonist muscles around ankle joint up to a higher frequency domain. Because the ankle has to be located right above MP joint during ballet specific tiptoe standing (Grieg 1994), the ankle might be locked due to co-activations of antagonist muscles, and this could cause the preference for in-phase coordination between MP and ankle joints. Although the activation of antagonist muscles is said to decrease via training associated with training-related increase in motor cortex activation (Dal Maso et al. 2012), the stability of the ankle might

be so vulnerable during tiptoe standing that co-activation of antagonist muscles was required. The in-phase coordination between MP and ankle joints was accompanied by muscle co-activations in the alpha, beta, and gamma frequency bands (Ushiyama 2013). Although the gamma range has been linked to strong contraction (Brown et al. 1998; Mima and Hallett 1999) or dynamic force output (Marsden et al. 2000; Omlor et al. 2007), our result demonstrated the existence of fast muscular activation in the gamma band during static tiptoe standing and raised the possibility that only in-phase coordination could be related with the motor control of CNS which creates the muscle activation in the gamma band. Our results indicate that in-phase coordination might result from the stabilization process; that is, a relatively unstable joint such as the MP and ankle during tiptoe standing could be locked by muscle co-activations to be stabilized, and as a result, in-phase coordination might be generated.

In contrast, there were similar muscle co-activation patterns among three coordination patterns of ankle-knee and knee-hip (Fig 5 right). This result suggested that each joint coordination pattern from ankle to hip joints might not be generated from the co-activation patterns of two muscles. One possibility is that the time lags between the timings of multiple muscle activation result in a specific joint coordination. Also, the pairs of aforementioned antagonist muscles around ankle joints, that is, LG vs. other lower limb muscles, and RF vs. SR, showed significant level of coherence up to higher frequency domain during tiptoe standing (Fig 5). It was suggested that lower limb muscles swayed in a coupled manner up to the fluctuations in higher frequency domain to stabilize the

ankle right above the MP joint. The reason why LG took the lead in the co-activations of lower limb muscles might be that first, LG plays a major role to generate the gravitational toppling torque while standing, and second, it is possible for LG to modulate its activation along with the sway of both the ankle and knee because LG is a bi-articular muscle, and last, the origin of LG is lateral epicondyle of femur and this direction of attachment might anatomically contribute to the turn out of knee joint. Also, the reason of RF-SR coupling up to fast oscillations might be that these muscles ' origins are close and their insertions are opposite sides of knee joint: tibial tuberosity for RF, proximal part of the tibia for SR. Thus, the coupling of the two muscles can contribute to the stabilization of the knee.

Although our discussion in this section of this study is much based on qualitative observation of coherence analysis, it was demonstrated the possibility of one-to-one relationships between kinematic coordinative structure and muscle activation coupling for at least MP-ankle coordination. This is an important point for understanding human postural control because this will be the first step for examining how human body segments are actuated leading to embody a certain pattern of kinematic coordination and investigating what functions of control strategies via muscle activities result in joint coordinative structure. In further analysis, it will be necessary for different EMG frequency bands to be analyzed separately, and it will be important to investigate the relationship between temporal phase transition and muscle activities.

Kinematic dimensionality during standing

In general, a few modes are sufficient to describe the variability of a spatially distributed coherent system (Kelso 1995; Haken 1996). The results in this study reveal that the low dimensional description of lower limb joints' fluctuations is possible under a variety of leg positions, and that the multiple degrees of freedom can be compressed to two or three. Ballet specific positions for tiptoe standing with legs turned out are so unstable that non-dancers lose balance easily with those positions; this is the main reason we did not recruit non-dancers. Such highly constrained mechanical leg positions may require a simple control mode; that is, dancers might have learned kinematic control of a few dimensions to maintain balance under unstable standing conditions.

In conclusion, there were two findings in this study: first, ballet dancers showed in-phase oscillation as MP-ankle and ankle-knee coordination under most of the leg positions among six kinds of tiptoe standing; second, MP-ankle in-phase coordination was associated with EMG-EMG coherence up to 50 Hz. Because in-phase oscillation was seen as characteristic of dancers' joint coordination patterns during tiptoe standing (Tanabe et al. 2014), our result indicates that ballet dancers' in-phase coordination between leg segments is controlled by higher frequencies of muscle co-activations compared with anti-phase coordination.

STUDY3

Temporal phase transition as lower limb inter-joint coordination and corresponding muscle activity during expert-specific postural control

Abstract

Lower limb joints fluctuate in a coordinative way during standing to compensate. Understanding the properties of temporal change in joint coordination and the mechanism of its generation remains a fundamental question in postural control strategy. Also, the plasticity of human motor control system can be observed by the investigation of postural control strategy for well-trained subjects such as dancers. The purpose of this study was to investigate the expert-specific temporal phase transition properties of lower limb joints during tiptoe standing and to examine the relationship between muscle activities and joint phase transitions. Seven female non-professional ballet dancers performed tiptoe standing with four kinds of leg positions. We measured the angular displacements of four lower limb joints in the sagittal plane. The temporal phase transition between two adjacent joints was calculated by using the Hilbert transformation. This methodology allowed us to compute the cross correlation between phase transition and electromyography (EMG) from twelve leg muscles. Peaks of phase-EMG cross-correlation were detected to investigate the relationship between muscle activities and kinematic phase

transition. Inter-joint phase transitions occurred a few times during 10 seconds of tiptoe standing. More importantly, we observed the cross correlation between phase transition and EMG signals, suggesting that phase transitions can be controlled via muscle activities. In addition, muscles that showed relationship with phase transitions varied individually and depended on leg configuration, and even small muscle activities can be temporally associated with joint phase transitions.

Introduction

Human bipedal stance is inherently unstable with the pendulum-like behavior of linking segments of the whole body. Visual, vestibular, and somatosensory systems function cooperatively to achieve the postural stability of such unstable mechanical dynamics (Dietz 1992). Human can learn to maintain more unstable posture through training, such as ballet dancers that can perform tiptoe standing with minimal body fluctuation. Understanding the postural control mechanism for well-trained subjects will lead us to comprehend the plasticity of human motor control system. During tiptoe standing, the corporative structure of sensory information will change due to the increased articular joints of the body with different innervation, narrower base of support, and less cutaneous information from the sole compared with quiet standing. Hence, the stochastic and deterministic properties of center of pressure (COP) during tiptoe standing were different from those of quiet standing (Nolan and Kerrigan 2004) and more meticulous control of COP by muscle activities was observed (Tanabe et al. 2012). However, the control mechanism of unstable tiptoe

standing, for which there might be a remarkable expert-specific control mechanism, is not fully understood from the aspect of kinematic body oscillations and its relationship with muscle activities.

The control strategies of human upright posture have been assessed by observing the joint coordination. For example, reciprocal coordination between the ankle and hip accelerations has been reported during quiet standing (Aramaki et al. 2001), and this converse two-joint oscillation was reduced through the aging process (Kato et al. 2014). In addition, we have recently found that the feature of joint coordination of ballet dancers was in-phase between ankle-knee and knee-hip segments during tiptoe standing (Tanabe et al. 2012). These findings support the idea that kinematic coordinative structure, which consists of assembled patterns among multi-segment oscillations, might change through the adaptation process. Joint fluctuations are partially the outcome of kinetic control via muscle activities. During quiet standing, lower leg muscle activities compensate for mechanically unstable body oscillation (Masani et al. 2003; Sasagawa et al. 2009; Kouzaki and Shinohara 2010; Kouzaki and Masani 2012; Day et al. 2013; Sozzi et al. 2013). This kinetic-kinematic coupling was stronger during tiptoe standing (Tanabe et al. 2012). Joint coordination affects the variability of COM acceleration (Sasagawa et al., 2014) and COM-COP relationship (Wang et al., 2014). These findings indicate that joint coordination has relationship with postural stabilization based on COM-COP control, and thus, it might be controlled by muscle activities.

Temporal change in center of pressure (COP) center of mass (COM)

coordination during standing was found to be accordance with the change of platform moving frequency (Ko et al., 2014), suggesting that the coordinative structure of the body can also change over time according to the postural task. Ballet dancers learn tiptoe standing with variety of leg positions. Such expert-specific tiptoe standing is so unstable that the change of leg configuration may lead the temporal change in kinematic coordinative structure. In addition, there might be individual differences in the control mechanism of temporal kinematic coordination because multi-segment body sways is affected by the individual body configuration. However, both joint coordination and muscle activation patterns during standing have been evaluated as their tendencies of whole sampling duration by using such as principal component analysis (for kinematics: Kuo et al. 1998; Aramaki et al. 2001; Pinter et al. 2008; Tanabe et al. 2014, and for muscle synergies: Wang et al. 2006; Krishnan et al. 2011), uncontrolled manifold (for kinematics: Hsu et al. 2007; 2013), or non-negative factorization (for muscle synergies: Chiovetto et al. 2012). Such methodologies have made it difficult to assess the temporally and adaptively changing control strategy of unstable postures that require experts' skills. On the other hand, the Hilbert transformation (Pikovsky 2001), which we used to calculate the instantaneous phase difference as kinematic coordination over time, is useful to examine its relationship with muscle activities by examining the cross-correlation between electromyography and phase difference time series. This would be a further step to understand the neural-muscular-skeletal postural control mechanism as a postural adaptation of ballet dancers. The purpose of this

study was to investigate the postural control adaptation through ballet training from the aspect of the temporal properties of phase transition between adjacent body segments during tiptoe standing and to examine the individual difference in phase transition control strategies by muscle activities.

Materials and Methods

All procedures used in this study were in accordance with the Declaration of Helsinki and were approved by the Ethics Committee of the Graduate School of Human and Environmental Studies at Kyoto University. Approval was based on an appropriate risk/benefit ratio and a study design wherein the risks were minimized. All procedures were conducted in accordance with the approved protocol. Informed consent is a process beginning with both written and oral description of the study and insurance of participant understanding followed by a signed consent form. Informed consent continued throughout the study via a dialogue between the researcher and participants.

Participants

Seven female non-professional classical ballet dancers (age = 24.1 ± 5.0 yr, height = 160.8 ± 5.1 cm, body mass = 53.0 ± 7.9 kg) participated in this study. The dancers we recruited had enough experience of ballet training to perform tiptoe standing; the average number of years of their ballet training was 14.4 ± 3.6 yr. None of the participants had a significant medical history or signs of gait, postural, or neurological disorders,

and no one had vision problems.

Experimental protocol and measurement

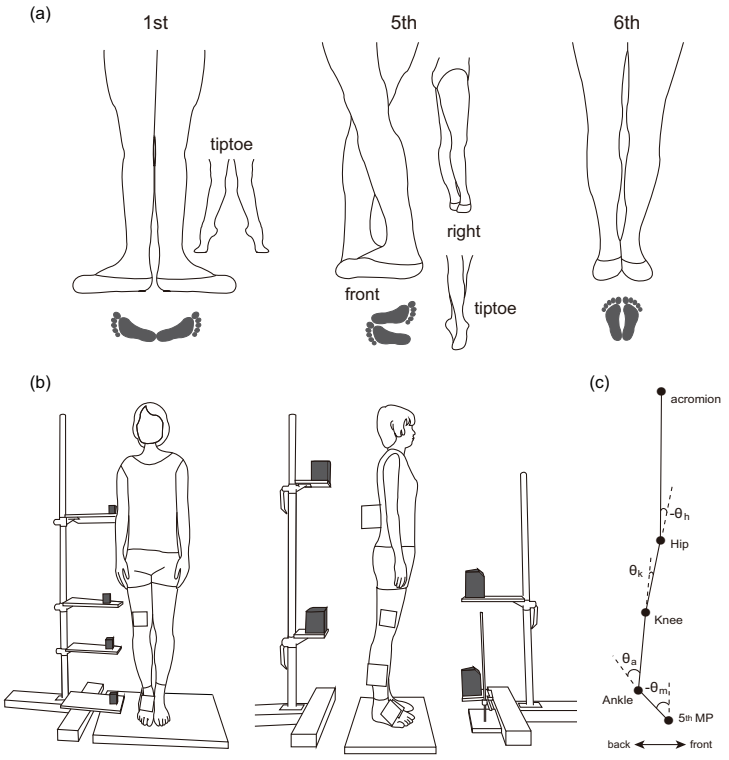

Figure 1: Three leg positions and experimental setup. (a) Three ballet specific leg positions (1st, 5th, and 6th positions) used in this study. 1st position: the balls of both feet are completely turned out, and the heels touch each other. 5th position: both feet touch each other so that the toe of one foot reaches the heel of the other. Right side view is also shown. Dancers performed this position with their right legs are both front and rear (5th-f and 5th-b positions, respectively). 6th position: both feet are stuck together. (b) Joint displacements were measured by eight laser sensors. Reflective boards (10cm × 10cm) were attached to each joint. (c) the definition of joint angles in the sagittal plane.

Each participant was instructed to stand quietly with her eyes open and to look at a fixed point on a plain wall about 1.5m ahead of them. We placed a handrail in front of the participants at a height of approximately 1m for their safety. The participants stood barefoot with their

arms crossed in front of their chest and performed tiptoe (relev or demi pointe in ballet) standing with three leg positions of classical ballet: 1st, 5th and 6th positions. Leg configuration for each position is shown in Figure 1(a). For 5th position, participants performed two kinds of leg configurations: right-leg-front and right-leg-rear (referred to as 5th-f and 5th-b, respectively). Each of the total four positions lasted for 10 s and five trials were conducted for each position. A sufficient rest period of at least 5 min was allowed between the conditions.

Before the experiment, we measured the circumferences of each ankle, knee, hip, and anterior superior iliac spine (ASIS) and segment length between metatarsophalangeal (MP)-ankle, ankle-knee, knee-hip, and hip-ASIS for every participant. These circumferences were used to calculate the depth of each joint center from the skin surface, based on the approximation that horizontal sections of ankle, knee, and hip are close to circle and that the section around ASIS are close to a rectangle with two semicircles stuck to both sides. Then we attached reflective boards for lasers (10cm × 10cm) to the front and the right side of the participants' ankle, knee, hip, and ASIS. The coordinate of each joint center corresponds to the coordination of each reflective board subtracted by each joint's radius. Eight laser sensors were used (four sensors in front of the participants: resolution of 10 m, LK-500, Keyence, Japan, and four additional sensors by the right side of the participants: resolution of 4 m, IL-S100, Keyence, Japan) to obtain precise displacements of the ankle, knee, hip, and ASIS in anteroposterior and mediolateral directions with sampling frequency of 2 kHz. The arrangement of the eight laser sensors was illustrated in Fig-

ure 1(b). The determination range of the laser sensors was 10 cm, and the horizontal displacement of each joint during tiptoe standing was a few centimeters at most. Thus, we assumed that participants' movement was not restricted by the experimental set up and that we could hold the accuracy of horizontal displacement of each joint.

Surface electromyograms (EMGs) from the skin surface over the rectus femoris (RF), sartorius (SR), vastus lateralis (VL), long head of biceps femoris (BFL), semimembranosus (SM), medial gastrocnemius (MG), lateral gastrocnemius (LG), soleus (SOL), peroneus longus (PL), tibialis anterior (TA), extensor digitorum longus (EDL), and flexor hallucis brevis (FHB) muscles were recorded from participants' right legs with Ag-AgCl electrodes with an interelectrode distance of 12 mm (DL-141, S&ME, Japan). To minimize the cross talk between adjacent muscles, we first ascertained the location of the belly of each muscle by using an ultrasound method, and then we placed the electrodes over the belly. The reference electrode for the EMGs was placed over the lateral malleolus of left leg. The electrodes were connected to a preamplifier with a bandwidth of 5.2500 Hz (DL-741, S&ME, Japan). All signals were stored with a sampling frequency of 2 kHz on the hard disk of a personal computer using a 16-bit analog-to-digital converter (PowerLab/16SP, ADInstruments, Sydney, Australia). Data processing was done with Matlab 6.5 (The MathWorks, Natick, MA).

Data analysis

Time series of kinematics data of 10 s were passed through a 20 Hz Butterworth low-pass filter. The displacements of ankle, knee, hip, and ASIS measured by the laser sensors were then converted to position coordinates (X_i, Y_i, Z_i) (i = 1, 2, $\cdots$, 5, corresponding to MP, ankle, knee, hip, and ASIS, respectively) of the center of the individual joints using the measured segment length and joints' radius as follows: for i = 1 (MP joint), the coordinate (X_1, Y_1, Z_1) is the origin (0, 0, 0), and for $i > 1$ (ankle to ASIS),

$$X_i = Ls_i + R_i$$
$$Y_i = Lf_i + R_i$$
$$Z_i = \sqrt{A_i^2 - (X_i - X_{i-1})^2 - (Y_i - Y_{i-1})^2} + Z_{i-1}$$

where Ls_i and Lf_i are the displacements of ith joint from z axes to the reflective board attached to the front and right side of the ith joint, respectively, R_i is the ith joint's radius, and A_i is the segment length between ith joint and $(i-1)$th joint.

Because participants' legs were turned out during the 1st and 5th positions (see Fig 1(a)), we defined the segment-specific sagittal plane of each segment for every trial. This segment-specific sagittal plane of the ith joint was defined as the plane which crosses the initial locations of the $(i-1)$th, ith, and $(i+1)$th joints. Then we calculated the joint angles along the defined sagittal plane, the definition of which is shown in Figure 1(c).

We used the Hilbert transformation, which was originally introduced by Gabor (1946), to calculate the temporal phase of each angular displacement. This method provides a true measurement of the instantaneous phase and amplitude for a signal, s(t), via construction of an analytic signal, $\zeta(t)$, which is a complex function of time defined by:

$$\zeta(t) = s(t) + iH(t) = A(t)e^{i\phi(t)}$$

where the imaginary part $H(t)$ is the Hilbert transform of s(t), which is a version of the original real sequence with a 90° phase shift, and A and ϕ are the amplitude and the phase, respectively. The phase of a signal represents the angular distance that the signal covered since the time origin and is obtained by:

$$\phi(t) = arctan(iH(t)/s(t))$$

The numerical algorithms are available in the standard control design packages of Matlab; the function *hilbert* was used to obtain the results of this paper. The Hilbert transformation was applied to each angle separately, and then the two phase signals of adjacent joints were subtracted to calculate the temporal phase transition. Figure 2 represents an example of the MP and ankle angles during one trial (top) and its MP-ankle phase transition time series calculated by the Hilbert transformation (middle). The Figure 3 bottom is in/anti switching detected by the two joints' angle relationship (the same sign for in-phase and the opposite sign for anti-phase), indicating that in-phase $(0 \pm 2n\pi[rad]; nisaninteger) and anti-phase(\pi \pm 2n\pi[rad]; nisaninteger)$ between two joints (solid and dashed

vertical lines in Fig 3 middle, respectively) calculated by the Hilbert transform mean that both joints' angular locations deviate from their individual mean angular position in the same and different direction, respectively.

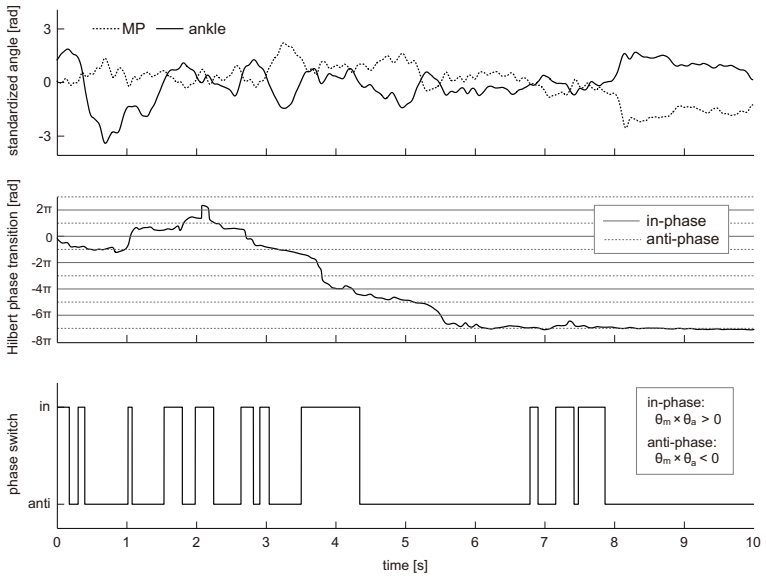

Figure 2: Hilbert phase transition and angular displacements. Top: an example of a set of MP (dashed line) and ankle (solid line) angular displacements during tiptoe standing for 10 seconds. Both time series are standardized with a mean of zero for a visually clear comparison between the two angular oscillations. Middle: temporal phase transition between the MP and ankle calculated by Hilbert transformation. The vertical solid and dashed lines represent in-phase and anti-phase, respectively. Bottom: phase switch defined by the angular displacements (the same sign for in-phase and the opposite sign for anti-phase). The acute switches for less than 50 ms were excluded for visual clarity. This phase switch mostly matches the Hilbert phase transition (middle figure), and indicates what the Hilbert phase transition means.

Then we detected the period of time when the phase difference moves from in-phase/anti-phase to anti-phase/in-phase. After that, we unified the phase transition between in-phase and anti-phase period to be an upward curve by x-axial reflection, that is, in-to-anti transition starts from 0 to π and anti-to-in transition starts from π to 2π. We calculated the phase transition frequency by counting the number of phase transition

from in-phase to anti-phase, which is almost the same number from anti- to in- phase. The phase transitions occurred within 100 ms were removed to exclude the transition derived from reflex loop. Also, EMG signals were high-pass filtered with 35 Hz butterworth filter and then rectified and low-pass filtered with 4 Hz butter-worth filter. Then we calculated cross correlation between phase transition and the processed EMG signals for each of the same transition period. As phase transition series of target periods were upward curves, positive and negative correlations represent muscle activation and attenuation, respectively, associated with phase transition. The pairs of phase and EMG were as follows: MP-ankle phase transition vs. EMGs of FHB, PL, TA, EDL, SOL, MG, and LG, ankle-knee phase transition vs. EMGs of PL, TA, EDL, SOL, MG, LG, RF, SR, VL, BFL, and SM, and knee-hip phase transition vs. EMGs of MG, LG, RF, SR, VL, BFL, and SM. Mean cross correlations among the all phase transition events during five trials were calculated for each pair of joints and muscles for all dancers and leg positions. Because our sample size was more than 200 (duration $> 0.1s$ and sampling frequency of 2 kH) in this study, we focused on the peaks over the value of 0.139, which represents the Pearson's product-moment correlation coefficient for a sample size of 200 at a significance level of 0.05. We also focused on the time lag of 100 to 350 ms to identify the contribution of muscles to the phase transitions because the time lag between lower limb muscle activities and COP or COM displacements has been reported to be around 200 ms during quiet standing (Masani et al. 2003).

Statistical analysis

Statistically significant difference in the phase transition frequency between dancers and leg positions was tested with a three-factor (individual dancers, leg positions, and joint pairs) ANOVA. The following Tukey's post hoc analysis was conducted for mean values for each dancer, leg position, and joint pair: the effect size was estimated using partial eta-squared (η_p^2). If there were any significant differences detected by the post hoc analysis, we implemented a one-factor ANOVA to examine the differences between dancers in the phase transition frequency. One participant (dancer 4) could not complete this task, thus, we excluded the 5th-b leg position from the statistical analysis because we focused on individual variation rather than the difference in postural stance in this study. We conducted all statistical analyses with SPSS 12.01 for Windows (SPSS, Inc., Chicago, IL, USA), and $p < 0.05$ was accepted as significant for all of these calculations.

Results

Phase transition frequency

We calculated how many times the phase transition between in- and anti- phase occurred to examine the difference in the phase frequency between leg positions or dancers. Figure 3 represents the mean phase transition frequency from in- to anti- phase for five trials between MP-ankle (top), ankle-knee (middle), and knee-hip (bottom), and we compared them between four leg positions (black, open, gray, and

hatched bars are for the 1st, 5th-f, 6th, and 5th-b positions, respectively) and between dancers. Dancer 4 could not complete the 5th-b trials, thus her data of 5th-b condition is missing. The three-way ANOVA (excluding 5th-b data) revealed the significant main effect of dancers ($F_{6.0,84} = 4.6, p = 4.3 \times 10^{-4}; \eta_p^2 = 0.25$). The following one-factor ANOVA showed that the knee-hip phase transition frequency of dancer 7 was significantly higher than dancer 1 and 5 during 1st position ($p = 3.7 \times 10^{-3}$), than dancer 5 during 5th-f position ($p = 7.8 \times 10^{-3}$), and than dancer 1, 2, and 6 during 6th position ($p = 1.7 \times 10^{-2}$). There was also a significant interaction between joint pairs and leg positions ($F_{4.0,168} = 4.5, p = 1.7 \times 10^{-3}; \eta_p^2 = 9.7 \times 10^{-2}$), which is not a target for our discussion in this study. There was no other statistically significant difference observed.

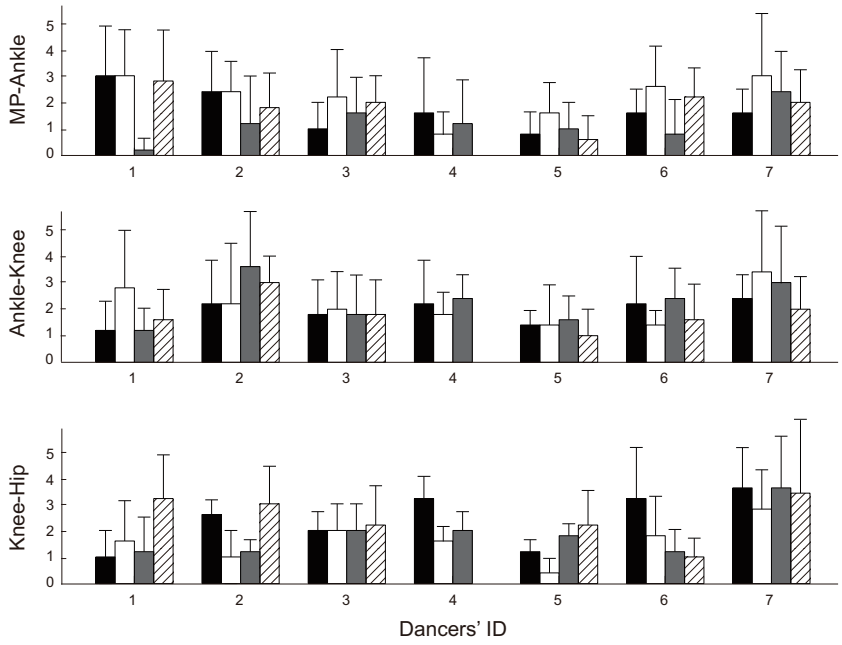

Figure 3: Phase transition frequency for each dancer. Top, middle, and bottom figures represent the mean phase transition frequency for five trials, which

refers to the number of times transition events occurred during 10 seconds of trial, for each dancer between MP-ankle, ankle-knee, and knee-hip pairs, respectively. Black, open, gray, and hashed bars are of 1st, 5th-f, 6th, and 5th-b positions, respectively.

Cross correlation between transition and EMG

		ID 1	ID 2	ID 3	ID 4	ID 5	ID 6	ID 7
6th	toA^+			E, S_o				
	toA^-			F				
	toI^+	P, T S_o, M	L		L		F, S_o M, L	L
	toI^-	F, E L	M			F, P T, E S_o, M	T, E	
1st	toA^-					E		
	toI^+			T, E M	T, S_o L	F, P T, E S_o	P	L
	toI^-	P, E		L			T	F, P E, S_o
5th-f	toI^+	T		P	P			
	toI^-			S_o, M				
5th-b	toA^+		P		F, L			
	toA^-		F				P, L	
	toI^+	F			T, M		P, T E, S_o M, L	
	toI^-					F		

Table 1: Muscles associated with MP-ankle phase transitions. Muscles that showed cross correlation peaks with MP-ankle phase transitions for each leg positions and dancer. Numbers represent time lags to take phase switch from in-phase to anti-phase (toA+ and toA- represent muscle activations and attenuations before the phase moves to anti-phase, respectively) and from anti-phase to in-phase (toI+ and toI- represent muscle activations and attenuations before the phase moves to in-phase, respectively). Blank cells indicate that there was

no muscle that showed correlation with phase transitions. Dancer 4 could not complete 5th-b position trials.

We calculated cross correlation ensemble for all phase transition events through five trials and its time lag between phase transitions and EMG signals for each standing position and joint pair of all dancers. This allows us to see whether joint phase transitions occur after the activities of agonist or antagonist muscles. Positive and negative peaks of the cross correlation represent the phase transitions associated with muscle activation and attenuation, respectively. Table 1 lists muscles that showed cross correlation peak values above 0.139 between MP-ankle phase transitions and EMGs and their time lag of all leg positions.

The relationship between MP-ankle phase transition and muscle activities was dancer dependent (Table 1). In particular, dancer 5's anti-to-in phase transition was associated with muscle activities for all leg positions. In addition, some of the others showed phase-EMG relationship for specific leg positions (dancer 1, 3, 6, and 7). There was less association for the rest (dancer 2 and 4). The anti-to-in transitions were more likely to be associated with muscle activities than in-to-anti transitions.

Figure 4 shows examples of the cross correlation between phase transition and EMG signals for each joint pair. Figures (a)-(c) represent the cross correlation associated with MP-ankle, ankle-knee, and knee-hip phase transitions, respectively. Figure 4a top represents the cross correlations between anti-to-in phase transition (represented by red lines) and EMGs of dancer 5 during 1st position. They all showed positive peaks with similar time lag. On the other hand, during 6th position, this

dancer 5 showed negative correlation between anti-to-in phase transition and EMGs (Fig 4a middle). Moreover, a positive correlation was observed between anti-to-in phase transition and six EMGs (red lines) for dancer 7 during 5th-b position, and a negative correlation was also found between in-to-anti transition and two EMGs (blue lines) (Fig 4a bottom).

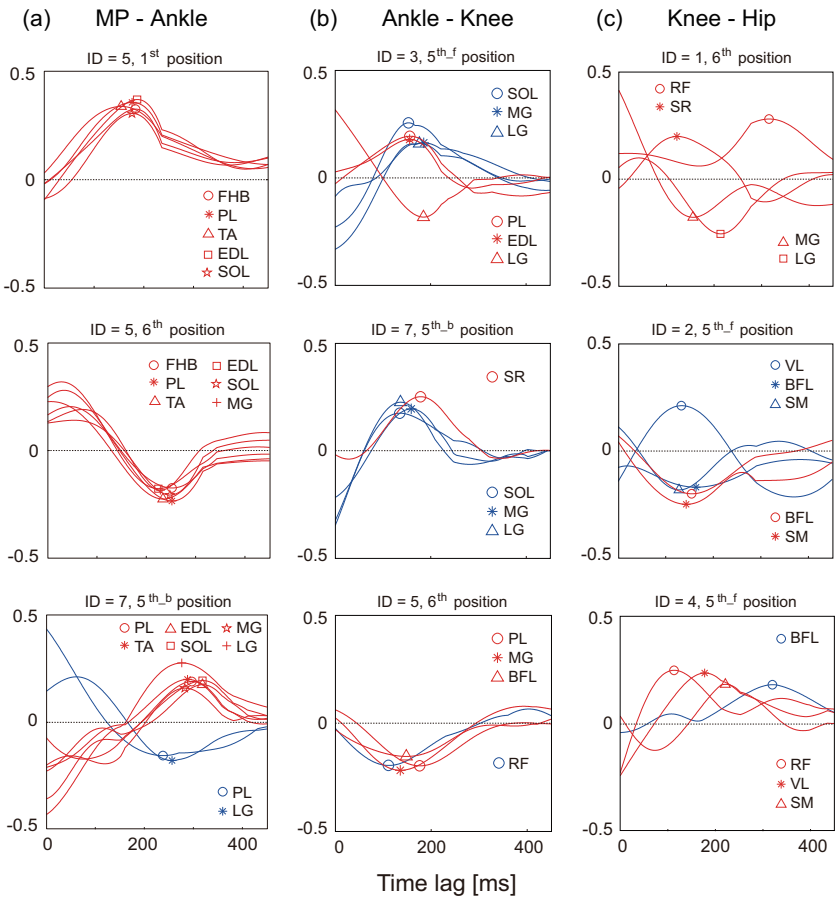

Figure 4: Examples of cross correlation between phase transition and EMG. (a) MP-Ankle phase transition vs. EMG: dancer 5 during 1st position (top), dancer 5 during 6th position (middle), and dancer 7 during 5th-b position (bottom). (b) Ankle-Knee phase transition vs. EMG: dancer 3 during 5th-f position (top), dancer 7 during 5th-b position (middle), and dancer 5 during 6th position (bottom). (c) Knee-Hip phase transition vs. EMG: dancer 1 during 6th position (top), dancer 2 during 5th-f position (middle), and dancer 4 during 5th-f position (bottom). Red and blue lines represent cross correlations for anti-to-in transition and in-to-anti transition, respectively. Each line represents the ensemble cross correlation for all events of phase transition through

five trials, and each symbol indicates each muscle written inside of each figure.

Figure 5 represents seven rectified EMG signals for the four cases that correspond to the dancers and leg positions in Figure 4a: EMGs of one trial out of five of dancer 5's 1st position, dancer 5's 6th position, and dancer 7's 5th-b position. In most cases, FHB activated predominantly followed by PL, EDL, or MG. In each case, note that there tended to be no relation between the amplitude of muscle activation and its contribution to phase transition (that is, peaks in cross correlation).

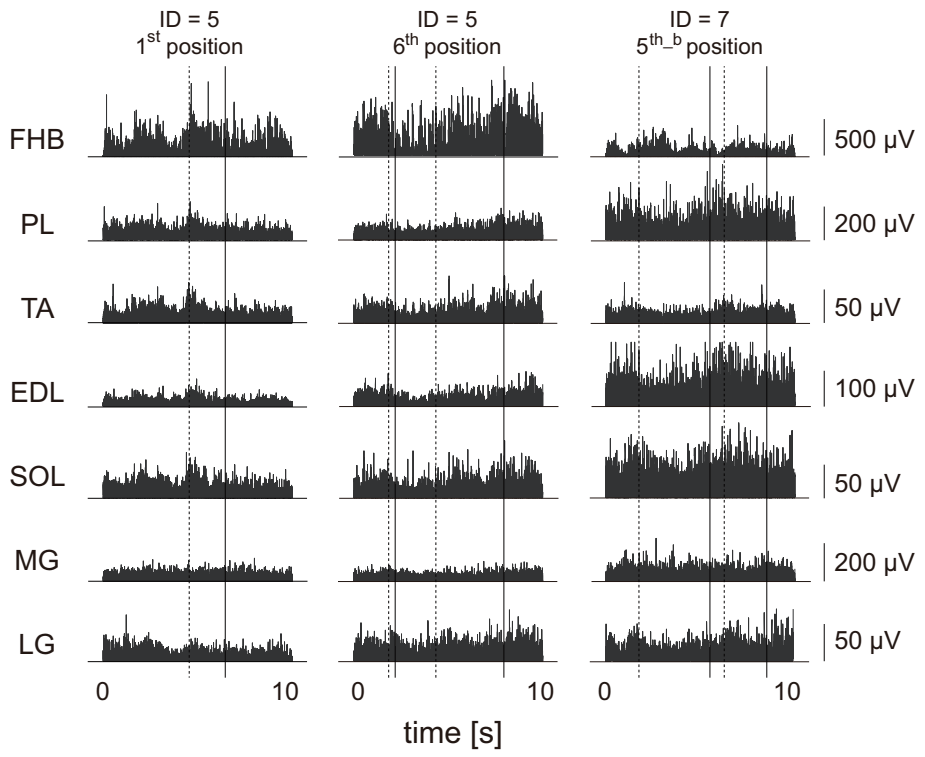

Figure 5: Rectified EMGs corresponding to Fig 4a. Rectified EMGs (no filtered) of seven muscles that were associated with the fluctuations of the MP and ankle are shown. The figures of each row are of one trial out of five for the dancer and leg position corresponding to Figure 4a. The solid and dashed vertical lines represent the time when the MP-ankle phase difference were in-phase and anti-phase, respectively.

Table 2 lists the muscles that showed correlation with ankle-knee phase transition for each dancer and leg position. The relationship between the ankle-knee phase difference and EMG activities was dancer dependent in this case as well. Phase transitions of dancer 1, 3, and 5 tended to be associated with muscle activities during all leg positions. On the other hand, the rest of the dancers showed a relationship between phase transition and muscle activities only during 5th position. Figure 4b shows the phase-EMG cross correlations of dancer 3, 5, and 7 as examples to describe some generation patterns of phase transition. In most cases, muscle activities occurred before phase transitions with similar time lag. As with the MP-ankle phase transition, there tended to be no relationship between the amplitude of muscle activities and its contribution to phase transition.

Table 3 lists the muscles that showed correlation with knee-hip phase transition for each dancer and standing position. Only dancer 1 showed the relationship between phase transitions and muscle activities during all leg positions. For the other dancers, the relationship was seen only during 5th-f position (dancer 2, 4, and 5) or there was almost no relationship (participants 3, 6, and 7). Some of these examples are shown in Figure 4c. Dancer 1 (Fig 4c top) and dancer 4 (Fig 4c bottom) showed correlation peaks with inconsistent time lag. Again, we should note that there tended to be no relationship between the amplitude of muscle activities and its contribution to phase transition.

		ID 1	ID 2	ID 3	ID 4	ID 5	ID 6	ID 7
6th	toA^+			V				
	toA^-			P, S_o M, L	B	R		M
	toI^+	P, S_o L	L					M
	toI^-	M	R	R	V	P, M B		
1st	toA^+	L, B,		M				
	toA^-		V	P, S_o R		P, T E, S_o M, L		
	toI^+	P, B			B	V, B	P	S_o, L
	toI^-	M			S_o, R		S_r	
5th-f	toA^+	E, L	B	S_o, M L		E, M		S_r
	toA^-	S_m			P, E	L	S_m	
	toI^+			P, E				
	toI^-			L	R, S_r B, S_m			
5th-b	toA^+	R	P, E B	P			P, T M, R S_r	S_o, M L
	toI^+	R, B	E, S_r	S_r, V S_m		V	T, R S_r	S_r
	toI^-	P, M		E			L	

Table 2: Muscles associated with ankle-knee phase transitions. Muscles that showed cross correlation peaks with ankle-knee phase transitions for each leg positions and dancer. 'toA+' and 'toA-' represent muscle activations and attenuations before the phase moves to anti-phase, respectively and 'toI+' and 'toI-' represent muscle activations and attenuations before the phase moves to in-phase, respectively.

		ID 1	ID 2	ID 3	ID 4	ID 5	ID 6	ID 7
6th	toA^+			V	R	S_r	R	
	toA^-				B	R		
	toI^+	R, S_r	L	B		S_r		
	toI^-	M, L		S_r				
1st	toA^+	M, S_m					L	
	toA^-					M		S_m
	toI^+				M			B
	toI^-	M, R S_m						
5th-f	toA^+	M, V S_m	V		B		L	B
	toA^-		B, S_m	S_m				
	toI^+			R	R, V S_m	S_r, V S_m	V	
	toI^-		B, S_m			M, L		
5th-b	toA^+		L					R
	toA^-	V						
	toI^+	B						
	toI^-	V	B			R, B	M, S_m	

Table 3: Muscles associated with knee-hip phase transitions. Muscles that showed cross correlation peaks with knee-hip phase transitions for each leg positions and dancer. 'toA+' and 'toA-' represent muscle activations and attenuations before the phase moves to anti-phase, respectively, and 'toI+' and 'toI-' represent muscle activations and attenuations before the phase moves to in-phase, respectively.

Discussion

The relationship between phase transition and muscle activities

In this study, we found that phase transitions between in- and anti-phase occurred a few times during 10 seconds of tiptoe standing (Fig 3). Joint coordination has been traditionally assessed as its spatial tendencies, however, tiptoe standing used in ballet is unstable, which may

disturb a spatially fixed kinematic coordination and make the body oscillation unpredictable. Our results suggest that such adaptively changing postural control mechanism needs to be examined by instantaneous evaluation method such as described by Pikovsky et al. (2001).

Regarding the kinetic-kinematic relationship, the central nervous system (CNS) generates desired muscle contractions by combining a small number of predefined modules, called muscle synergies, and it combines them in a task-dependent fashion to generate the muscle contractions that lead to the desired movement (Tresch et al. 2002; Bizzi et al. 2008). In this study, phase transitions occurred after the muscle activations or attenuations for most of the dancers (Table 1 to 3). Such muscle activities associated with synchronized oscillations of adjacent joints can be explained by considering muscle modules organized for tiptoe standing to get the information of each joint's fluctuation and to output the command of activations or attenuations to their governing muscles. The conventional concept of muscle synergies is that the muscles that compose synergies are similar across subjects and motor tasks in many cases (i.e., robustness of muscle synergies), however, they were inconsistent in this study. The difference in the composition of modules between dancers or leg positions might reflect the fact that in some cases the desired task requires a change in the organization of modules for its effective accomplishment.

On the other hand, there was almost no cross correlation peak between phase transitions and EMG signals for some dancers or leg positions. This result was dependent on two facts: one is that the cross-

correlation peaks were variable and uneven for each event of phase transition during one trial; the second that there was no cross-correlation at all throughout trials. The former might be because of the variability of commands that modules output. In the latter case, the phase transitions might be generated by biomechanical reasons such as viscoelasticity or constraints of leg positions. The relationship between joint coordination and mechanical components or joint control strategies by CNS is under consideration in our current research by computer simulation, which allows us to divide kinematic oscillations into passive and active components and to investigate the contribution of each component to joint coordination.

Differences between dancers

The dancers participated in this study had similar ballet training experience and similar joint coordination patterns (they were the same dancers recruited in (Tanabe et al. 2014)). However, how they controlled their joint fluctuations (i.e., which muscles to use) varied a lot between dancers. These inter-dancer differences might come from their postural control strategy controlled by the CNS or their mechanical structures such as the external rotation angle of the hip, the height of the center of mass, muscle properties, or joint viscoelasticity. As Alessandro et al. (2013) states, muscle synergy extraction methods should take into account task execution variables from the aspect of command input from CNS, and this study reinforces this suggestion and further proposes that the temporal modules for individual dancers may result in the effective accomplishment

of the desired task for their own. This study indicates that the temporal relationship between single muscles and joint coordination is a useful way to analyze the individual variation in neuromuscular postural control mechanism.

In addition, dancer 7 showed higher phase transition frequency than some of the others (Fig 3). The differences between dancers in muscle activation patterns associated with phase transitions and in the phase transition frequency might be the outcome of the optimization to minimize energy consumption or stabilize the posture of each dancer. It is impossible to experimentally understand the individually optimal postural control strategies because human postural control is a complex system due to individually different mechanical components and physiological properties. Whether the change in control strategies of joint torques, which assumes different muscle activation patterns, cause variety in postural stability is currently being investigated in our research by simulation.

Phase transitions and postural stability

Each joint should be controlled during standing to maintain the postural stability with high COM kept in a small base of support. Sasagawa et al. (2014) demonstrated that joint coordination affected the COM acceleration during standing. Thus, the temporal phase transitions might contribute greatly to the postural stability. The characteristics of dancers' postural control are as follows: 1) although the sway amplitude during tiptoe standing was not affected by ballet experience (Tanabe et al. 2014), ballet dancers obviously have superb balance ability compared with non-

dancers in terms of the postural maintenance duration and the degree of fatigue, 2) the feature of dancers' joint coordination during tiptoe standing was in-phase fluctuations between adjacent joints (Tanabe et al. 2014), and 3) the phase transitions from anti-phase to in-phase was more likely to be associated with muscle activities in this study (i.e., there tended to be more red cross-correlation lines in Fig 4). Thus, dancers' postural stability can be considered to be dependent partially on the in-phase joint coordination temporally generated by muscle activities. On the other hand, the amplitude of muscle activities was not related to its relationship with phase transitions (Fig 5). This result suggests that small amplitude of muscle activities will be sufficient to control phase transitions, giving a biological benefit to postural control from the aspect of energy consumption, and that the rest of the activities are for other postural maintenance purposes such as heightening joint stiffness or replying the deviation of current body configuration from the equilibrium. Small changes in muscle activities have often been neglected in the consideration of muscle activities during whole sampling duration such as muscle synergies, however, out results in this study suggests the possibility that muscle activities have some function towards temporal change of joint fluctuations even if the amplitude is quite small.

In summary, we demonstrated that kinematic phase transition between anti- and in-phase occurs during tiptoe standing, suggesting that temporal analysis of joint coordination is essential to understand the postural control mechanism. More importantly, we observed the cross correlation between phase transitions and EMG activities, indicating that

phase transitions can be controlled via muscle activities. In addition, muscles that showed relationship with phase transitions varied individually and depended on leg configuration, and even small muscle activities can temporally modulate joint phase transition. Our study is a first step to investigate the temporal properties of kinematic coordinative strategies and gives a great insight to the neuromuscular postural control strategy of the temporal joint coordination.

STUDY4
Intermittent control of tiptoe standing: robustness based on joint viscoelasticity

Abstract

Human standing has been recently modeled using an intermittent feedback control strategy, but its necessity is still controversial because the model of human quiet standing can also be stabilized with conventional continuous control. Also, it is still unclear whether intermittent control is necessary for the stabilization of intrinsically unstable tiptoe standing. In this study, a quadruple inverted pendulum model with intermittent control has been used as a model of human tiptoe standing in the sagittal plane. The aim of this study was to investigate whether intermittent feedback control is necessary for the stabilization of the human body during tiptoe standing and to examine the sensitivity of joint viscoelasticity and joint control strategy on postural robustness. We first reproduced joint fluctuations similar to those of actual human tiptoe standing.

We simulated a motion of the quadruple inverted pendulum model as each of four links represents metatarsophalangealankle, ankleknee, kneehip, and headarmtrunk segments in the sagittal plane during tiptoe standing. We set three kinds of simulation parameters: three pairs of passive viscoelasticity coefficients, three kinds of joint control strategies for each joint (continuous active, intermittent, and no active controls), and two values of α, which determines the location of the switching boundary for

intermittent control. We assumed that the active torques are generated by linear proportional-derivative feedback controllers with delay of 0.2 s.

Among the 480 pairs of parameters, we found 30 pairs that can stabilize the pendulum for more than 60 s, in which the hip must be controlled intermittently. We also found that each parameter set has different sensitivity to the postural robustness. In conclusion, intermittent feedback control was necessary for the stabilization of the quadruple inverted pendulum. Also, postural robustness varied by joint control strategies, which accompanied with the change in kinematic joint coordination.

Introduction

Inverted pendulum model has been used as a method to investigate human bipedal standing and its control strategy (Peterka 2002; Lakie et al. 2003; Bottaro et al. 2005; Asai et al. 2009; Suzuki et al. 2012). Although actual human control system is nonlinear, this inverted pendulum model can be linearized at the vicinity of the equilibrium points because joint fluctuations are small enough to approximate the coriolis force to be zero during standing. This simple model allows us to understand the mechanism underlying experimentally observed phenomena, such as the difference in joint coordination, and to speculate the robustness of a controller. It has been shown that a multi-segment with multi-input model is more valid as a model of human quiet standing (Pinter et al. 2008; Gnter et al. 2009; 2011; 2012).

Human bipedal postural control has been conventionally modeled as feedback controller based on proportional and derivative feedback (PD

control) model (Peterka 2000; Masani et al. 2003; Maurer and Peterka 2005). Joint viscoelasticity refers to material properties with spring-like (elasticity) and damping (viscosity) behaviors, which contributes to body posture stabilization. The passive stiffness caused by viscoelasticity of the muscle-tendon-ligament system is insufficient to compete with gravitational toppling torque (Loram and Lakie 2002; Casadio et al. 2005). This leads human upright posture to unstable equilibrium of saddle type in multi-dimensional state space (spanning angular position and velocity). The state of the system moves in a phase space converging towards the equilibrium along stable manifolds but diverging away from the equilibrium along unstable manifolds as time elapses. Thus, the state of the system must be controlled actively in the vicinity of the equilibrium to maintain upright posture.

Many studies have advocated the computational theory of the intermittent control for quiet standing (Bottaro et al. 2005; 2008; Asai et al. 2009; Gawthrop et al. 2011; 2014; Suzuki et al. 2012). The intermittent feedback control strategy used in this study exploits the fact that the state point of the system transiently approach to the equilibrium along stable manifolds that appears during active control is turned off (off-period) (Bottaro et al. 2008; Asai et al. 2009; Suzuki et al. 2012). This type of intermittent control produces postural stability by the movements of the state point along stable manifolds during off-periods and pulling it back in the vicinity of stable manifolds during on-periods. At this point, this nonlinear stability during off-periods in this study is different from the classical concept of stability of a linear system. Such intermittent control

strategy is biologically plausible from the aspect of energy consumption for muscle activities and the physiological phenomena of alternate muscle activity which reduce muscle fatigues (Kouzaki and Shinohara 2006). The paper of Suzuki et al. (2012) used a double inverted pendulum model with intermittent on/off switching for each joint and it showed that the change in hip elastic coefficients lead the differences in the stability region, joint fluctuation amplitudes, and postural control strategy. Thus, it can be speculated that the intrinsic joint viscoelastic component and joint control strategy are sensitive to the postural stabilization.

Gawthrop et al. (2011) have mathematically demonstrated that intermittent control was necessary for the stabilization of human quiet standing during different postural tasks. Tiptoe standing is intrinsically unstable compared with quiet standing because of its narrow base of support and the accompanying decrease in afferent proprioceptive information. We can examine the postural control mechanism of inherently unstable postures through studying tiptoe standing, where base of support is very narrow and is accompanied with less afferent proprioceptive information. Metatarsophalangeal (MP) joint must be controlled and the anatomical properties around MP joint, such as muscles, tendon, and aponeurosis, are smaller than those around the ankle joint for quiet standing. In addition, muscle activations are larger during tiptoe standing and the enhanced muscle co-activation (Tanabe et al. 2012) should lead the change in joint impedance control for postural stability. In this study, we aimed to investigate whether intermittent control is necessary for the stability of tiptoe standing, which intrinsically require different

control strategy from quiet standing. Computer simulation of a quadruple inverted pendulum as a model of tiptoe standing is also useful to investigate the changing mechanism of human postural control strategy because the change in joint coordination through balance training was observed only for tiptoe standing (Tanabe et al. 2014). If experimentally valid output of joint fluctuations were observed with the simulation of quadruple inverted pendulum, the generality of the model can be enhanced, and we will also be able to estimate the factor of the change in joint coordination, which can never be understood by experimentally observing coordinative phenomena.

As a simple motor output out of an infinite number of neuralmusculars keletal control strategies of human movement, many studies have extracted such joint coordination for human standing (Kuo et al. 1998; Aramaki et al. 2001; Pinter et al. 2008; Hsu et al. 2013; Kato et al. 2014; Tanabe et al. 2014), some of which focused on the age-related changes in joint coordination during quiet standing (Hsu et al. 2013; Kato et al. 2014) or differences in joint coordination patterns based on expertise level of balance ability during tiptoe standing (Tanabe et al. 2014). These studies indicate that joint coordination during standing can adaptively change according to the neuromuscular aging process or special balance training. Such investigations of joint coordination as a global aspect of motor system are essential to understand the postural control mechanism. Also, joint coordination has relationships with the center of mass (CoM) acceleration (Sasagawa et al. 2014) and the mutual relationship between the center of pressure (CoP) and CoM (Wang et al. 2014). So

joint coordination has some function associated with body stabilization.

In this study, we established a computer simulation of a quadruple inverted pendulum with intermittent feedback control as a model of human tiptoe standing, which is an intrinsically unstable posture. The aim of this study was to investigate whether intermittent feedback control is necessary for the stabilization of the human body during tiptoe standing and to examine the sensitivity of joint viscoelasticity and joint control strategy to postural robustness. We first reproduced joint fluctuations similar to those of actual human tiptoe standing with exploratory selected joint viscoelasticity coefficients. This is also for giving generality of the intermittent control model of multi-segment inverted pendulum.

Materials and Methods

Ethics statement

All procedures used in this study were in accordance with the Declaration of Helsinki and were approved by the Ethics Committee of the Graduate School of Human and Environmental Studies at Kyoto University. The approval was based on an appropriate risk/benefit ratio and a study design wherein the risks were minimized. All procedures were conducted in accordance with the approved protocol. The individuals participating in this study has given written informed consent to participate in this study and to publish these case details. Informed consent continued throughout the study via a dialog between the researcher and participants.

A quadruple inverted pendulum model

In this study, the motion of a quadruple inverted pendulum mimics the human upright posture of tiptoe standing in the sagittal plane. The distal end of the lowest segment is fixed in the space by a pin joint, corresponding to the metatarsophalangeal (MP) joint. A pin joint also connects each pair of adjacent segments. Four segments of the model represent MPankle (foot), ankleknee (shank), kneehip (thigh), and headarmtrunk (HAT) segments, respectively. The model and its definition of joint angles are shown in Figure 1.

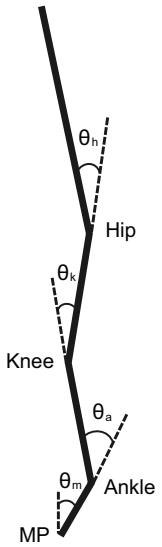

Figure 1: A quadruple inverted pendulum model. A model for a human standing tiptoe in the sagittal plane. Each of four links represent foot (MPankle), shank (ankleknee), thigh (kneehip), and HAT segments, from the bottom. Joint angles were defined as relative angles between adjacent joints except for joint angle of the MP being relative to the vertical line.

Because the joint angles, $\theta = [\theta_m, \theta_a, \theta_k, \theta_h]$, and the corresponding angular velocities are small during quiet tiptoe standing, the second and higher order terms can be neglected, leading to the following linearized

equation of motion for the quadruple inverted pendulum model:

$$M\ddot{\theta} + G\theta = Q \tag{1}$$

where M is the inertia matrix, $G\theta$ the gravitational toppling torque vector, and $Q = [\tau_m, \tau_a, \tau_k, \tau_h]^T$ the joint torque vector. The matrices M and G are defined in the Supporting Information (A1). Parameter values are listed in Table 1 for an adult woman with a height of 1.6 m and weighting 55 kg based on our previous experiment and the anthropometric parameters of Japanese athletes (Ae et al. 1992).

When we consider the continuous control of inverted pendulum, the joint torque $\tau_i (i = m, a, k, h)$ is modeled as the sum of passive torque that is determined mechanically without feedback delay and active torques determined by the CNS with feedback delay as follows:

$$\tau_i = K_i\theta_i + B_i\dot{\theta}_i + P_i\theta_{i\Delta} + D_i\dot{\theta_{i\Delta}} \tag{2}$$

where subscript Δ represents that the state variable include delay which we consider a physiologically plausible value of 0.2 s that includes sensory transduction, neural processing, transmission, and muscle activation delays as reported in (Peterka 2002) (we did not consider local feedback at the spinal level with shorter delay), and $\theta_\Delta = \theta(t - \Delta)$. The first two terms on the right hand side of the equation represent passive feedback torques with no time delay corresponding to the intrinsic mechanical impedance of each joint: joint stiffness and damping that we consider to include tonic muscle activities (not via CNS control) as well as intrinsic muscle-tendon properties as materials. The third and fourth terms repre-

sent the active neural feedback torques that are determined as functions of delay-affected angular displacement and velocity, respectively.

Body mass [kg]	55
Segment length [m]	[0.13, 0.35, 0.40, 0.72]
Segment mass ratio [%body mass]	[2.2, 10.6, 24.6, 62.6]
Segment center of mass ratio [%]	[50.0, 41.0, 45.8, 33.0]
Gyration radius ratio [%]	[18.4, 27.5, 28.5, 40.0]

Table 1: Anthropometric parameters of quadruple inverted pendulum. Four values of each line (except for body mass) are for segment 1 to 4 from the left. Segment center of mass ratio is with respect to segment length from the upper end. Gyration radius is relative to frontal (mediolateral) axis and the presented as percentage of each segment length.

Continuous passive joint torques

The passive joint torques are modeled as linear torsional viscoelastic elements with passive elastic (K_i) and viscosity (B_i) coefficients. The passive torques are continuously acting on the joints because they are generated by intrinsic mechanical properties. We used the three pairs of viscoelastic coefficients $VE\{j\}(j = 1, 2, 3)$ to investigate the effect of passive musculotendinous properties to the joint coordination:

$$VE\{1\} = \begin{cases} (K_m, K_a, K_k, K_h) = (0.8, 10, 10, 0.2) \cdot mgh \\ (B_m, B_a, B_k, B_h) = (4, 100, 100, 10) \end{cases} \tag{3}$$

$$VE\{2\} = \begin{cases} (K_m, K_a, K_k, K_h) = (0.8, 8, 8, 0.2) \cdot mgh \\ (B_m, B_a, B_k, B_h) = (4, 50, 50, 10) \end{cases} \tag{4}$$

$$VE\{2\} = \begin{cases} (K_m, K_a, K_k, K_h) = (0.8, 4, 4, 0.2) \cdot mgh \\ (B_m, B_a, B_k, B_h) = (4, 20, 20, 10) \end{cases} \tag{5}$$

We set these values by referring to previous studies of quiet standing (Loram and Lakie 2002; Casadio et al. 2005; Maurer and Peterka 2005; Bottaro et al. 2008; Asai et al. 2009; Suzuki et al. 2012). We consider passive joint torques include muscle tonic activities as well as intrinsic muscletendon properties. Because muscle activity levels are very high during tiptoe standing compared with those during quiet standing, we set relatively higher viscoelasticity values particularly for the ankle and knee. In addition, we set the elasticity values of the hip to be relatively small. This is because larger elasticity values require larger active feedback gain (that is, larger gain P), which is liable to cause delay-induced instability. Regarding the hip viscosity value, Suzuki et al. (2012) set this value to be 10 for the double inverted pendulum model, so we decided it to be the same value. Despite setting the exploratory values of viscoelasticity for the ankle and knee, the model fell down easily with these values at ¡ 20 and 4, respectively.

Active joint torques for intermittent control

As for active joint torques (the third and fourth terms in eq. 2), we assumed three types of control theories for each joint: continuous-time, intermittent, and non-active control. Continuous-time control assumes the continuous active torques generated by linear PD feedback controllers with proportional (P_i) and derivative (D_i) gains and are conveyed with a feedback delay of $\Delta = 0.2$ s. Such simple neural controllers have been used in previous studies based on a single inverted pendulum model (Masani et al. 2003; Maurer and Peterka 2005; Van Der Kooij and De Vlugt 2007;

Vette et al. 2010). We set that the equilibrium points of joint angles and velocities are the origin of the phase plane because we deal with the divergence of the state point from the actual equilibrium generated by tonic activities of antagonist muscles. Regarding the active feedback gains (P and D), Suzuki et al. (2012) set P of the ankle and hip to be 0.4 and 0.6, respectively, and both D gains at 10 for the double inverted pendulum model of human quiet standing. We first found, in the preliminary study, that P values for the MP and hip were sensitive to the model stability, so we set these values based on a previous study by Suzuki et al. (2012). On the other hand, P values of the ankle and knee were less sensitive to the stability, thus, we selected arbitrary values, but close those from previous studies. In addition, although we also tested various D values ranging from 1 to 100 in the preliminary study, such change in D did not affect the model stability. Thus, we set the D values of 10 for all joints (Suzuki et al. 2012). Eight parameters of active feedback gains (P_i and D_i) used in this study were:

$$\begin{cases} (P_m, P_a, P_k, P_h) = (0.4, 0.3, 0.3, 0.6) \\ (D_m, D_a, D_k, D_h) = (10, 10, 10, 10) \end{cases} \tag{6}$$

On the other hand, non-active control means that no active torque works throughout the sampling duration (P_i and D_i to be zero in eq. 2). Intermittent control switches the active torque in an event-driven way as described in the following section. Because we found that the quadruple inverted pendulum could not be stabilized with continuous-time control for all joints in the preliminary examination, we investigated eighty pairs

(= 34 1) of joint control strategies (JCS) in this study.

The active torques were turned on and off by the CNS for the intermittent control. That is, when the active torques are turned on, the motion equation follows the eq. 2 with the viscoelastic parameters of eq. 3 and active feedback gain of eq. 4, and in the rest case, the third and fourth terms of eq. 2 is set to be zero. We assume that the switching surface, which is an on/off boundary of the active control, is based on stable and unstable manifolds of the system when all of the active torques are turned off (off model; the dynamics of the uncontrolled system). Although this idea of switching surface has not been validated physiologically, the idea that using the stable manifold of the off model to stabilize posture can avoid the postural instability due to time lag that takes for neural control. Hence, this idea gives biological benefits to the model from the aspect of control efficiency. To decompose the current state into the components of stable and unstable manifolds, we expressed eq. 1 as the state space representation:

$$\begin{cases} \dfrac{dy}{dt} = Ay \\ y = [\theta_m, ..., \theta_h, \omega_m, ..., \omega_h]^T \end{cases} \tag{7}$$

where y is a state variable vector consisted of four joint angles (θ) and four angular velocities (ω; derivative of each θ) and A is a state matrix of off model shown in Supporting Information (A2). After this transformation (eq. 5), the state space of the system was eight dimensional (determined by four joint angles and four angular velocities), which we referres to as θ - ω space. Another state space representation X = [x1,⋯,x8],

whose bases are eigen vectors of the system, is obtained from a linear mapping as follows:

$$X = V^{-1}y \tag{8}$$

where V is a transformation matrix from $\theta - \omega$ space to the new coordinate, which consists of the eight eigen vectors of the state matrix A. The new coordinate is useful for the intermittent control based on stable manifolds. The state space discussed in this study comprised a one-dimensional unstable manifold (whose real part of eigenvalue is positive, denoted by x_1) and a seven-dimensional stable manifold (whose real part of eigenvalues are negative, denoted by x_2 to x_8). We assume the inside of the switching surface (where off model is used) as follows:

$$|x_1| = \alpha\sqrt{|x_2|^2 + \cdots + |x_8|^2} \tag{9}$$

where α denotes the neighborhood of unstable manifold (the first row of the V). The intermittent control was turned off (no active torque) when eq. 7 is satisfied in terms of the dynamics of the uncontrolled system. We used two α values of 1/30 and 1/50. We found that values α of 1/10 and 1/100 were inappropriate to stabilize the quadruple inverted pendulum model in our preliminary analysis.

Simulation and analysis

We set the initial angular position [rad] as $[\theta_m, \theta_a, \theta_k, \theta_h] = [-0.02, 0.03, -0.005, 0.01]$, which is based on joint angle variability of our experimental data in our previous study (Tanabe et al. 2014), and the angular velocity

as zero for all joints. We executed computer simulations with some different initial values (even large values that violate the linearization of eq. 1) in the preliminary study, and obtained similar results to those in this study. We assume that the model was unstable when at least one of the angles is greater than $\pi/3$. Although this borderline of $\pi/3$ is outside of the linearization of eq.1, joint angles that were stable at this borderline fluctuated asymptotically towards zero (upright position), and thus, this borderline did not violate the linearization. The stability of the system can be analyzed mathematically by root loci of the model: the sign of the real parts of the system coefficient matrix' ' s eigenvalues represents the stability of the system. However, calculating eight eigenvalues of the system with delayed feedback is quite complicated. Instead, we decided the system to be leading to the equilibrium point insofar as the model does not fall down for more than 50 s. Thus, we detected the simulation trial during which the model keeps standing for 50.2 s as the provisional stability of the model (the additional 0.2 s are for the exclusion of the initial 0.2 s of data in the subsequent data analysis because no active torque is generated at this period due to delayed feedback).

Among 480 simulation trials ([VE, α, JCS] = 3·2·80), we searched the condition to meet the provisional stability of the model and extracted the pairs of joint control strategy for the postural stability. Then, we calculated the phase difference between two angular positions of adjacent joints by the Hilbert transformation to investigate the joint coordination under a variety of simulation parameters. The Hilbert transformation is originally introduced by Gabor (1946) and provides a true measurement of

the instantaneous phase and amplitude for a signal, s(t), via construction of an analytic signal, $\zeta(t)$, which is a complex function of time defined by:

$$\zeta(t) = s(t) + iH(t) = A(t)e^{i\phi(t)} \tag{10}$$

where H(t) is the Hilbert transform of s(t), and A and ϕ are the amplitude and the phase, respectively (Pikovsky et al. 2001). The phase of a signal represents the angular distance that the signal covered since the time origin and is obtained by:

$$\phi(t) = arctan(iH(t)/s(t)) \tag{11}$$

The numerical algorithms are available in the standard control design packages of Matlab; the function hilbert was used to obtain the results of this paper. The temporal phase transition between two adjacent joints, that is the continuous relative phase between two joint angle signals, was obtained by the subtraction of those phase time series. The distribution of joint coordination is then represented as a histogram of the time series of relative phase difference.

Thus far, we used the fixed values of active gain parameters (P_i and D_i) to investigate the contribution of passive joint viscoelasticity to joint coordination. Then we moved the feedback gain parameter P_i for each joint under some pairs of VE and JCS and examined the range of gain P that did not lead unstable posture for 50 s. These stability regions of feedback gain P_i (and D_i as well) represents the flexibility for CNS to control the upright posture; the wider the stability region is, the more robust the system is. The conditions, under which the stability region of

each joint's P was investigated, are shown in the Results section and the corresponding figures.

Comparison with experimental data

We measured the actual angular displacements of four lower limb joints during tiptoe standing experimentally from seven female participants (age = 24.1 ± 5.0 years, height = 160.8 ± 5.1 cm, body mass = 53.0 ± 7.9 kg). All experimental protocols and calculation method of joint angles are described in our previous study (Tanabe et al. 2014). In this simulation case, we set all initial angular positions and velocities to be zero and added Gaussian white noise. The second order equation of motion is written as the following ordinary delay differential equation:

$$\dot{y}(t) = f(y(t), t(t-\Delta)) + \sigma\xi(t) \tag{12}$$

where, $\xi(t)$ is a normal random process obtained by Matlab function randn, σ is the corresponding amplitude of 0.001, and Δ is the feedback delay time of 0.2s. Even when this white noise was added, the joints fluctuated with small amplitude under the condition for the model's stability (see Results in Fig. 6), and therefore again, the stability judgment of $\pi/3$ did not violate the linearization.

We performed computer simulation with noise for 30 pairs of simulation variables out of 480, in which inverted pendulum did not fall for 50 s (see Results). We compare the resultant angular displacements of four joints with those derived from experiment from the aspect of their amplitude and frequency characteristics. Both simulation and experimen-

tal data were down sampled to 1000 Hz and then we calculated power spectrum for each angular displacement.

Results

Control strategy for model's stabilization

u	JCS{u}	alpha	VE
1	[N C C I]	1/50	VE{1, 2}
2	[N C N I]		
3	[N C I I]		
4	[N N C I]		
5	[N N N I]		
6	[N N I I]		
7	[N I C I]		
8	[N I N I]		
9	[N I I I]		
10	[I C C I]	1/30	VE{2}
11	[I C N I]		
12	[I C I I]		
13	[I N C I]		
14	[I I C I]		
15	[I I N I]		
16	[I N N I]	1/30	VE{1}
		1/50	VE{3}
17	[I N I I]	1/30	VE{1, 2}
18	[I I I I]	1/30	VE{2}
		1/50	VE{3}

Table 2: Thirty pairs of simulation variables for provisional stability. Index u is for joint control strategy (JCS). Capital letters 'N', 'C', and 'I' represent the model is under no active control, continuous control, and intermittent control, respectively.

We implemented simulations of quadruple inverted pendulum under 480 different conditions (3 pairs of VE, 2 values of α, and 80 pairs of

JCS) and examined the conditions during which the model were stable for 50.2 seconds (provisional stability in this study) and the four segments' angles converge to zero asymptotically. We found that the model was provisionally stable for 30 conditions that are listed in Table 2.

As Table 2 indicates, the quadruple inverted pendulum stabilized only during hip was controlled intermittently and the MP joint must be controlled intermittently or passively. There are two findings here: first, intermittent feedback control is necessary for the stabilization of the quadruple inverted pendulum (at least the hip must be controlled intermittently), and second, there seems to be an appropriate switching surface (that is, the value of α) depending on joint viscoelasticity and/or joint control strategies.

Joint coordination and model variables

Next, we investigated joint coordination for the condition during which the model was stabilized (30 conditions in Table2). The Hilbert transformation was used to calculate the time series of relative phase between two adjacent joints, and then its distribution was plotted as a histogram. The tendencies of joint coordination observed by the histogram were investigated for all of the 30 conditions. Figure 2 represents two examples of relative phase distribution between MP-ankle (black), ankle-knee (brace), and knee-hip (gray). When the relative phase has the tendency of distribution around zero-phase bin or pi-phase bin, we decided the joint coordination to be in-phase or anti-phase, respectively. Although this is a qualitative classification, the difference between in-

phase and anti-phase was obvious for most of the conditions (like shown in Fig. 2). Then we counted the number of parameter conditions for each joint coordination pattern and calculated its ratio among the thirty conditions with which the model was stabilized.

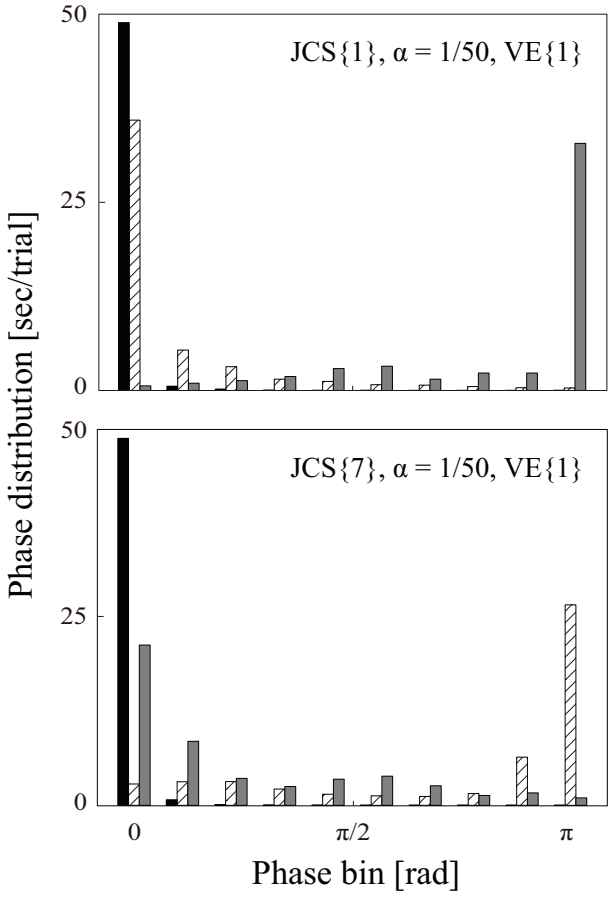

Figure 2: Two examples of phase distribution. Phase difference between two adjacent joints is separated into ten bins. The sum of each colored bar is 50 s (the whole trial length). Black, brace, and gray bars represent MP-ankle, ankle-knee, and knee-hip phase distributions, respectively. Each parameter conditions are shown in the top-right corner of each figure.

The majority of joint coordination (20 conditions; 66.7%) was as follows: [MP-ankle, ankle-knee, knee-hip] = [in-phase, in-phase, anti-phase] (shown in Fig. 2 top), followed by [in-phase, anti-phase, in-phase] (3

conditions; 10%, shown in Fig. 2 bottom) and [in-phase, in-phase, wide-range distribution] (3 conditions; 10%). The rest of the conditions showed the following joint coordination: [in-phase, wide-range, wide-range] for two conditions (6.7%), [anti-phase, in-phase, in-phase] for one condition (3.3%), and [in- or anti-phase, in-phase, anti-phase] for one condition (3.3%). Thus, joint coordination was affected by the passive viscoelasticity and/or joint control strategy.

Parameter sensitivity to postural robustness

We also investigated the stability region of feedback gain P for each joint in which the model can be stabilized with fixed values of K, B, and D. The wider this region, the wider choice of active feedback gain P for the CNS, so this region could represent the parameter sensitivity to postural robustness. Fig. 3 shows the stability region of feedback gain P_a with $JCS\{u\}$ of u = [1, 2, 3, 7, 8, 9], $\alpha = 1/50$, and $VE\{j\}$ of j = [1, 2]. The simulation data with $JCS\{u\}$ of u = [4, 5, 6] were excluded because the ankle was continuously switched off under these conditions. The stability region of the ankle gain P_a varied depending on joint control strategy and viscoelasticity. Smaller viscoelasticity of the ankle and knee ($VE\{2\}$) showed larger size of the region. Also, the stability region tended to be larger when the ankle was controlled intermittently compared with the continuous active control of ankle. In addition, the size of the region tended to be larger when the knee was controlled intermittently or given no active control ($JCS\{u\}$: u = [2, 3, 8, 9]) compared with continuous control for the knee ($JCS\{u\}$: u = [1, 7]).

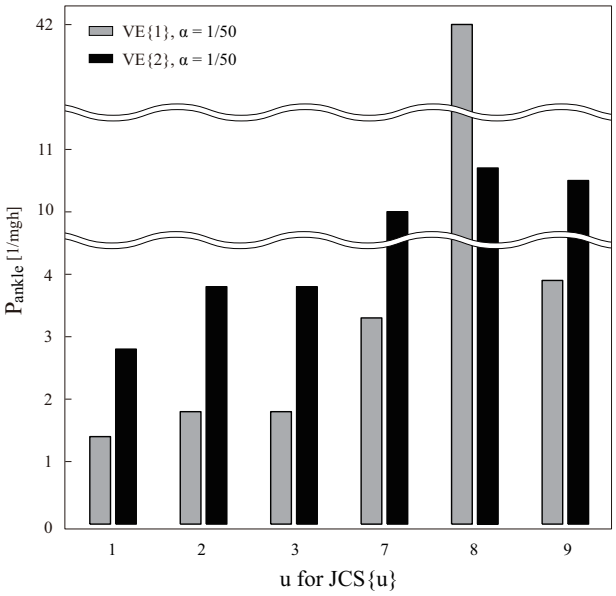

Figure 3: Stability region of the ankle gain P for six JCS pairs. Each $JCS\{u\}$ corresponds to the ones shown in Table 2. Gray and black bars represent two different viscoelasticity parameters shown in the top-left corner. The minimum P value was 0.1 for all conditions.

Fig. 4 shows the stability region of P for the knee (P_k) with $JCS\{u\}$ of u = [1, 3, 4, 6, 7, 9] and the same value of α (= 1/50) and $VE\{1, 2\}$ as Fig. 3. As with the case of the knee feedback gain, the size of its stability region was dependent on joint control strategy and viscoelasticity. Also, the size of the region tended to be larger when the knee was controlled intermittently ($JCS\{u\}$: u = [3, 6, 9]) compared with continuous control for the knee ($JCS\{u\}$: u = [1, 4, 7]). In this case, in contrast, larger viscoelasticity of the ankle and knee ($VE\{1\}$) showed larger size of the region.

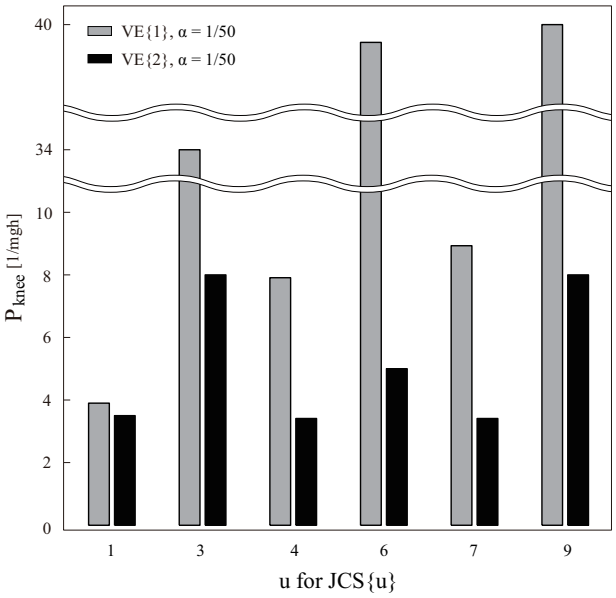

Figure 4: Stability region of the knee gain P for six JCS pairs. Each JCS$\{u\}$ corresponds to the ones shown in Table 2. Gray and black bars represent two different viscoelasticity parameters shown in the top-left corner. The minimum P value was 0.1 for all conditions.

On the other hand, we observed slightly smaller stability region of P_m and P_h (for the MP and hip, respectively) as shown in Fig. 5, which are the results of simulations with $JCS\{u\}$ of u = [10, $\cdots$, 18] in Table 2 where both MP and hip were intermittently controlled. These results indicate that the model parameters of the MP and hip were very sensitive to the postural stability compared with those for the ankle and knee. There existed some width of P_m and P_h for all of the nine JCS pairs with only $VE\{2\}$, suggesting that $VE\{2\}$ is the optimal to obtain the robustness of the MP and hip among the three VEs. This means that the difference in viscoelastic coefficients of the ankle and knee affected the robustness of the MP and hip.

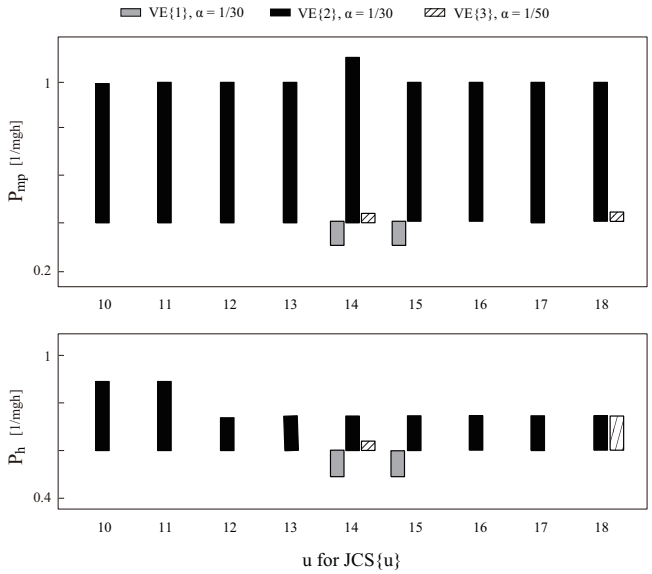

Figure 5: Stability region of the MP and hip gain P for nine JCS pairs. Top and bottom figures represent P regions for the MP and hip, respectively. Each $JCS\{u\}$ corresponds to the ones shown in Table 2. Gray, black, and brace bars represent three different pairs of viscoelasticity and alpha shown on the top.

Comparison with experimental data

Fig. 6 shows examples of angular displacements during tiptoe standing derived from simulation with noise and experiments. The amplitudes of each angular displacement for experiments and simulation data were θ_{exp} = [0.02 - 0.1, 0.03 - 0.09, 0.003 - 0.06, 0.02 - 0.15] and θ_{sim} = [0.01 - 0.35, 0.004 - 0.03, 0.002 - 0.03, 0.05 - 1.15] [rad], respectively. The scatter plots of sway amplitude and its standard deviation are shown in a supporting figure (A3). Some simulation data reproduced joint fluctuations with similar sway amplitude and variability to those from experiment. The animation of the simulation data (Fig. 6 left) can be available as a supporting material (A4). The left bottom of Fig. 6 represents the time series of on/off switching for intermittent control, and the distribution

of its on interval is shown in Fig. 6 right bottom. The intermittent on-interval (and off interval as well) was mostly distributed to < 0.02 seconds, which represent non-physiological high frequency component. There was another peak for only on-interval around 0.2 0.25 seconds. The power of these angular displacements is shown in Fig. 7 as logarithmic plots. The slope of the power spectrum was fitted to a third-order polynomial; its power law approximated a linear curve (the MP, ankle, and hip) or a polynomial curve (especially for the knee) for both simulation and experimental data.

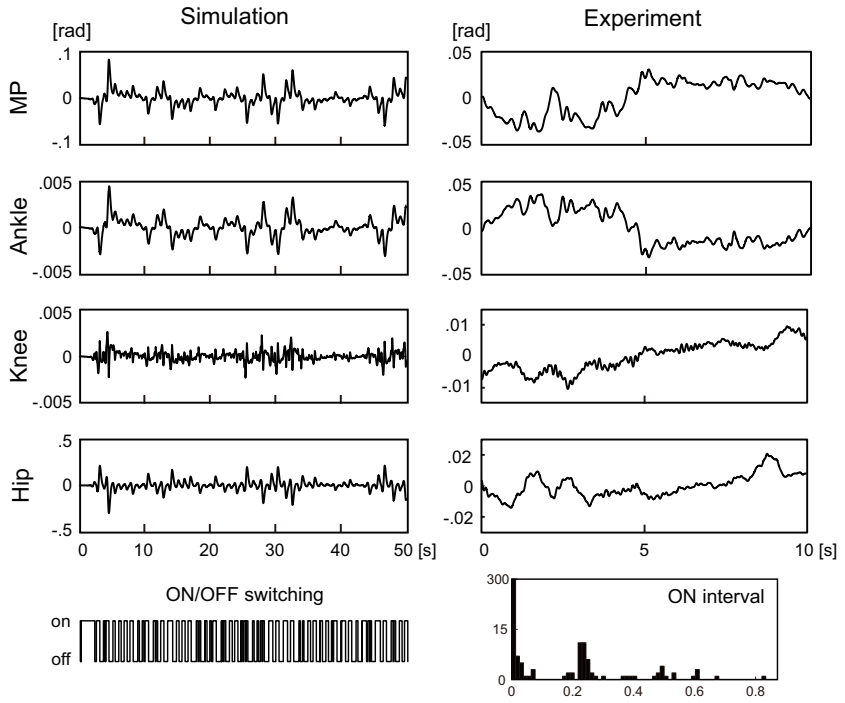

Figure 6: Joint angular displacements for simulation and experimental data. Left: time series for 50 seconds of the four joints' angular displacements obtained by simulation with Gaussian white noise. Intermittent switching of the active torque (on/off) is shown in the bottom. Right: experimentally observed four joints angular displacements during tiptoe standing for 10 seconds.

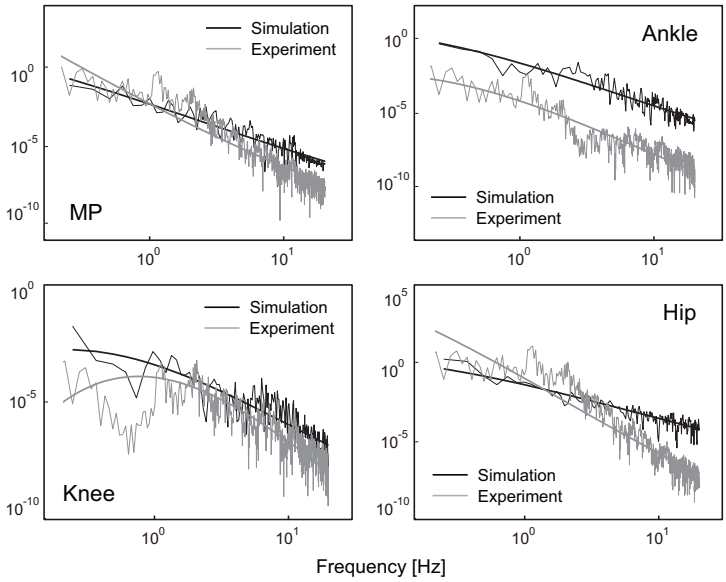

Figure 7: Comparison in the power spectrum of angular displacements between simulation and experiment. Black and gray lines are the logarithm plots of the power spectrum of each angular displacement for simulation and experiment, respectively. The power spectrum was shown up to 20 Hz, which is physiologically relevant range of frequency component of joint oscillations.

Discussion

The validity of the model

The purpose of this study was to investigate whether intermittent feedback control is necessary for the stabilization of the quadruple inverted pendulum as a model of human tiptoe standing in the sagittal plane. When we choose joint viscoelasticity parameters in this study, we set viscoelastic parameters of the MP and hip to be relatively small. This is because MP torque during tiptoe standing might be smaller, and because the approximation of the upper body segments into one HAT segment causes the model to destabilize more easily owing to the absence of mutual compensation between upper body segments, as is seen in the

actual human body segments. As a consequence of simulation with the parameters, which we selected, we obtained joint fluctuations whose amplitudes were similar to those from actual experiments (Fig. 6 and 7). We also calculated CoP location from the MP joint for simulation data. It was slightly ($<$ 0.5 - 1.5 cm) far from the actual location (about 3 cm from the MP) but it was entirely inside of the base of support (6 - 7 cm from the MP for women).

However, there are still some gaps between simulation and experimental data, especially in sway size of the hip (A3). The large sway size of the hip was obtained with some simulation parameter sets, which is possible in actual human tiptoe standing but such a large sway will be generally excluded from experimental data (and probably also by other researchers for quiet standing tasks) because it does not appear quiet. Thus, simulation data with a large body sway may reflect such experimentally excluded but practically possible body sway during tiptoe standing. We should also mention that the behavior of the model was determined not only by the control system but also by the noise properties, i.e., the noise can be selected such that the behavior is similar to experimentally obtained behavior. Although there are limitations to the model validation, the power law distribution of the simulation data had some degree of slope (Fig. 7) and it was not white-noise-like non-scaled flat PSD shape. Thus, the model behavior in this study was not significantly influenced by the noise.

The reason for the apparently less lowfrequency component of joint angles for simulation results (Fig. 6) may be that there was no restric-

tion for switching frequency. The switching intervals in this study were mostly distributed < 0.02 s (Fig. 6), which may cause non-physiologically fast components of joint fluctuations, leading to lower lowfrequency components than those which actually occur in humans. The modeling of intermittent timing strategy needs further investigation; however, we obtained the simulated joint angles similar to those during human tiptoe standing from the aspect of sway amplitude and power-law distribution. Although this is a qualitative similarity, we can conclude that we could partially reproduce joint fluctuations by simulation that is similar to those of experimental data.

The stability of the model was so sensitive to the joint viscoelasticity that small changes (approximately 1 10 %) caused the large sway of the inverted pendulum resulting in its falling down. Thus, the gaps with experimental data may be because of the simplicity of the inverted pendulum model, such as the approximation of the HAT segment or constant active feedback gain parameters. However, it is still important that we were able to stabilize the four-dimensional inverted pendulum for understanding the complicated human multi-segment postural control mechanism. Also, the essential result here is that simulation parameters used in this study affected the joint coordination and they were sensitive to the robustness of the inverted pendulum.

Intermittent control gives a degree of freedom of control strategy to the motor controller. Human motor performance, such as joint coordination can change by training or aging. In addition, alternate muscle activity, which is a neuromuscular level of switching between motor con-

trol strategies, has been reported experimentally and this phenomenon reduces mechanical stress or fatigue (Kouzaki and Shinohara 2006). In addition, there was a peak of distribution of on-interval around 0.2 0.25 s (Fig. 6), which indicates that active torques were switched off soon after delay-induced instability ($\tau = 0.2$ s) violates the stability of the model. As discussed in the following section, this study suggests that the switching of joint control strategies yielded by intermittent control is one of the factors that may produce plasticity or conversion of motor performance.

Simulation parameters and body fluctuations

The intermittent feedback control mechanism used in this study achieves nonlinear stability towards the equilibrium along stable manifolds during off-periods. Active control was utilized for pulling the state point back in the vicinity of stable manifolds and not for directly moving the state point towards equilibrium. This concept of stability is different from the classical one for linear system. However, it has recently been reported that human postural control mechanism adopted this type of intermittent strategy for the postural control in which antagonist muscle activities were measured (Asai et al. 2013). Although the definition of human postural stability needs further investigation, we assumed that this type of intermittent feedback control strategy was useful for acquiring postural stability of the model.

In this study, the quadruple pendulum with anthropometric parameters was stabilized for 30 pairs of parameters (VE, α, and JCS). Hips should always be controlled intermittently and the MP has to be under

no active control or intermittent control for all of those 30 stabilized conditions. This indicates that intermittent control was necessary at least for the hip control, which is an important finding to validate the need for intermittent control. Inside of the switching surface (when the current state's components of stable manifolds are dominant), we assumed the active torque to be zero, which is termed zero control (Gawthrop et al. 2014). Someone may imagine that zero control means all muscles associated with the sway of each joint have zero activation and that zero control is unrealistic. However, we should emphasize here that we consider the passive torque in our model to be involved in not only intrinsic stiffness and damping properties but also tonic muscle activities that are not related to the closed feedback loop, which are not influenced by equilibrium feedback loop.

The simulation parameter α in this study represents the switching surface of intermittent control, and the value range of α means the region of switching surface that stabilize the pendulum. We found that there were upper and lower limits of α that includes the values used in our simulations (α of 1/30 and 1/50) and this region of switching surface. Also, the region of switching surface was slightly shifted depending on viscoelasticity and joint control strategy (Table 2). Therefore, these results suggest that the region of switching surface might vary individually because of inherent viscoelastic properties and that it is possible to change the region of switching surface by learning different joint control strategies to accomplish the desired task.

Joint coordination during standing has plasticity and training could

change ankleknee joint coordination during tiptoe standing from in-phase to anti-phase (Tanabe et al. 2014). The ankle-hip anti-phase relationship was reduced during quiet standing, as a result of aging (Kato et al. 2014). A majority of joint coordination in our simulation was [MPankle, ankleknee, kneehip] = [in-phase, in-phase, anti-phase] (71 %) or [in-phase, anti-phase, in-phase] (16 %). The former coordination pattern is consistent with our experimental data (Tanabe et al. 2014). Although we were not able to find any regularity in the relationship between joint coordination patterns and simulation parameters, our results suggest that the changes in passive joint viscoelasticity or active joint control strategy, through training or aging, might be factors of the plasticity of joint coordination during human bipedal standing.

Parameter sensitivity to the robustness of the model

We investigated the parameter sensitivity to the robustness of the model by the stability region of active gain parameters P as degrees of CNS flexibility for postural control. Asai et al. (2009) and Suzuki et al. (2012) demonstrated the difference in the area of this stability region (in PD coordinate system) depending on the location of switching boundary and passive hip stiffness, respectively. Our study further revealed that joint control strategies (intermittent, continuous, or only passive) could affect the robustness of the inverted pendulum model. This implies the possibility that humans can acquire the stability of tiptoe standing via learning not only the optimal switching boundary but also the optimal joint control strategy, which leads our postural control strategy to more

robust manner.

Fig. 3 showed that the stability region of P_a varied depending on joint control strategies and passive joint viscoelasticity. First, the smaller viscoelasticity of the ankle and knee showed the larger P_a stability region (black vs. gray bars for each JCS). However, extremely small viscoelasticity intimidated the stability of the inverted pendulum, and the P_a stability region was actually smaller for the smallest viscoelasticity parameters ($VE\{3\}$), suggesting that an optimal viscoelasticity could maximize the stability region, and that the joint robustness varies individually depending on his or her joints' viscoelastic properties. In addition, the P_a stability region tended to be larger when the ankle was controlled intermittently rather than by continuous control ($JCS\{[1,2,3]\}$ vs. $JCS\{[7,8,9]\}$). It also tended to be large when the knee was controlled intermittently or with no active control ($JCS\{[2,3,8,9]\}$ vs. $JCS\{[1,7]\}$). Although it might be difficult to change passive joint viscoelasticity properties to acquire greater robustness, it may be possible to enhance the robustness by optimizing the joint control strategy through training. The fact that intermittent control leads to more robust posture might support the biological plausibility of the intermittent control model for multi-link inverted pendulum as a model of human standing.

The result of P_k region (Fig. 4) will reinforce the discussion above. The P_k region was also dependent on joint control strategy and viscoelasticity; the size tended to be large when the knee was controlled intermittently, and the larger viscoelasticity of the ankle and knee led the larger stability region. Again, there might be optimal viscoelasticity for each

mechanical body configuration, and we can maximize the robustness by learning the optimal joint control strategy and switching boundary depending on our own joint viscoelasticity. Also, the viscoelasticity of the ankle and knee affected their P regions mutually: the control strategy of the knee affected the ankle robustness, and vice versa. This is an interesting result that mathematically showed the interaction between multi-segments involving mutual robustness.

On the other hand, the size of P_m and P_h stability regions are considerably small (Fig. 5), suggesting that the proportional gains for the MP and hip joints were limited to acquire the stability of these joints. The small size of P_m might be because the MP is the lowest joint; its fluctuation affects all the joints above it. Table 2 shows that we can choose no active control for the MP joint apart from intermittent control. Therefore, it would be reasonable not to control MP joint actively rather than exerting intermittent control by carefully selecting its feedback gain parameter. On the other hand, the HAT segment is almost half the length of the human body and thus, the location of HAT segment's center of mass might be high enough to destabilize the body at the hip joint, with a small change in active gain parameters. There is no choice to control the hip intermittently for the stability of the inverted pendulum (Table 2). Thus, CNS should select an appropriate P_h value rigorously according to the other joints' viscoelasticity, switching boundary, and joint control strategies. Our result suggests that most of the attention among the four joints should be given to the hip to control tiptoe standing.

Conclusion

In this study, we were able to generate fluctuations of quadruple inverted pendulum that are similar to those of four lower limb joints during tiptoe standing. We conclude that the intermittent feedback control was necessary for the stabilization of the quadruple inverted pendulum as a model of human tiptoe standing, which is an intrinsically unstable posture. At least the hip control must be controlled intermittently. Furthermore, changes in joint viscoelasticity and joint control strategies affect postural robustness accompanying the change in joint coordination. This study also provides an insight for the improvement of the performance of tiptoe standing from the aspect of postural robustness.

Appendix

A1. Model definition

$$
\begin{aligned}
M_{11} &= I_1 + I_2 + I_3 + I_4 \\
&\quad + r_1^2 m_1 + l_1^2 m_2 + 2 l_1 m_2 r_2 + r_2^2 m_2 \\
&\quad + l_1^2 m_3 + 2 l_1 m_3 l_2 + 2 l_1 m_3 r_3 + l_2^2 m_3 + 2 r_3 m_3 l_2 + r_3^2 m_3 \\
&\quad + l_1^2 m_4 + 2 l_1 m_4 l_2 + 2 l_1 m_4 l_3 + 2 l_1 m_4 r_4 + l_2^2 m_4 \\
&\qquad + 2 l_2 m_4 l_3 + 2 l_2 m_4 r_4 + l_3^2 m_4 + 2 r_4 m_4 l_3 + r_4^2 m_4 \\
M_{12} &= I_2 + I_3 + I_4 \\
&\quad + l_1 m_2 r_2 + r_2^2 m_2 \\
&\quad + l_1 m_3 l_2 + l_1 m_3 r_3 + l_2^2 m_3 + 2 l_2 m_3 r_3 + r_3^2 m_3 \\
&\quad + l_1 m_4 l_2 + l_1 m_4 l_3 + l_1 m_4 r_4 + l_2^2 m_4 \\
&\qquad + 2 l_2 m_4 l_3 + 2 l_2 m_4 r_4 + l_3^2 m_4 + 2 r_4 m_4 l_3 + r_4^2 m_4 \\
M_{13} &= I_3 + I_4 \\
&\quad + l_1 m_3 r_3 + l_2 m_3 r_3 + r_3^2 m_3 \\
&\quad + l_1 m_4 l_3 + l_1 m_4 r_4 + l_2 m_4 l_3 + l_2 m_4 r_4 + l_3^2 m_4 + 2 r_4 m_4 l_3 + r_4^2 m_4 \\
M_{14} &= I_4 + l_1 m_4 r_4 + l_2 m_4 r_4 + l_3 m_4 r_4 + r_4^2 m_4 \\
M_{21} &= I_2 + I_3 + I_4 \\
&\quad + r_2 m_2 l_1 + r_2^2 m_2 \\
&\quad + l_2 m_3 l_1 + l_2^2 m_3 + r_3 m_3 l_1 + 2 r_3 m_3 l_2 + r_3^2 m_3 \\
&\quad + l_2 m_4 l_1 + l_2^2 m_4 + 2 l_2 m_4 l_3 + 2 l_2 m_4 r_4 \\
&\qquad + l_3 m_4 l_1 + l_3^2 m_4 + r_4 m_4 l_1 + 2 r_4 m_4 l_3 + r_4^2 m_4 \\
M_{22} &= I_2 + I_3 + I_4 \\
&\quad + r_2^2 m_2 \\
&\quad + l_2^2 m_3 + 2 l_2 m_3 r_3 + r_3^2 m_3
\end{aligned}
$$

$$
\begin{aligned}
&+ l_2^2 m_4 + 2 l_2 m_4 l_3 + 2 l_2 m_4 r_4 + l_3^2 m_4 + 2 r_4 m_4 l_3 + r_4^2 m_4 \\
M_{23} &= I_3 + I_4 \\
&+ l_2 m_3 r_3 + r_3^2 m_3 \\
&+ l_2 m_4 l_3 + l_2 m_4 r_4 + l_3^2 m_4 + 2 r_4 m_4 l_3 + r_4^2 m_4 \\
M_{24} &= I_4 + l_2 m_4 r_4 + l_3 m_4 r_4 + r_4^2 m_4 \\
M_{31} &= I_3 + I_4 \\
&+ r_3 m_3 l_1 + r_3 m_3 l_2 + r_3^2 m_3 \\
&+ l_3 m_4 l_1 + l_3 m_4 l_2 + l_3^2 m_4 + r_4 m_4 l_1 + r_4 m_4 l_2 + 2 r_4 m_4 l_3 + r_4^2 m_4 \\
M_{32} &= I_3 + I_4 \\
&+ r_3 m_3 l_2 + r_3^2 m_3 \\
&+ l_3 m_4 l_2 + l_3^2 m_4 + r_4 m_4 l_2 + 2 r_4 m_4 l_3 + r_4^2 m_4 \\
M_{33} &= I_3 + I_4 \\
&+ r_3^2 m_3 + l_3^2 m_4 + 2 r_4 m_4 l_3 + r_4^2 m_4 \\
M_{34} &= I_4 + r_4 m_4 l_3 + r_4^2 m_4 \\
M_{41} &= I_4 + r_4 m_4 l_1 + r_4 m_4 l_2 + r_4 m_4 l_3 + r_4^2 m_4 \\
M_{42} &= I_4 + r_4 m_4 l_2 + r_4 m_4 l_3 + r_4^2 m_4 \\
M_{43} &= I_4 + r_4 m_4 l_3 + r_4^2 m_4 \\
M_{44} &= I_4 + r_4^2 m_4 \\
G_{11} &= -g(r_1 m_1 + l_1 m_2 + l_1 m_3 + l_1 m_4 + r_2 m_2 \\
&+ l_2 m_3 + l_2 m_4 + r_3 m_3 + l_3 m_4 + m_4 r_4) \\
G_{12} &= -g(r_2 m_2 + l_2 m_3 + l_2 m_4 + r_3 m_3 + l_3 m_4 + m_4 r_4) \\
G_{13} &= -g(r_3 m_3 + l_3 m_4 + m_4 r_4) \\
G_{14} &= -g m_4 r_4 \\
G_{21} &= -g(r_2 m_2 + l_2 m_3 + l_2 m_4 + r_3 m_3 + l_3 m_4 + m_4 r_4) \\
G_{22} &= -g(r_2 m_2 + l_2 m_3 + l_2 m_4 + r_3 m_3 + l_3 m_4 + m_4 r_4)
\end{aligned}
$$

$$G_{23} = -g(r_3 m_3 + l_3 m_4 + m_4 r_4)$$

$$G_{24} = -g m_4 r_4$$

$$G_{31} = -g(r_3 m_3 + l_3 m_4 + m_4 r_4)$$

$$G_{32} = -g(r_3 m_3 + l_3 m_4 + m_4 r_4)$$

$$G_{33} = -g(r_3 m_3 + l_3 m_4 + m_4 r_4)$$

$$G_{34} = -g m_4 r_4$$

$$G_{41} = -g m_4 r_4$$

$$G_{42} = -g m_4 r_4$$

$$G_{43} = -g m_4 r_4$$

$$G_{44} = -g m_4 r_4$$

where I_i, m_i, l_i, and r_i represent the ith segment's inertia moment of around the distal end, the mass, the length, and the length between the distal end and center of mass, respectively.

A2. First order differential equation of off model

The passive joint torque in the motion equation (eq. 1) can be represented as follows:

$$Q = -[diag(K)\ \ diag(B)] \cdot y$$

where K and B are vectors of elastic and viscosity components, respectively, and y is the state variable vector consisted of four joint angles and four velocities (eq. 5 in Sect. 2.3). The expression diag(v) is a diagonal matrix composed by vector v.

Therefore, the motion equation (eq. 1) with no active torque (off model) can be written as a following eight-dimensional ordinary first order

differential equation:

$$\begin{bmatrix} E & O \\ O & M \end{bmatrix} \cdot \frac{dy}{dt} = \begin{bmatrix} O & E \\ -diag(K) + G & -diag(B) \end{bmatrix} \cdot y$$

where E is a 4-by-4 unit matrix. This elicits the coefficient matrix A in eq. 5 as follows:

$$A = \begin{bmatrix} E & O \\ O & M \end{bmatrix}^{-1} \begin{bmatrix} O & E \\ -diag(K) + G & -diag(B) \end{bmatrix}$$

A3. Scatter plots of sway amplitude and its standard deviation for the comparison between simulation and experimental data.

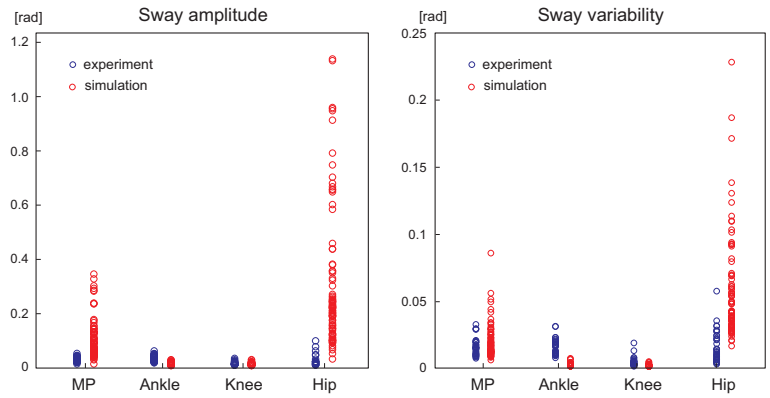

Figure A3: Left and right figures represent sway amplitude and its standard deviation (variability) of the four joints, respectively, from experiment (blue; 35 trials from 7 subjects) and simulation (red; 30 conditions in Table 2 with three different white noise; 90 trials in total).

STUDY5
Phasic muscle activation and its function: Intermittent feedback control of quiet standing

Abstract

Human upright posture is controlled both passively and actively for resisting against the gravitational toppling torque that expose to the body, which is mechanically leaning forward during quiet standing. Active feedback control via the central nervous system includes intermittent system, which plays an important role to the stabilization dynamics in the vicinity of the equilibrium. However, it is still unknown the intermittent control strategy at the muscular level, and the functions of intermittent muscle activity to control input (i.e., torque generation). Thus, in this study, we investigated the relationship between timing of intermittent muscle activity and joint fluctuation (i.e., location of the state point in the phase space) and between intermittent muscle activity and joint torque output. Eight healthy male participants stood quietly on the force platform for 120 sec, while we measured angular displacements and joint torque of the ankle, knee, and hip in the sagittal plane. Surface electromyography from six leg muscles of both legs were also recorded to determine phasic muscle activation (on-period) and inactivation (off-period) for each muscle by using two low-pass filters. We found that muscle activation and inactivation periods related to the current joint position

and velocity, and that intermittent muscle activities were associated with torque fluctuations in anatomical action direction. These results suggested that intermittent muscle activation/inactivation are triggered by the state point location in the phase space, leading to joint actuation via torque generation along with anatomical action direction, which is a function of intermittent muscle activity.

Introduction

Human multi-joint body is controlled both passively and actively to maintain upright posture, which is mechanically leaning forward and is always exposed to gravitational force. The passive stiffness caused by joint viscoelasticity of the muscle-tendon-ligament is insufficient to compete with the gravitational toppling torque during quiet standing (Loram and Lakie 2002a; Casadio et al. 2005). This leads human upright posture to be an unstable equilibrium of saddle type in multi-dimensional state space, in which the state point converges to the equilibrium along stable manifolds and diverges away from the equilibrium along unstable manifolds as time elapses. Therefore, human bipedal standing should be actively controlled through integrated sensory cues from the visual, vestibular, and somatosensory systems (Peterka 2002).

Generally, human motor control systems must include continuous and intermittent processes incorporating discrete switching. Continuous systems integrate visual, vestibular, and somatosensory information, represented by the spinal and transcortical reflexive pathways, and provide high-bandwidth feedback at short latency (Brookes 1986; Rothwell

1994; Pruszynki and Scott 2012). Intermittent systems exist within the basal ganglia, prefrontal cortex, and premotor cortex and provide low-bandwidth feedback at longer latency (Redgrave et al. 1999; Cisek and Kalasla 2005; Dux et al. 2006). In the context of human bipedal standing, continuous system, involving muscle spindle and Goldi tendon organ feedback, provide tonic equilibrium joint moments via tonic stretch reflexes (Sherrington 1947) and partial dynamic stabilisation in the unstable state space (Marsden et al. 1981; Fitzpatrick et al. 1996; Loram and Lakie 2002a,b). However, the continuous control strategy itself is insufficient to regulate the dynamics of the postural system (Marsden et al. 1981), and intermittency of the postural control mechanism plays an important role to the stabilization dynamics in the vicinity of the equilibrium.

Regarding the control mechanism of such unstable postural system, impedance control, which resists destabilizing motion by regulating co-activation levels of antagonist muscles, has been proposed in the field of neuroscience (Hogan 1984; 1985). The CNS stabilizes unstable dynamics by learning optimal impedance, in which antagonist muscles co-activate in a preprogrammed manner (Burdet et al. 2001; Franklin et al. 2007). Such a feed-forward, non-reactive control decreases a risk of delay-induced instability and enhances the robustness to internal or external perturbations. However, this strategy has a trade-off that increasing impedance causes high metabolic cost consumed by muscle co-activations. This is critical for maintaining postural stability as a fundamental human activity (Weyand et al. 2009). Internal model could optimize such trade-off for modulating the relation between motor command and movement during

human bipedal standing (Gomi and Kawato 1993; Morasso et al. 1999).

Asai et al. (2013) demonstrated that some of their participants adopted a discontinuous, intermittent strategy for a virtual pendulum-balancing task using an EMG-based human-computer interface. They observed "on-periods" and "off-periods" in the antagonist muscle activations, which represent muscle activation and inactivation, respectively, among phasic component of EMG signals. The extraction methodology used in their study has possibility to investigate the direct relationship between intermittent muscle activities and joint motion/torque output, however, their experimental task was far from natural quiet standing (i.e., it was based on postural control of a inverted pendulum only with two shank muscles) and only two muscles were examined. Nomura et al. (2007) have reported the methodology that decomposes EMG signals from soleus muscle during quiet standing into tonic and phasic, intermittent components by using two low-pass filtering, and this methodology may be applied to extract intermittent activations of other muscles.

Joint movement during quiet standing shows stochastic fluctuation, which is unavoidable during postural fixation. Whether these stochastic, intermittent fluctuations have any functional role has been being attention (Stephen and Mirman 2010; Engbert et al. 2011). Because multi-joint of the body is actuated by muscle activities, the nature of the function of intermittency of joint fluctuations could exist in the intermittent muscle activities and emerge as a torque output that is a control output of postural control feedback loop. Therefore, in this study, we aimed to elucidate the origin and function of intermittent muscle activity

during quiet standing. To do so, we investigated the relationship between timing of intermittent muscle activity and joint fluctuation (i.e., location of the state point in the phase space) and between intermittent muscle activity and joint torque output.

Materials and Methods

Ethics statement

All procedures used in this study were in accordance with the Declaration of Helsinki and were approved by the Ethics Committee of the Graduate School of Human and Environmental Studies at Kyoto University. The approval was based on an appropriate risk/benefit ratio and a study design wherein the risks were minimized. All procedures were conducted in accordance with the approved protocol. The individuals participating in this study has given written informed consent to participate in this study and to publish these case details. Informed consent continued throughout the study via a dialog between the researcher and participants.

Experimental protocol and measurement

Eight healthy males (age, 22.3 ± 1.7 year; height, 170.9 ± 7.9 cm; body mass, 63.5 ± 5.7 kg) participated in this study. None of the participants had a significant medical history or signs of gait, postural, or neurological disorders, and no one had vision problems.

Participants were instructed to stand quietly with their eyes open and to look at a fixed point on a plain wall about 1.5 m ahead of them. They

stood on a force platform (EFPA1.5kNSA13B, Kyowa, Tokyo, Japan) and kept standing for 120 sec. We collected five trials data for each participant with sufficient rest between trials (about a few minutes). Participants held their arms comfortably by their sides with their feet were stuck together. One split (600 g) was strapped to the back of the participant at the forehead, chest, and pelvis for ensuring correct triple inverted pendulum model approximation of quiet standing by allowing joint motions to occur around the ankle, knee, and hip joints. Although this restriction could disturb the natural characteristics of quiet standing, we used it to measure the motion of a three-segmented body without ambiguity.

Joint motion data was obtained with a three-dimensional (3D) optical motion capture system (OptiTrack V100:R2; NaturalPoint, Corvallis, OR) composed of twelve infrared cameras in a semicircular arrangement. Spherical reflective markers, 13 mm in diameter, were affixed to the lateral side of fifth metatarsophalangeal (MP), ankle (lateral malleolus), knee (lateral condyle of femur), hip (greater trochanter), anterior superior iliac spine (ASIS), and shoulder (acromion) on the both sides of the participants ' body. We also placed one reflective marker on the reference point of the force platform to make coordinate system of the platform agree with that of motion capture system. The kinematic signals were sampled at a rate of 100 Hz and stored on the hard disk of a personal computer for later off-line analysis.

Surface electromyography (EMG) from the skin surface over the rectus femoris (RF), long head of biceps femoris (BFL), medial gastrocnemius (MG), lateral gastrocnemius (LG), soleus (SOL), tibialis anterior

(TA) were recorded from both legs with Ag-AgCl electrodes of 5 mm and an interelectrode distance of 20 mm. To minimize the cross talk between adjacent muscles, we first ascertained the location of the abdomen of each muscle by using an ultrasound method for attaching electrodes. After careful shaving and abrasion of the skin, the electrodes were placed over the abdomen of muscles. The reference electrode for EMG was placed over the lateral malleolus of left leg. The electrodes were connected to a preamplifier and a differential amplifier with a bandwidth of 5-1000 Hz (MEG6116M, Nihonkohden, Tokyo, Japan). All EMG signals were stored with a sampling frequency of 2000 Hz on the hard disk of a personal computer using a 16-bit analog-to-digital converter (PowerLab/16SP, ADInstruments, Sydney, Australia). Data processing was done with Matlab (MathWorks, USA).

Data analysis

Time series of kinematics data (each marker data) and the displacement of center of pressure (CoP) from the MP joint of 120 sec were passed through a second-order Butterworth low-pass filter with cutoff frequency of 20 Hz ($filtfilt$ function in the Matlab signal processing toolbox). The standing body was modeled as a triple inverted pendulum consisting of three rigid segments, i.e., shank, thigh, and head-arm-trunk (HAT). The coordinates of the MP, ankle, knee, and top end of HAT were determined by the middle points of markers affixed on the both sides of the MP, ankle, knee, and shoulder, respectively. Coordinate of the hip was calculated by using the maker location data of greater trochanter and

ASIS (Kurabayashi et al. 2003). We then computed the segment lengths (MPankle, ankleknee, kneehip, and HAT) and joint angles (q_a, q_k, and q_h, where subscripts 'a', 'k', and 'h' stand for the ankle, knee, and hip, respectively) in the sagittal plane. The angular velocities and angular accelerations were computed by numerically differentiating the angular displacement data with a three-point central difference formula (Winter 1990). Joint torques (T_a, T_k, and T_h) were calculated by inverse dynamics using vertical grand reaction force. The calculation procedures for joint angles and torques are presented in Appendix A. Joint angles and torques were defined as positive in extension.

All EMG signals were first numerically rectified and processed by the second order Butterworth low-pass filter with a cutoff frequency of 12 Hz (iEMG). We determined phasic on/off switching of muscle activity (activation/inactivation) from EMG data by using two low-pass filtered EMG signals, each of which represents phasic/tonic component of muscle activations based on Asai et al. (2013). The second order Butterworth low-pass filter with a cutoff frequency of 0.02 Hz was applied to all iEMG signals to obtain trend curves, which represent tonic muscle activity components. This cutoff frequency of 0.02 was selected based on the following two reasons. First, the cross-correlation between the center of mass (CoM) and low-pass filtered EMG of SOL during quiet standing was the highest when its cutoff frequency ranged between 0.02 and 0.06 Hz (Nomura et al. 2007). Second, the findings in this study were not affected by this cutoff frequency when we changed it to 0.01 or 0.05 Hz. We also obtained smoothed iEMG signals by applying the second order

Butterworth low-pass filter with a cutoff frequency of 2 Hz. We assumed that the trend curve subtracted from these smoothed iEMG signal represents phasic muscle activation. If the smoothed iEMG was above the trend curve for a time interval, we considered that the muscle activity was high in that interval. In this way, we obtained time intervals in which the muscle activity was high. Then, for each interval with high muscle activity, we further computed the maximum value of the smoothed iEMG. If half of the maximum value was greater than the trend curve, it was defined as the threshold of the interval. Otherwise, the trend curve itself was defined as the threshold of the interval. We determined the threshold curve by performing this procedure for every interval with high muscle activity.

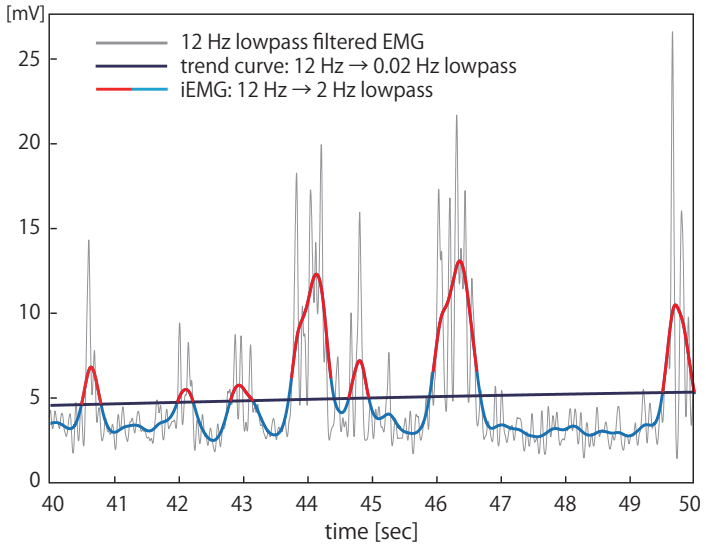

Figure 1: Muscle activation/inactivation (on/off) discrimination. Sample EMG signal is shown. Gray plot represents 12 Hz low-pass filtered EMG signal after full wave rectification. Dark blue plot is a trend curve, which is 0.02 Hz low-pass filtered EMG signal. 2 Hz low-pass filtered iEMG signal is consisted of red and light blue curves, which represent muscle activation and inactivation, respectively.

An example of on/off periods determined by a single iEMG signal is shown

in Figure 1. We believe that this cutoff frequency of 2 Hz was validate for detecting phasic muscle activations because the shape of each on/off period was mainly unimodal or bimodal, representing a fact that we could successfully extract each on/off period as a single smooth curve.

We then investigated the information that triggers muscle phasic on/off switching by dividing the dynamics (time history) of a state point in the phase planes of ankle, knee, and hip joints into on and off periods for each 12 muscles. We call these areas as on area and off area, and an example is shown in Figure 2. Each on/off area was fit into a second order mixed Gaussian distribution for every muscle (Fig 2, middle), and we plotted their centers in the phase planes for all trials (Fig 2, right). In the same way, we examined the distribution of on/off area in the torque plane of the ankle, knee, and hip (torque vs. torque velocity) for each muscle by fitting them to mixed Gaussian distributions and calculated their centers.

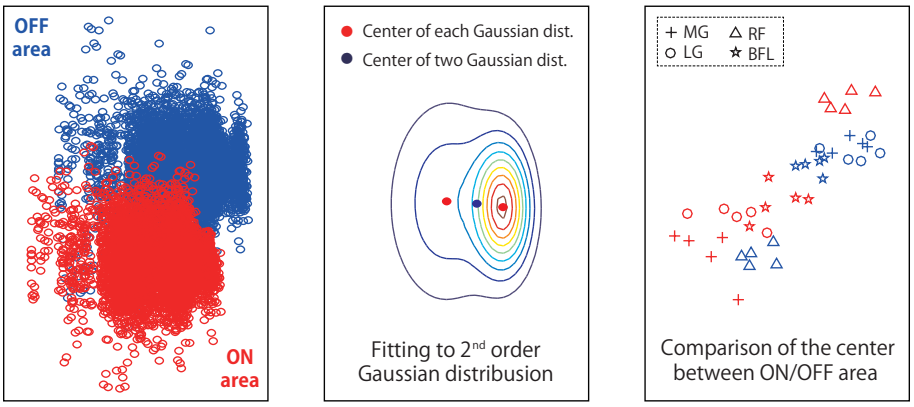

Figure 2: Mixed Gaussian distribution fitting of on/off area. Left: sample distribution of on/off area during a 120-sec trial. Middle: Example of a mixed (2nd order) Gaussian distribution. Two red points and one blue point represent each center of two Gaussian distributions and their center, respectively. Right: examples of the distribution of on/off centers in the knee torque plane for five

trials of one participant. Symbols of +, ○, △, and ☆ were for on/off area of MG, LG, RF, and BFL, respectively. Red and blue symbols represent on and off area centers for each muscle, respectively.

We further investigated the similarity between actual dynamics of state point based on phasic on/off muscle activities and dynamics in the phase space of a triple inverted pendulum without active feedback control. In the concept of intermittent feedback control strategy (e.g. Asai et al. 2009), the state point is assumed to move towards the equilibrium along stable manifolds during off period, and to run counter to the dynamics and go back in the vicinity of stable manifolds when it is diverging away from the equilibrium along unstable manifolds during on period. The motion of a triple inverted pendulum mimics the human upright posture in the sagittal plane during quiet standing in this study. Three segments of the pendulum represent shank, thigh, and head-arm-trunk segments. The motion equation of the triple inverted pendulum can be linearized as follows because joint angles and velocities are small during quiet standing, allowing us to neglect the second and higher order term:

$$M\ddot{\theta} + G\theta = T \tag{13}$$

where θ is a joint angle vector, M the inertia matrix, $G\theta$ the gravitational toppling torque vector, and T the joint torque vector. Eq. 1 can be expressed as the state space representation:

$$dx/dt = Ax \tag{14}$$

where x is a state variable consisted of three joint angle (θ) and three angular velocities (ω): $x(t) = (\theta(t), \omega(t))^T$ at a time instant t, and A is a

state matrix of off period (without any active feedback control). Matrices M and G in eq. 1 determine state matrix A, and they were calculated by using Japanese anthropometric parameters shown in Table 1 (Ae et al. 1992). The definitions of these two matrices and the state space representation of the motion equation are described in Appendix B. The eigen values and eigen vectors of state matrix A determine the dynamics of the state point in the phase space. The pendulum should be governed by the saddle type vector field defined by Ax without any control input. As a parameter of similarity between the dynamics of a triple inverted pendulum and actual dynamics of state point from experiment data, we calculated directional cosine (DC) during a course of 120 sec of quiet standing as follows:

$$DC = \frac{v_{exp}(t) \cdot v_{saddle}(t)}{|v_{exp}(t)||v_{saddle}(t)|} \tag{15}$$

where $v_{exp}(t)$ is defined as $x(t+\Delta)x(t)$ for experimentally obtained data and $v_{saddle}(t)$ is $Ax(t)$ (Bottaro et al. 2008). The numerator is the inner product of $v_{exp}(t)$ and $v_{saddle}(t)$. We set Δ to be 0.1 sec in this study. Notice that if the actual movement of state point follows the dynamics of the phase space of saddle type, DC would become unity. In this study, we calculated DC at every event of on-point (at instant from off to on period) and off-point (on to off period) for each trial and made it into a histogram to investigate the similarity between the dynamics of phase space of saddle type and actual behavior of state point.

Body mass [kg]	for each subject
Segment length [m]	
Segment mass ratio [%body mass]	[10.2, 22.0, 67.8]
Segment center of mass ratio [%]	[40.6, 47.5, 49.3]
Gyration radius ratio [%]	[27.4, 27.8, 34.6]
Elastic component $[K_a, K_k, K_h]$	[0.8, 0.5, 0.5]$\cdot$ mgh
Viscosity component $[B_a, B_k, B_h]$	[4, 10, 10]

Table 1: Anthropometric parameters of a triple inverted pendulum. Three values of each line (except for body mass and segment length) are for shank, thigh, and HAT segments from the left. Segment center of mass ratio is with respect to segment length from the upper end. Gyration radius is relative to frontal (mediolateral) axis and the presented as percentage of each segment length.

Statistical analysis

To determine the distribution of the center of mixed Gaussian distribution in the phase plane or torque plane, we conducted one sample t-test for coordinates (angular displacement/torque and angular velocity/torque velocity) of on/off area centers from five trials for each muscle. Significant levels of differences between five-sample data and zero value (i.e. significant distance from x or y axis) were tested using ttest in the statistical toolbox of Matlab. The statistical significance threshold was set at $p = 0.05$.

Results

Switch timing: on/off area in the phase plane

We calculated the center of mixed Gaussian distribution for each on/off area in the phase plane to investigate the trigger information between muscle activation and inactivation. Figure 3 shows 80 samples

(from 8 subject of 5 trials, both legs) of on-area center (red) and off-area center (blue) for each muscle in the phase planes of the ankle (top), knee (middle), and hip (bottom) joints. Gastrocnemius muscles (MG and LG) tended to activate when the state point located in dorsiflexion of the ankle and extension of the knee and to inactivate when it located in planterflexion of the ankle and flexion of the knee. Similarly, SOL activation and inactivation tended to occur when the state point located in dorsiflexion and planterflexion of the ankle, respectively. In contrast, TA activated and inactivated when the ankle had position and velocity in planterflexion and dorsiflexion, respectively. RF and BFL also tended to activate in knee flexion and extension, respectively, and to inactivate vice versa. In addition, although triceps surae muscles do not directly (anatomically) actuate the hip joint, their on/off area was isolated in the hip phase plane, and they activated and inactivated when the hip fluctuated in backward and forward, respectively.

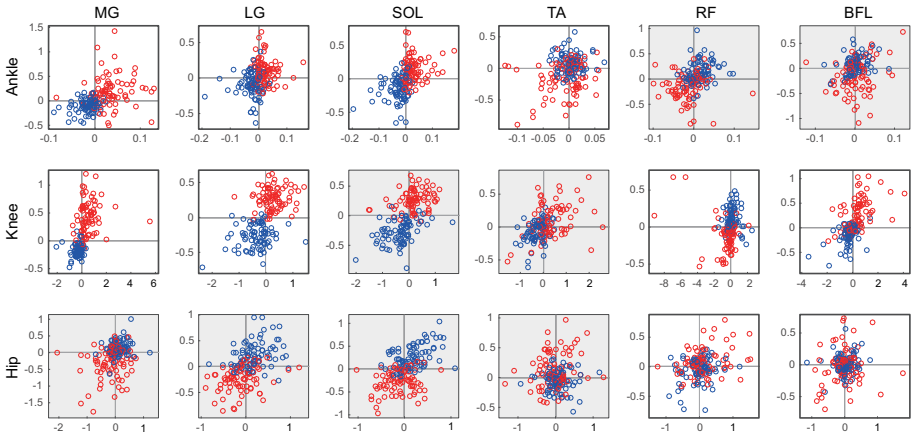

Figure 3: Centers of on/off area in the phase planes. Red and blue plots represent on and off area centers, respectively, of five trials from eight participants' both legs (80 samples in total for each figure). Top, middle, and bottom figures show distributions in the phase planes of the ankle, knee, and hip, respectively.

We further conducted one sample t-test on the five-trial data of on/off area center coordination in the phase plane (angular position and velocity) to evaluate the key information to muscle phasic activation/inactivation for each participant. Table 2 4 shows such on/off trigger information (angular position, velocity, or both), which was determined by statistical divergence from the x- and y- axes, in the phase planes of the ankle, knee, and hip, respectively. Although there were individual variation and laterality in the trigger information (position, velocity, or both), in general, each muscle activated when the state point located in anatomically opposite area in the phase plane and inactivated when it is in the anatomical action direction.

	ON						OFF					
	$\theta+$	$\theta-$	$\omega+$	$\omega-$	1^{st}	3^{rd}	$\theta+$	$\theta-$	$\omega+$	$\omega-$	1^{st}	3^{rd}
MG_L	1678		3		45			168		37		45
LG_L	3		246		58		(7)	3		2467		58
SOL_L	138		4		256			138		4		256
TA_L	(5)			12				(5)	21			
RF_L			(5)	(4)		(238)			(1)	(5)	(238)	
BFL_L	(5)			(238)				(5)	(238)			
MG_R	48		23		1			4		2		1
LG_R	346				12			46				12
SOL_R	46		3	(8)	12			46	(8)	3		12
TA_R	(4)			58		1			8	(7)	1	
RF_R		(4)				(128)	(4)				(128)	
BFL_R				(23)		(8)		(4)	(23)	(7)	(8)	

Table 2: Distributions of on/off area centers in the ankle phase plane. Distributions of on/off area centers (both θ and ω) were tested by one-sample t-test for five samples of each participant. Subject numbers are shown separately depending on their distributions of on/off area centers for each muscle: only angular position is statistically apart from zero and its sign is positive ($\theta+$)

or negative ($\theta-$), only angular velocity is statistically apart from zero and its sign is positive ($\omega+$) or negative ($\omega-$), the centers are statistically apart from the origin; the 1^{st} or 3^{rd} quadrant. The subject numbers inside of parentheses represent anatomically opposite direction of on/off timing (that is, anatomical action direction for on-area centers and vice versa for off-area centers) or anatomically irrelevant muscle for the ankle oscillation.

	ON						OFF					
	$\theta+$	$\theta-$	$\omega+$	$\omega-$	1^{st}	3^{rd}	$\theta+$	$\theta-$	$\omega+$	$\omega-$	1^{st}	3^{rd}
MG_L	2		34		17			25		34		17
LG_L	2		46		137			2		46		137
SOL_L			(2347)		(1)					(2347)		(1)
TA_L			(47)						(2)	(47)		
RF_L		5		1237					1237			
BFL_L	8		46		25			8		46		25
MG_R			38		2457					368		2457
LG_R			2568		1347					258		1347
SOL_R			(257)		(1348)					(257)		(1348)
TA_R			(8)		(3)					(8)		(3)
RF_R				1237		4			12357		4	
BFL_R			6	(5)	12			4	(5)	6		12

Table 3: Distributions of on/off area centers in the knee phase plane. Distributions of on/off area centers (both θ and ω) were tested by one-sample t-test for five samples of each participant. Subject numbers are shown separately depending on their distributions of on/off area centers for each muscle: only angular position is statistically apart from zero and its sign is positive ($\theta+$) or negative ($\theta-$), only angular velocity is statistically apart from zero and its sign is positive ($\omega+$) or negative ($\omega-$), the centers are statistically apart from the origin; the 1^{st} or 3^{rd} quadrant. The subject numbers inside of parentheses represent anatomically opposite direction of on/off timing (that is, anatomical action direction for on-area centers and vice versa for off-area centers) or anatomically irrelevant muscle for the knee oscillation.

	ON						OFF					
	$\theta+$	$\theta-$	$\omega+$	$\omega-$	1^{st}	3^{rd}	$\theta+$	$\theta-$	$\omega+$	$\omega-$	1^{st}	3^{rd}
MG_L				(24)			(6)		(34)			
LG_L				(246)		(3)	(5)	(7)	(24)		(3)	
SOL_L				(234)		(6)	(1)		(234)		(6)	
TA_L			(6)							(6)		
RF_L	6				(3)							(3)
BFL_L				(1)		(6)			(1)		(6)	
MG_R				(136)				(7)	(1236)			
LG_R				(12)		(346)			(1)		(346)	
SOL_R				(1256)		(3)	(4)		(12456)		(3)	
TA_R			(4)	(38)					(38)			
RF_R												
BFL_R												

Table 4: Distributions of on/off area centers in the hip phase plane. Distributions of on/off area centers (both θ and ω) were tested by one-sample t-test for five samples of each participant. Subject numbers are shown separately depending on their distributions of on/off area centers for each muscle: only angular position is statistically apart from zero and its sign is positive ($\theta+$) or negative ($\theta-$), only angular velocity is statistically apart from zero and its sign is positive ($\omega+$) or negative ($\omega-$), the centers are statistically apart from the origin; the 1^{st} or 3^{rd} quadrant. The subject numbers inside of parentheses represent anatomically opposite direction of on/off timing (that is, anatomical action direction for on-area centers and vice versa for off-area centers) or anatomically irrelevant muscle for the hip oscillation.

Function of switching: on/off area in the torque plane

We also obtained the center of mixed Gaussian distribution for each on/off area in the torque plane to examine the relationship between phasic muscle activation/inactivation and joint torque fluctuations as a control output. Figure 4 shows 80 samples (from 8 subject of 5 trials, both legs) of on-area center (red) and off-area center (blue) for each muscle in the torque planes of the ankle (top), knee (middle), and hip (bottom) joints.

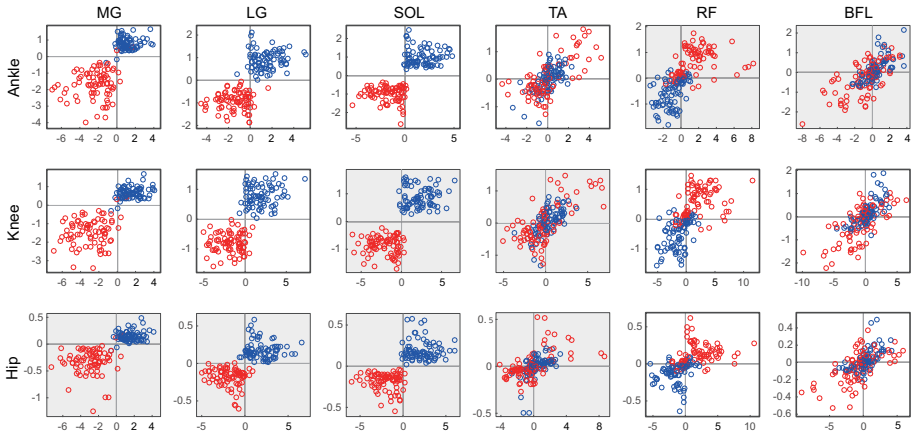

Figure 4: Centers of on/off area in the torque planes. Red and blue plots represent on and off area centers, respectively, of five trials from eight participants' both legs (80 samples in total for each figure). Top, middle, and bottom figures show distribution in the torque planes of the ankle, knee, and hip, respectively.

The distributions of on/off area centers in torque planes were relatively small compared with those in phase planes (Fig 3). Centers of on-area and off-area of triceps surae muscles distributed in the third and first quadrants, respectively, in the ankle and knee torque planes, indicating that their phasic activation and inactivation were associated with torque generations in anatomical action direction (ankle plantar flexion and knee flexion during their activation and ankle dorsiflexion and knee extension during their inactivation). In addition, centers of on-area and off-area were separated in the third and first quadrant, respectively, in the anatomically non-involving hip torque plane, which may represent the effect of phasic muscle activities to multi-link interaction. Similarly, RF on-area and off-area also distributed in the first and third quadrants, respectively, in the knee and hip torque planes. This implies that RF phasic activation and inactivation were associated with torque generations in anatomical action direction (knee extension and hip flexion during ac-

tivation and knee flexion and hip extension during inactivation). Also, its on/off distributions were separated in the first and third quadrants of anatomically irrelevant ankle torque plane.

On the other hand, the on/off area centers of TA and BFL were not separated clearly, although both distributed in the first and third quadrants of torque planes. Table 3 shows the result of one sample t-test on the five-trial data of on/off area center coordination in the torque planes (torque and torque velocity), which was for evaluating each muscle's contribution to torque output fluctuations. Statistical analysis for on/off area distribution showed that the variability for TA and BFL in torque planes was mainly due to variability between participants and laterality. The results of t-test for the other muscles (triceps surae muscles and RF) statistically showed that phasic activation/inactivation of these muscles involved in torque generations in anatomical action directions.

	ON						OFF					
	T_+	T_-	$T_{\Delta+}$	$T_{\Delta-}$	1^{st}	3^{rd}	T_+	T_-	$T_{\Delta+}$	$T_{\Delta-}$	1^{st}	3^{rd}
MG_L						1,3-8					1,3-8	
LG_L				27		1,3-6,8			27		1,3-6,8	
SOL_L				45		1-3,6-8			45		1-3,6-8	
TA_L			12	(7)		(8)			(7)	12	(8)	
RF_L			(7)		(238)					(7)		(238)
BFL_L		(2)	(8)	(4)		(56)	(2)		(4)	(8)	(56)	
MG_R				8		1-7			8		1-7	
LG_R				8		1-7			8		1-7	
SOL_R						All					All	
TA_R		(5)			1	(38)	(5)				(38)	1
RF_R					(1-4,8)					(5)		(1-4,8)
BFL_R			(8)			(6)	(4)			(8)	(6)	

Table 5: Distributions of on/off area centers in the ankle torque plane. Distributions of on/off area centers (both ankle torque (T) and its velocity (T_Δ)) were tested by one-sample t-test for five samples of each participant. Subject numbers are shown separately depending on their distributions of on/off area centers for each muscle: only torque is statistically apart from zero and its sign is positive (T_+) or negative (T_-), only torque velocity is statistically apart from zero and its sign is positive ($T_{\Delta+}$) or negative ($T_{\Delta-}$), the centers are statistically apart from the origin; the 1^{st} or 3^{rd} quadrant. The subject numbers inside of parentheses represent torque output in anatomically opposite action direction or anatomically irrelevant muscle for the ankle oscillation. 'All' represents all participants' subject number.

	ON						OFF					
	T_+	T_-	$T_{\Delta+}$	$T_{\Delta-}$	1^{st}	3^{rd}	T_+	T_-	$T_{\Delta+}$	$T_{\Delta-}$	1^{st}	3^{rd}
MG_L						1,3-8					1,3-8	
LG_L				27		1,3-6,8			27		1,3-6,8	
SOL_L				(45)		(1-3,6-8)			(45)		(1-3,6-8)	
TA_L			(12)	(7)		(8)			(7)	(12)	(8)	
RF_L			7		238					7		238
BFL_L		2	(8)	4		56	2		4	(8)	56	
MG_R				8		1-7			8		1-7	
LG_R				8		1-7			8		1-7	
SOL_R						(All)					(All)	
TA_R					(1)	(38)					(38)	(1)
RF_R		(5)			1-4,8		(5)			5		1-4,8
BFL_R			(8)	1		6	4		1	(8)	6	

Table 6: Distributions of on/off area centers in the knee torque plane. Distributions of on/off area centers (both knee torque (T) and its velocity (T_Δ)) were tested by one-sample t-test for five samples of each participant. Subject numbers are shown separately depending on their distributions of on/off area centers for each muscle: only torque is statistically apart from zero and its sign is positive (T_+) or negative (T_-), only torque velocity is statistically apart from zero and its sign is positive ($T_{\Delta+}$) or negative ($T_{\Delta-}$), the centers are statistically apart from the origin; the 1^{st} or 3^{rd} quadrant. The subject numbers inside of parentheses represent torque output in anatomically opposite action direction or anatomically irrelevant muscle for the knee oscillation. 'All' represents all participants' subject number.

	ON						OFF					
	T_+	T_-	$T_{\Delta+}$	$T_{\Delta-}$	1^{st}	3^{rd}	T_+	T_-	$T_{\Delta+}$	$T_{\Delta-}$	1^{st}	3^{rd}
MG_L						(1,3-8)					(1,3-8)	
LG_L				(27)		(1,3-6,8)			(27)		(1,3-6,8)	
SOL_L				(45)		(1-3,6-8)			(45)		(1-3,6-8)	
TA_L			(12)	(7)		(8)			(7)	(12)	(8)	
RF_L					238					1		238
BFL_L		2	(8)	4		56	2		4	(8)	56	
MG_R				(8)		(1-7)			(8)		(1-7)	
LG_R				(8)		(1-7)			(8)		(1-7)	
SOL_R						(All)					(All)	
TA_R					(1)	(38)					(38)	(1)
RF_R		(5)			1-4,8		(5)			5		1-4,8
BFL_R			(8)			6	4		7	(8)	6	

Table 7: Distributions of on/off area centers in the hip torque plane. Distributions of on/off area centers (both hip torque (T) and its velocity (T_Δ)) were tested by one-sample t-test for five samples of each participant. Subject numbers are shown separately depending on their distributions of on/off area centers for each muscle: only torque is statistically apart from zero and its sign is positive (T_+) or negative (T_-), only torque velocity is statistically apart from zero and its sign is positive ($T_{\Delta+}$) or negative ($T_{\Delta-}$), the centers are statistically apart from the origin; the 1^{st} or 3^{rd} quadrant. The subject numbers inside of parentheses represent torque output in anatomically opposite action direction or anatomically irrelevant muscle for the hip oscillation. 'All' represents all participants' subject number.

Dynamics in the phase space

Furthermore, we calculated directional cosine (DC) that represents the similarity between the dynamics of a triple inverted pendulum and actual dynamics of state point from experiment data. The typical histogram of DC during one trial is shown in Figure 5. The absolute value of DC stayed around unity for most of on-point and off-point, indicating that the actual state point of the participants' skeletal system moved

along (DC(t) of 1) or against (DC(t) of -1) the saddle-type vector field for the triple inverted pendulum model.

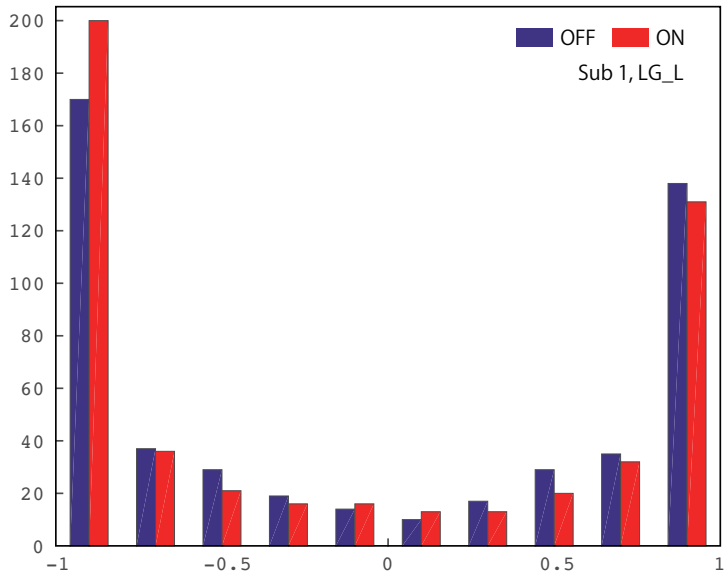

Figure 5: Sample DC histogram. Red and blue bar represent DC of on-points and off-points, respectively, during a 120-sec trial (LG of subject no. 1). DC of 1 and -1 means that the actual state point moves forward and against the model dynamics of a triple inverted pendulum, respectively.

Discussion

In this study, we aimed to make clear the relationship between intermittent (phasic) muscle activities and postural control mechanism during quiet standing. To this end, we investigated the relationship between phasic muscle activation/inactivation timing and location of state point in the phase planes (trigger information) or torque output (function of phasic muscle activities).

Feedback loop with intermittent muscle activity

The centers of on/off areas distributed on the phase planes so that each muscle activated when the state point located in anatomically opposite position and inactivated when the state point located in anatomical action direction (Fig 3). This result correspond to our hypothesis of intermittent feedback control strategy, in which control input (i.e. active torque actuation) are triggered based on the location of the state point in the phase plane. That is, our results indicate that phasic muscle activities during quiet standing, as actuators, are triggered based on such mechanism described as a dynamics in the phase space of saddle type. This tendency is particularly pronounced in the ankle and knee phase planes (Fig 3, top and middle). In addition, on/off area separation in the hip phase plane was much more obvious for anatomically irrelevant triceps surae muscles but not for thigh muscles (Fig 3, bottom). This may be because activities of shank muscles are indirectly affected the fluctuations of the hip joint via skeletal transmission of force and because anatomically more complicated structure around the hip does not allow the efferent information to the thigh muscles (at least RF and BFL) to be precise enough to activate/inactivate these muscles along with the anatomical action direction. In this study, extracting phasic components of muscle activities allowed us to observe the direct relationship between kinematics and muscle activity during quiet standing, which has been difficult to demonstrate because joint fluctuations are aperiodic and muscle activities are small and contain a lot of frequency components during quiet

standing without any disturbances.

The on/off distribution in the phase planes (Fig 3) varied more widely compared with that on the torque planes (Fig 4). Statistical test revealed that this variability were due to individual variation and laterality (Table 2-4). There are three possible explanation of this result. One is that transfer lag of afferent feedback is individually and laterally different. Second, efferent control input via muscular and skeletal system varies individually and laterally. This laterality could be affected by the difference in the EMG electrode placement positions between legs. The last possibility is that the on/off trigger timing of intermittent muscle activities (i.e., the reference value of the state point for each muscle) is modulated depending on individually or laterally different mechanical/structural body properties (such as segment length, joint viscoelasticity, or physiological cross-sectional area of muscles) so as to precisely generate joint torque in the anatomical action direction. Distributions of on/off area should also be quantified for the further analysis to investigate the causality of variability of on/off area in the phase planes. Figure 6 represents a block diagram including intermittent muscle activation on/off switching, which is the overall postural control system assumed in this study. Further analysis of the on/off timing for each muscle should clarify whether there can be seen the synchronization of switch timing among different muscles (i.e., modules for intermittent muscle activity).

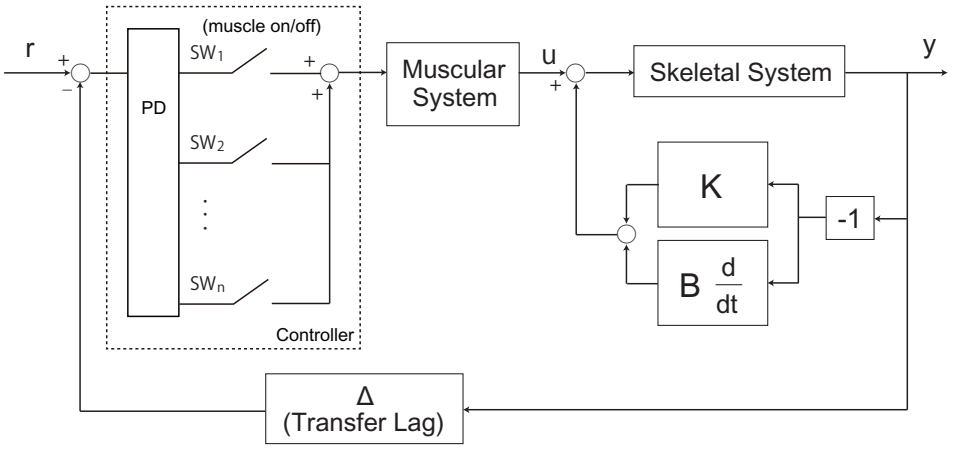

Figure 6: Block diagram of intermittent feedback control of human quiet standing. Each muscle (or each module) on/off switching (SW_k) is triggered depending on the error between current state y (consisted of angular displacements and velocities) and reference value r. The reference value of r could be set for each muscle or each module. The intermittent muscle activities generate joint torque, and together with passive torque (stiffness and damping component K and B) without time delay, control input u actuate the skeletal system and joint fluctuations occur.

Function of intermittent muscle activity

The centers of on/off areas on the torque planes showed that phasic muscle activation and inactivation were associated with joint torque generation in anatomical action direction and opposite direction, respectively (Fig 4). In particular, on/off areas of triceps surae muscles explicitly distributed over the third and first quadrant, respectively, of the ankle and knee torque planes, suggesting that anti-gravity muscles intermittently activate or inactivate in order to accurately handle the ever-present gravitational toppling torque during quiet standing. In addition, RF activation and inactivation was also associated with torque generation in anatomical action direction of the knee and hip (i.e., knee extension and flexion, and hip flexion and extension, respectively). Although RF on/off area on the

hip phase plane was widely distributed, RF on/off area on the hip torque plane explicitly separated into the first and third quadrant. One of the most important results in this study was that muscle inactivation itself was also associated with the torque generation in anatomically opposite direction. Thus, the individual differences and laterality of the on/off area distribution were relatively small on the torque planes in contrast with those on the phase planes. These results indicate that the function of intermittent muscle activity is to generate joint torque precisely along with the action direction and that such on/off trigger is modulated based on mechanical properties of the body or afferent/efferent transmission time lag.

Intermittent feedback control strategy for human bipedal standing has been discussed at kinematic level and relevant muscle activities have been missing. This study further deepened the understanding and validity of the intermittent control model to the musculoskeletal level. We also observed on/off area separation on anatomically irrelevant torque planes (Fig 4, gray background figures). Further analysis of skeletal fluctuations should clarify the contribution of intermittent muscle activity to reciprocal interaction between multi body segments.

State point behavior of actual human skeletal system

Intermittent feedback control model for human bipedal standing assumes that on/off switching of active control via CNS was triggered based on the dynamics towards the equilibrium along with stable manifolds of the dynamical system (Bottaro et al. 2005; 2008; Asai et al. 2009).

Thus, we hypothesized that state point of the system was dominated by the dynamics of the unstable equilibrium of the saddle type during off period and that it moved against the current of such dynamics during on period to go back to the vicinity of the stable manifolds or the equilibrium. The DC histogram in this study distributed around 1 or -1 for both on-points and off-points, suggesting that state point keep moving forward and backward with the dynamics of a triple inverted pendulum. However, intermittent control model presumes that the state point moves back forward and backward during off period and on period, respectively (Fig 7). This inconsistency between model assumption and actual state point behavior may come from errors in estimating joint viscoelasticity or from simple assumption of a triple inverted pendulum. Because it is difficult to experimentally measure the viscoelasticity components for all joints, further constitutional analysis for seeking inferences on human postural control dynamics is necessary, which is accomplished by comparing model behavior and actual skeletal fluctuation with changing mechanical properties of the model.

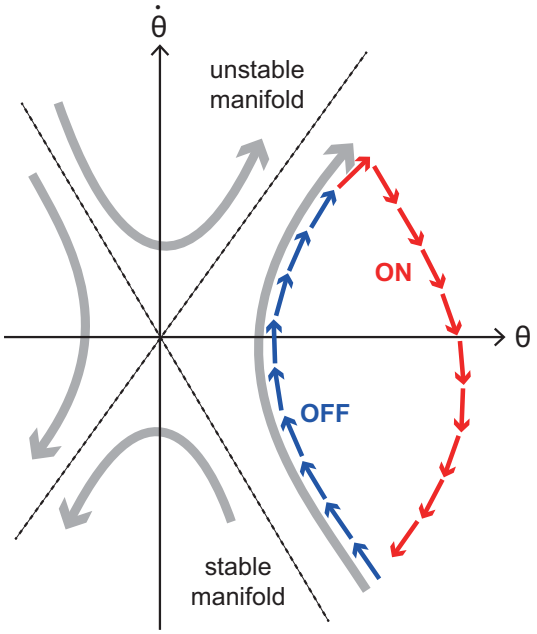

Figure 7: Concept of intermittent feedback control strategy. Although actual human body consists of multiple segments and the phase space is multidimensional, the concept is explained in 2D phase plane for visual purpose. Human body is an unstable equilibrium of saddle type, which means that there is at least one unstable manifold in a dynamical system. Thus, without any active control, the state point of the body diverges away from the equilibrium along the unstable manifold(s) as time elapses (gray arrow). To avoid this falling divergence, active control should be switched on for moving the state point toward the equilibrium or the vicinity of stable manifolds (red arrow), and otherwise, active control could be off (blue arrow).

Conclusion

In this study, we demonstrated the direct relationship between joint fluctuation, muscle activities, and torque output during quiet standing by extracting phasic components from EMG signals. In conclusion, our results suggested that intermittent muscle activation/inactivation occurs depending on the state point location in the phase space, leading to joint actuation via torque generation along with anatomical action direction.

Appendix A

Joint angle and torque calculation

Definitions of angular displacements of the ankle, knee, and hip are shown in Figure A1. Ankle dorsiflexion, knee extension, and hip forward flexion were defined to be positive direction.

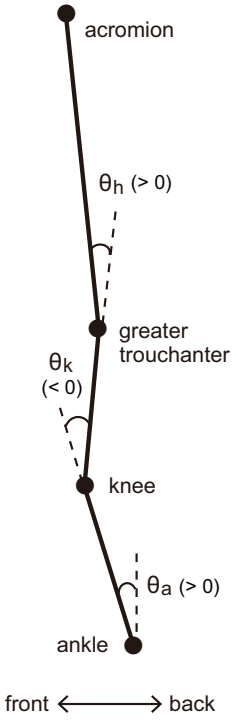

Figure A1: Definition of joint angles. Ankle dorsiflexion, knee extension, and hip forward flexion were defined to be positive direction. Signs of joint torque were set to be the same directions.

Joint torque was calculated by inverse dynamics. The x and y axes represent anteroposterior and vertical directions, respectively. Due to the equilibrium of force at the lowest segment (i.e., the foot),

$$R_{ax} + F_x = 0$$

$$R_{ay} + F_y - m_f g = 0$$

where R_{ax} and R_{ay} represent the joint reaction force at the ankle in anteroposterior and vertical directions, respectively. F_x and F_y are the grand reaction force, where subscripts represent each direction of axis. The term $m_f g$ is gravitational force applied to the foot (i.e., m_f is a mass of the foot). The equilibrium of moment around the center of mass (COM) of foot segment leads to the following equation,

$$M_a + rR_{ay} - pF_y = 0$$

where M_a is the ankle moment in the planterflexion direction, and r and p are a horizontal distances between the ankle and foot COM and between foot COM and the center of pressure. Because we defined the ankle dorsiflexion direction to be positive, the ankle torque T_a is the opposite sign of M_a.

The motion equation of the upper segments (i.e. shank, thigh, and upper body) is expressed as follows:

$$m_i a_x = R_{xp} + R_{xd}$$

$$m_i a_y = R_{yp} + R_{yd} - m_i g$$

where m_i is a mass of ith segment, a_x and a_y are acceleration of ith segment's COM in anteroposterior and vertical directions, respectively, R_{xp} and R_{yp} are joint reaction forces at the proximal end in the anteroposterior and vertical directions, and R_{xd} and R_{yd} are joint reaction forces at the distal end in the anteroposterior and vertical directions (i.e., joint reaction force at the ankle for the shank). These two equations lead the joint reaction force at the proximal end. Then, joint moment at the ith

segment (equivalent to M_d in the following equation) can be derived from the following Euler's momentum equation:

$$I_i\ddot{\theta}_i = M_{pi} - M_{di} + R_{xp}r_i cos\theta_i - R_{yp}r_i sin\theta_i - R_{xd}(l_i - r_i)cos\theta_i + R_{yd}(l_i - r_i)sin\theta_i$$

where the subscript i represents the ith segment, I is the inertial moment, θ is the angular displacement, M_p and M_d are the joint moment in the backward direction (i.e., the ankle plantarflexion, knee flexion, and hip backward flexion) at the proximal and distal ends, respectively, r is a length between proximal end and segment COM, and l is a segment length. Because we defined the knee extension and hip forward flexion to be positive, the torque at the knee and hip is the opposite sign of M_p of shank and thigh segments, respectively.

Appendix B

B1. Model definition

$$M_{11} = I_1 + I_2 + I_3 + r_1^2 m_1 + r_2^2 m_2 + l_1^2 m_2 + 2 l_1 m_2 r_2 + r_3^2 m_3 + l_1^2 m_3 + l_2^2 m_3 + 2 l_1 m_3 l_2 + 2 l_2 m_3 r_3 + 2 l_1 m_3 r_3$$

$$M_{12} = I_2 + I_3 + r_2^2 m_2 + l_1 m_2 r_2 + r_3^2 m_3 + l_2^2 m_3 + l_1 m_3 l_2 + 2 l_2 m_3 r_3 + l_1 m_3 r_3$$

$$M_{13} = I_3 + r_3^2 m_3 + l_2 m_3 r_3 + l_1 m_3 r_3$$

$$M_{21} = I_2 + I_3 + r_2^2 m_2 + l_1 m_2 r_2 + r_3^2 m_3 + l_2^2 m_3 + l_1 m_3 l_2 + 2 l_2 m_3 r_3 + l_1 m_3 r_3$$

$$M_{22} = I_2 + I_3 + r_2^2 m_2 + r_3^2 m_3 + l_2^2 m_3 + 2 l_2 m_3 r_3$$

$$M_{23} = I_3 + r_3^2 m_3 + l_2 m_3 r_3$$

$$M_{31} = I_3 + r_3^2 m_3 + l_2 m_3 r_3 + l_1 m_3 r_3$$

$$M_{32} = I_3 + r_3^2 m_3 + l_2 m_3 r_3$$

$$M_{33} = I_3 + r_3^2 m_3$$

$$G_{11} = -g(r_1 m_1 + l_1 m_2 + l_1 m_3 + r_2 m_2 + l_2 m_3 + r_3 m_3)$$

$$G_{12} = -g(r_2 m_2 + l_2 m_3 + r_3 m_3)$$

$$G_{13} = -g m_3 r_3$$

$$G_{21} = -g(r_2 m_2 + l_2 m_3 + r_3 m_3)$$

$$G_{22} = -g(r_2 m_2 + l_2 m_3 + r_3 m_3)$$

$$G_{23} = -g m_3 r_3$$

$$G_{31} = -g m_3 r_3$$

$$G_{32} = -g m_3 r_3$$

$$G_{33} = -g m_3 r_3$$

where I_i, m_i, l_i, and r_i represent the ith segment's inertia moment of around the distal end, the mass, the length, and the length between the distal end and center of mass, respectively.

B2. First order differential equation

The passive joint torque in the motion equation (eq. 1) can be represented as follows:

$$T_{passive} = -[diag(K)\ \ diag(B)] \cdot x$$

where K and B are vectors of elastic and viscosity components, respectively, and x is the state variable vector consisted of three joint angles and three angular velocities. The expression diag(v) is a diagonal matrix composed by vector v.

Therefore, the motion equation (eq. 1) with no active torque can be written as a following six-dimensional ordinary first order differential equation:

$$\begin{bmatrix} E & O \\ O & M \end{bmatrix} \cdot \frac{dx}{dt} = \begin{bmatrix} O & E \\ -diag(K) + G & -diag(B) \end{bmatrix} \cdot x$$

where E is a 3-by-3 unit matrix. This elicits the coefficient matrix A in eq. 2 as follows:

$$A = \begin{bmatrix} E & O \\ O & M \end{bmatrix}^{-1} \begin{bmatrix} O & E \\ -diag(K) + G & -diag(B) \end{bmatrix}$$

General Discussion

Control mechanism of unstable posture

In our daily life, we humans must stabilize our bodies in a variety of postures. The stability of unstable postures requires specific motor learning, which is a complex process determined by many cross-related factors such as joint mechanical properties and neural control strategies. Postural robustness against external perturbations significantly affects postural stability and its relationship with passive mechanical properties, and postural control strategies are essential for understanding the causality of postural stability. In STUDY4, I demonstrated the cross-relationship between postural robustness, passive joint viscoelasticity, and neural joint control strategies by computer simulation of a quadruple inverted pendulum as a model of tiptoe standing. Tiptoe standing is one of the unstable bipedal standing that is often used in daily life such as when we want to reach something at a high place. The instability of tiptoe standing comes from the very small base of support inside of which we have to keep CoP oscillation, accompanied by small amount of somatosensory information. Nolan and Kerrigan (2004) have investigated open-loop and closed-loop postural control dynamics of tiptoe standing from CoP oscillation and we have further demonstrated the contributions of muscle activities to such CoP non-linear dynamics (Tanabe et al. 2012). It would be beneficial to understand postural control mechanism of unstable standing in expert population such as ballet dancers for clinical applications such as

fall prevention of elderly people.

Many researchers have focused on dancers balance control expertise by investigating the behavior of CoP, which is the output of postural control mechanism via multi-joint fluctuations (see General Introduction). Although CoP analysis gives us some speculations on postural control mechanism, however, there is a limitation in examining the neural-muscular-kinematic control mechanism only from the CoP time series. Therefore, I focused on kinematic and kinetic properties of ballet dancers' body fluctuations in STUDY 1 to 3 and found the differences with non-dancers. Also, I observed the expertise of ballet dancers only during tiptoe standing (not during quiet standing) in STUDY1, revealing that unstable posture is a good experimental task to extract the expertise of postural control. The maintenance of unstable standing requires higher muscle activities, leading to higher joint impedance, which would partially contribute to non-reactive, impedance control for body stabilization. Also, I have already found that muscle activities contribute to the control of joint fluctuations of fast frequency components up to 20 Hz (Tanabe et al. 2012) and joint coordination specific to ballet dancers was associated with muscle co-activations in higher frequency components In STUDY1. Thus, we can maintain the stabilization of unstable postures both by increase in passive joint impedance due to enhanced tonic muscle co-activations and neural muscle coordination associated with multi-joint fluctuations.

Kinematic-kinetic coordination during human quiet standing

Motor learning is a process through which the neural control system achieves movement coordination by mastering redundant degrees of freedom of the body or limb system (Bernstein, 1967). As a simple motor output out of an infinite number of neuralmusculars keletal control strategies of human movement, many studies have extracted such joint coordination during bipedal standing. In STUDY 1 and 2, I focused on joint coordination during tiptoe standing in ballet dancers. PCA allowed me to investigate intra-joint coordination (between anteroposterior and mediolateral fluctuations) as well as inter-joint coordination in STUDY1. This methodology makes it possible to investigate postural control mechanism (especially kinematic coordinative structures) in three-dimensional space, and this is a big progress for investigating balance control mechanism during standing because body oscillations in mediolateral direction is linked to problems in balance maintenance (Maki et al. 1994) and associated with balance impairment represented by a history of falls (Mitchell et al. 1995).

I found MP-ankle in-phase coordination to be dancer-specific coordination during tiptoe standing and this in-phase coordination was associated with muscle co-activation in higher frequency domain (STUDY2). Non-reactive muscle co-activations enhance joint impedance and such rigid joint may be result in in-phase coordination, in which two adjacent segments fluctuate synchronously towards the same direction. Also,

higher joint impedance is robust to internal and external perturbations, although this enhances the biological risk regarding energy consumption. Thus, STUDY 1 and 2 suggest that ballet dancers achieve rigid joints by muscle co-contractions for robustness against internal perturbations during tiptoe standing, which as associated with in-phase joint coordination, and that ballet training allows dancers to perform such high energy consuming strategy associated with changes in VO_{2max} and anaerobic threshold (Guidetti et al. 2008).

PCA measurement enables us to capture only the tendency of joint coordination because joint coordination was measured by PC1 that contains only 70 80 % of information of each joint fluctuations. Also, in-phase and anti-phase kinematic coordination patterns simultaneously coexist during standing; Creath et al. (2005) reported a leg-trunk in-phase pattern for lower frequencies and an anti-phase pattern for higher frequencies. Therefore, I also examined the temporal phase transition between adjacent joints and its relationship between muscle activities in STUDY3. The result showed extremely high individual variation in cross correlation between EMG signals and temporal phase transition. This may be because of non-linearity of postural control system, such as in sway dynamics, muscle activation (tonic and phasic characteristics), and choice of neural control strategies inside of the CNS. Such inconsistent result on kinematic-kinetic relationship may be because active postural control through muscle activities switches on and off transiently during bipedal standing.

Function of intermittent feedback control during standing

Many researchers have tried to provide a computable algorithm to explain human motor behaviors by using computational theories (in the sense of Marr (1982)) as discussed by Shadmehr and Wise (2005) and Todorov and Jordan (2002). Intermittent control is, in essence, a sequence of open-loop trajectories determined by intermittent feedback. This gives a conceptually and computationally simple solution to the control of time-delayed system such as human motor control mechanisms. For the model of human bipedal standing, many researchers have used non-predictive continuous-time controllers of a proportional, integral, and derivative (PID) structure (Peterka 2002; Maurer and Peterka 2005; Lockhart and Ting 2007; Welch and Ting 2008). However, Gawthrop et al. (2009) have demonstrated that a predictive model explains actual body sway better than a non-predictive model with intermittent feedback control. This suggests the function of intermittent control for making time for prediction during the off-period. I have not considered predictive function inside of the internal model for our quadruple inverted pendulum model yet, therefore, the inclusion of the predictor to our model may make the oscillations of the pendulum much closer to the actual body sway during tiptoe standing.

Gawthrop et al. (2011) have also showed that intermittent control is necessary for the postural control under difficult conditions (pulse matching test). In STUDY4, intermittent control was necessary for the sta-

bilization of a quadruple inverted pendulum that is mechanically close to human tiptoe standing. Also, the robustness of the model was cross-related to passive joint properties and neural control strategies (including continuous, intermittent, and passive control). Why could intermittent control contribute to postural robustness is an important question for the understanding of postural control mechanism and its expertise. Mathematically, intermittent active control could provide some time to compensate for time delay of feedback loop (including sensory transduction, neural processing, transmission, and muscle activations; Peterka 2002) and psychological refractory period (Vince 1948; Navas and Stark 1968), and it could also give neural processing time for prediction, which is physiologically demonstrated by Hoff and Arbib (1993), Bhushan and Shadmehr (1999), Burdet and Milner (1998), Todorov and Jordan (2002), Shadmehr and Wise (2005), and Stanley and Miall (2009). From the physiological viewpoint, intermittent postural control can be achieved with less energy consumption as discussed in Suzuki et al. (2012). Controller of the internal model may prefer time-discrete intermittent feedback control for the reasons described above. Also, adequately tuned (or learned) intermittent control strategy depending on the individual mechanical properties (such as joint viscoelasticity and segment length) will produce robust postural control system against internal and external perturbations.

Intermittent muscle activations

In STUDY5, we were able to clearly show the kinematic-kinetic relationship by extracting the phasic on/off muscle activities. This suggests

that the relationship between muscle activities and joint fluctuations exists within the intermittent or phasic oscillations and not within the mixture of tonic and phasic components (like in STUDY3). Also, the center of on-area and off-area were distributed mainly in the first and third quadrant of the phase plane. This result supports the hypothesis of the intermittent control of human bipedal standing (Bottaro et al. 2005; 2008; Asai et al. 2009) that unstable body fluctuations are intermittently controlled depending on the location of the state variable in the state space. Although it is still controversial regarding the way of extracting phasic/tonic components from EMG signals (i.e. the cutoff frequency of EMG signal processing), the methodology used in STUDY5 for investigating kinetic-kinematic relationship is useful for examining the musculoskeletal mechanism of any kinds of motor control even if it is nonlinear, non-periodic, or static motor task such as quiet bipedal standing. During standing, interventional joint torques that push and pull body segments occur when a sensory organ with nonlinear threshold detects the body tilt. Moreover, medial gastrocnemius and tibialis anterior rather than soleus are responsible for the interventions (Yasutake et al. 2006; Bottaro et al. 2008). However, soleus and lateral gastrocnemius were switched on and off around the unstable manifolds and contributed to the joint torque in anatomical direction of action in STUDY5.

The cutoff frequency for extracting tonic muscle activities affects the detection of the timing of on/off switching. Nomura et al. (2007) investigated the optimal cutoff frequency for the tonic constant components of soleus by finding the highest cross-correlation between soleus trend and

CoM trend with changing cutoff frequency from 0.02 to 0.15 Hz. The results showed that the optimal cutoff frequency was individually different. Although frequency domain of tonic muscle component during bipedal standing is still an essential topic for the understanding of postural control mechanism especially when we assume the model with multi-link segments, we supplementary demonstrated that the change in cutoff frequency (from 0.01 to 0.05) did not affect the center of on/off area (the local maximum/minimum) both in phase plane and torque plane. Also, the actual dynamics of state variable (determined by angular position and velocity) was quite identical with the dynamics of a triple inverted pendulum. We will obtain further precise model for human bipedal standing by making the model dynamics closer to muscle on/off intermittent activities as well as the dynamics of state variables.

Future studies for postural control mechanism

As I mentioned above, frequency component of tonic/phasic EMG signals itself is big topic for investigating musculoskeletal mechanism of human bipedal standing. Nomura et al. (2007) estimated the tonic muscle activities from the assumption that human quiet standing can be approximated to a single inverted pendulum. However, actual human body consists of multi segments and this fact makes it difficult to estimate the tonic activities of individual muscles especially except for Toriceps surae muscles because kinematic trend reference for tonic muscle activities is absent for a multi-segment model (especially for bi-articular muscles). Such cross-relationship between multi segments from the aspect of kinetic

control mechanism is also an interesting topic for understanding human bipedal standing. Sasagawa et al. (2014) demonstrated kinematic level of cross-relationships between multi segments during quiet standing by induced acceleration analysis. The contribution of muscle phasic on/off activities to multi segment oscillations (even joint fluctuations that is not anatomically relevant) will be observed with mixture of joint torque decomposition (by induced acceleration analysis) and detection of muscle phasic on/off timing (like in STUDY5).

The 3D analysis of human bipedal standing is necessary for further understanding of postural control mechanism. Hip abduction and adduction moment predominantly control the postural sway in the mediolateral direction (Winter et al. 1996) and body sway in the mediolateral direction coordinates with the sway in the anteroposterior direction at the CoP level (King et al. 2012) and joint level (Tanabe et al. 2014). Although the direction of action of most lower leg muscles is along the anteroposterior direction, joint oscillations in the mediolateral directions must be also controlled by muscle activities. The understanding of such neural-muscular-kinematic control mechanism will be a beneficial knowledge of balance control expertise and balance instability due to aging and diseases because balance training enhances the postural control ability in lateral directions (Calavalle et al. 2008).

Psychological aspect of biomechanics in human movement (e.g. body expression and emotional body language) is gradually attracting attentions of researchers of bioengineering, biomechanics, and cognitive sciences. Felis et al. (2013) tried to extract the emotional aspect of walking

(anger, fear, sadness, and joy) from the emotionally acted kinematics. Static movement such as quiet standing must also have psychological aspects such as self-confidence or disappointment, even more, aesthetical properties may exist inside of the kinematic oscillations even though their fluctuations are very small during quiet standing. The optimization algorithm via changing objective functions can extract those emotional components of kinematics during human bipedal standing. Bipedal standing is one of the fundamental human behaviors, and therefore, the understanding of emotional aspects within its control mechanism will contribute to solve the nature of humanity.

Conclusion

I found various evidences regarding postural control mechanism from the viewpoint of the structure at musculoskeletal level (Study 2, 3 and 5), its function (Study 4 and 5), and expertise and plasticity (Study 1, 2, and 4). We humans have to control our bodies in a constantly changing indefinite situation (i.e. environment) and then the body system works well for serving the current control purpose. Thus, the human motor control mechanism should assume the mutual relationship with the environment to be its control law. This dissertation deepened the understanding of postural control mechanism in which the control system selects suboptimal control strategy among the redundant system for stabilizing the body in a constantly changing environment.

Acknowledgements

Firstly, I would like to express my sincere gratitude to my advisor Prof. Motoki Kouzaki for the continuous support of my Ph. D study and related research, for his patience, motivation, and immense knowledge. His guidance helped me in all the time of research and writing of this thesis. I could not have imagined having a better advisor and mentor for my Ph. D study.

Besides my advisor, I would like to thank the rest of my thesis committee: Prof. Toshio Moritani and Prof. Akihiko Ishihara, for their insightful comments and encouragement, but also for the hard question which incented me to widen my research from various perspectives.

My sincere thanks also goes to Dr. Keisuke Fujii, who always provides me insightful comments and makes me motivated throughout my Ph. D research. Without his precious support it would not be possible to conduct this research. I also thank my fellow lab mates for the stimulating discussions and for all the fun we have had in the last five years. In addition, I am grateful to Mr. Gregory Khezrnejat for giving me language support and for always cheering me up.

Last but not the least, I would like to thank my family: my mother and to my grand parents for supporting me spiritually throughout writing this thesis and my life in general.

Reference

Ackermann H, Scholz E, Koehler W, Dichgans J (1991) Influence of posture and voluntary background contraction upon compound muscle action potentials from anterior tibial and soleus muscle following transcranial magnetic stimulation. Electroencephalogr Clin Neurophysiol 81: 71-80.

Ae M, Tang H, Yokoi T (1992) Estimation of inertia properties of the body segments in Japanese athletes. Biomechanism 11: 23-33.

Albers D, Hu R, McPoil T, Cornwall MW (1992/1993) Comparison of foot plantar pressures during walking and en pointe. Kinesiol Med Dance 15(1 Fall/Win): 25-32.

Alessandro C, Delis I, Nori F, Panzeri S, Berret B (2013) Muscle synergies in neuroscience and robotics: from input-space to task-space perspective. Front Comput Neurosci 7:43.

Amjad AM, Halliday DM, Rosenberg JR, Conway BA (1997) An extended difference of coherence test for comparing and combining several independent coherence estimates: theory and application to the study of motor units and physiological tremor. Journal of Neuroscience Methods 73:69-79.

Applegate C, Gandevia SC, Burke D (1988) Changes in muscle and cutaneous cerebral potentials during standing. Exp Brain Res 71: 183-188.

Aramaki Y, Nozaki D, Masani K, Sato T, Nakazawa K, Yano H (2001) Reciprocal angular acceleration of the ankle and hip joints during quiet standing in humans. Experimental Brain Research, 136, 463-473.

Asai Y, Tasaka Y, Nomura K, Nomura T, Casadio M, Morasso P (2009) A model of postural control in quiet standing: robust compensation of delay-induced instability using intermittent activation of feedback control. PLoS One 4:e6169.

Asai Y, Tateyama S, Nomura T (2013) Learning an Intermittent Control Strategy for Postural Balancing Using an EMG-Based Human-Computer Interface. PLoS One 8: e62956.

Bernstein NA (1967) The co-coordination and regulation of movements. Oxford, England, Pergamon Press.

Bhushan N, Shadmehr R (1999) Computational nature of human adaptive control during learning of reaching movements in force field. Biol Cybern 81(1): 39-60.

Bizzi E, Cheung VCK, d'Avella A, Saltiel PF (2008) Combining modules for movement. Brain Res Rev 57:125-133.

Blsing B, Calvo-Merino B, Cross ES, Jola C, Honisch J, Stevens CJ (2012) Neurocognitive control in dance perception and performance. Acta Psychologica, 139, 300-308.

Boonstra TW, Daffertshofer A, van Ditshuizen JC, van den Heuvel MRC, Hofman C, Willigenburg NW, Beek PJ (2008) Fatigue-related changes in motor-unit synchronization of quadriceps muscles within and across legs. Journal of Electromyography and Kinesiology, 18, 717731.

Bormann R, Cabrera JL, Milton JG, Eurich CW (2004) Visuomotor tracking on a computer screen an experimental paradigm to study the dynamics of motor control. Neurocomputing 58-60: 517-523.

Bottaro A, Casadio M, Morasso P, Sanguineti V (2005) Body sway during quiet standing: is it the residual chattering of an intermittent stabilization process? Hum Mov Sci 24:588615.

Bottaro A, Yasutake Y, Nomura T, Casadio M, Morasso P (2008) Bounded stability of the quiet standing posture: an intermittent control model. Hum Mov Sci 27:473495.

Brookes VB (1986) The neural basis of motor control. Oxford University Press, New York.

Brown P, Salenius S, Rothwell JC, Hari R (1998) Cortical correlate of the Piper rhythm in humans. J Neurophysiol 80:29112917.

Bruyneel AV, Mesure S, Par JC, Bertrand M (2010) Organization of postural equilibrium in several planes in ballet dancers. Neuroscience Letters 485(3): 228-232.

Burdet E, Milner TE (1998) Quantization of human motions and learning of accurate movements. Biol Cybern 78(4): 307-318.

Burdet E, Osu R, Franklin DW, Milner TE, Kawato M (2001) The central nervous system stabilizes unstable dynamics by learning optimal impedance. Nature 414(6862): 446-449.

Byblow WD, Coxon JP, Stinear CM, Fleming MK, Williams G, Mller JFM, Ziemann U (2007) Functional connectivity between secondary and primary motor areas underlying head-foot coordination. Journal of Neurophysiology, 98, 414-422.

Cabrera JL, Milton JG (2002) On-off intermittency in a human balancing task. Phys Rev Lett 89(15): 158702/1-158702/4.

Calavalle AR, Sisti D, Rocchi MBL, Panebianco R, Del Sal M, Stocchi V (2008) Postural trials: expertise in rhythmic gymnastics increases control in lateral directions. Eur J Appl Physiol 104:643-649.

Casadio M, Morasso P, Sanguineti V (2005) Direct measurement of ankle stiffness during quiet standing: Implications for control modeling and clinical application. Gait and Posture 21: 410-424.

Chatfield SJ, Krasnow DH, Herman A, Blessing G (2007) A descriptive analysis of kinematic and electromyographic relationships of the core during forward stepping in beginning and expert dancers. Journal of Dance Medicine and Science 11(3): 9.

Chiovetto E, Patan L, Pozzo T (2012) Variant and invariant features characterizing natural and whole-body pointing movements. Exp Brain Res 218:419-431.

Chow JY, Davids K, Button C, Koh M (2007) Variation in coordination of a discrete multiarticular action as a function of skill level. Journal of Motor Behavior, 39, 463-479.

Cisek P, Kalaska JF (2005) Neural correlates of reaching decisions in dorsal premotor cortex: specification of multiple direction choices and final selection of action. Neuron 45(5): 801-814.

Collins JJ, De Luca CJ (1993) Open-loop and closed-loop control of posture: A random-walk analysis of center-of-pressure trajectories. Exp

Brain Res 95(2): 308-318.

Collins JJ, De Luca CJ, Burrows A, Lipsitz LA (1995) Age-related changes in open-loop and closed-loop postural control mechanisms. Exp Brain Res, 104(3): 480-92.

Cramr H (1999) Mathematical Methods of Statistics, Princeton University Press.

Creath R, Kiemel T, Horak F, Peterka R, Jeka J (2005) A unified view of quiet and perturbed stance: simultaneous co-existing excitable modes. Neurosci Lett 377: 75-80.

Crotts D, Thompson B, Nahom M, Ryan S, Newton RA (1996) Balance abilities of professional dancers on select balance tests. The Journal of Orthopaedic and Sports Physical Therapy 23(1): 12-17.

Daffertshofer A, Lamoth C J C, Meijer OG, Beek PJ (2004) PCA in studying coordination and variability: a tutorial. Clinical Biomechanics, 19, 415-428.

Dal Maso F, Longcamp M, Amarantini D (2012) Training-related decrease in antagonist muscles activation is associated with increased motor cortex activation: evidence of central mechanisms for control of antagonist muscles. Exp Brain Res 220:287-295.

Day JT, Lichtwark GA, Cresswell AG (2013) Tibialis anterior muscle fascicle dynamics adequately represent postural sway during standing balance. J Appl Physiol 115:1742-1750.

Deluzio KJ, Wyss UP, Zee B, Costigan PA, Sorbie C (1997) Principal component models of knee kinematics and kinetics: Normal vs. pathological gait patterns. Human Movement Science, 16, 201-217.

Dietz V (1992) Human neuronal control of automatic functional movements: interaction between central programs and afferent input. Physiol Rev 72:33-69.

Dux PE, Ivanoff J, Asplund CL, Marois R (2006) Isolation of a central bottleneck of information processing with time-resolved fMRI. Neuron 52(6): 1109-1120.

Engbert R, Mergenthaler K, Sinn P, Pikovsky A (2011) An integrated model of fixational eye movements and microsaccades. Proc Natl Acad Sci USA 108(39): E765-E770.

Eurich CW, Milton JG (1996) Noise-induced transitions in human postural sway. Phys Rev E 54(6): 6681-6684.

Felis ML, Mombaur K, Kadone H, Berthoz A (2013) Modeling and identification of emotional aspects of locomotion. Journal of Computational Science 4: 255-261.

Fitzpatrick R, Burke D, Gandevia SC (1996) Loop gain of reflexes controlling human standing measured with the use of postural and vestibular disturbances. J Neurophysiol 76(6): 3994-4008.

Frank J, Earl M (1990) Coordination of posture and movement. In Movement Science: An American Physical Therapy Association Monograph. Alexandria, VA, American Physical Therapy Association 108.

Franklin DW, Liaw G, Milner TE, Osu R, Burdet E, Kawato M (2007) Endpoint stiffness of the arm is directionally tuned to instability in the environment. J Neurosci 27(29): 7705-7716.

Gabor D (1946) Theory of communication. Journal of the Institution of Electrical Engineers 93:429-457.

Gawthrop PJ, Loram I, Lakie M (2009) Predictive feedback in human simulated pendulum balancing. Biol Cybern 101(2): 131-146.

Gawthrop P, Loram I, Lakie M, Gollee H (2011) Intermittent control: a computational theory of human control. Biol Cybern 104: 31-51.

Gawthrop P, Loram I, Gollee H, Lakie M (2014) Intermittent control models of human standing: similarities and differences. Biol Cybern 108: 159-168.

Gerbino PG, Griffin ED, Zurakowski D (2007) Comparison of standing balance between female collegiate dancers and soccer players. Gait & Posture, 26, 501-507.

Gimmon Y, Riemer R, Oddsson L, Melzer I (2011) The effect of plantar flexor muscle fatigue on postural control. J Electromyogr Kine-

siol, 21(6): 922-928.

Golomer E, Dupui P, Monod H (1997a) Sex-linked differences in equilibrium reactions among adolescents performing complex sensorimotor tasks. Journal of Physiology, 91, 4955.

Golomer E, Dupui P, Monod H (1997b) The effects of maturation on self-induced dynamic body sway frequencies of girls performing acrobatics or classical dance. European Journal of Applied Physiology and Occupational Physiology 76(2): 140-144.

Golomer E, Cremieux J, Dupui P, Isableu B, Ohlmann T (1999) Visual contribution to self-induced body sway frequencies and visual perception of male professional dancers. Neuroscience Letters, 267, 189192.

Golomer E, Dupui P (2000) Spectral analysis of adult dancers' sways: Sex and interaction vision-proprioception. International Journal of Neuroscience 105(1-4): 15-26.

Gomi H, Kawato M (1993) Neural network control for a closed-loop system using feedback-error-learning. Neural Networks 6(7): 933-946.

Grieg V (1994) INSIDE BALLET TECHNIQUE separating anatomical fact from fiction in the ballet class. New Jersey, A Dance Horizons Book Priceton Book Company.

Guidetti L, Emerenziani GP, Gallotta MC, Da Silva SG, Baldari C (2008) Energy cost and energy sources of a ballet dance exercise in female adolescents with different technical ability. Eur J Appl Physiol 103(3): 315-231.

Gnter M, Grimmer S, Siebert T, Blickhan R (2009) All leg joints contribute to quiet human stance: a mechanical analysis. J Biomech 42: 2739-2746.

Gnter M, Mller O, Blickhan R (2011) Watching quiet human stance to shake off its straitjacket. Arch Appl Mech 81: 283-302.

Gnter M, Mller O, Blickhan R (2012) What does head movement tell about the minimum number of mechanical degrees of freedom in quiet human stance? Arch Appl Mech 82: 333-344.

Haken H (1996) Principles of brain functioning. Berlin Heidelberg New York: Springer.

Halliday DM, Rosenberg JR, Amjad AM, Breeze P, Conway BA, Farmer SF (1995) A framework for the analysis of mixed time series/point process data-theory and application to the study of physiological tremor, single motor unit discharges and electromyograms. Prog Biophys Mol Biol 64:23778.

Higuchi T, Imanaka K, Hatayama T (2002) Freezing degrees of freedom under stress: Kinematic evidence of constrained movement strategies. Human Movement Science, 21, 831-846.

Hodges NJ, Hayes S, Horn RP, Williams AM (2005) Changes in coordination, control and outcome as a result of extended practice on a novel motor skill. Ergonomics, 48, 1672-1685.

Hoff B, Arbib MA (1993) Models of trajectory formation and temporal interaction of reach and grasp. J Mot Behav 25(3): 175-192.

Hogan N (1984) Adaptive control of mechanical impedance by coactivation of antagonist muscles. IEEE T Automat Contr AC-29(8): 681-690.

Hogan N (1985) The mechanics of multi-joint posture and movement control. Biol Cybern 52(5): 315-331.

Hsu WL, Scholz JP, Schner G, Jeka JJ, Kiemel T (2007) Control and Estimation of Posture During Quiet Stance Depends on Multijoint Coordination. J Neurophysiol 97:3024-3035.

Hsu WL, Chou LS, Woollacott M (2013) Age-related changes in joint coordination during balance recovery. Age (Dordr) 53:1299-1309.

Hubley-Kozey CL, Deluzio KJ, Landry SC, McNutt JS, Stanish WD (2006) Neuromuscular alterations during walking in persons with moderate knee osteoarthritis. Journal of Electromyography and Kinesiology, 16, 365-378.

Insperger T (2006) Act-and-wait concept for continuous-time control system with feedback delay. IEEE T Contr Syst T 14(5): 974-977.

Insperger T, Stpn G (2010) On the dimension reduction of system with feedback delay by act-and-wait control. IMA J Math Control I 27(4):

457-473.

Insperger T, Milton J, Stpn G (2013) Acceleration feedback improves balancing against reflex delay. J R Soc Interface 10(79): 20120763.

Ivanenko YP, Cappellini G, Dominici N, Poppele RE, Lacquaniti F (2005) Coordination of Locomotion with Voluntary Movements in Humans. Journal of Neuroscience, 25, 7238 7253.

Jola C, Davis A, Haggard P (2011) Proprioceptive integration and body representation: Insights into dancers ' expertise. Experimental Brain Research 213(2-3): 257-265.

Jolliffe IT (1986) Principal component analysis. New York, Springer-Verlag.

Kadel N, Donaldson-Fletcher EA, Sagal A, Falicov A, Orendurff M (2004) Kinematic, kinetic, and electromyographic (EMG) analysis of muscle activity during rise to the pointe position. In: Solomon R, Solomon J (eds): Proceedings of the 14th Annual Meeting of the Internal Association for Dance Medicine and Science, San Francisco, CA, IADMS, pp 244-247.

Kato T, Yamamoto S, Miyoshi T, Nakazawa K, Masani K, Nozaki D (2014) Anti-phase action between the angular accelerations of trunk and leg is reduced in the elderly. Gait Posture 40:107-112.

Kelso JAS (1995) Dynamics patterns. MIT press, Cambrige, MA.

Kiemel T, Zhang Y, Jeka J (2011) Identification of neural feedback for upright stance in humans: stabilization rather than sway minimization. J Neurosci 31:15144-15153.

Kilby MC, Newell KM (2012) Intra- and inter-foot coordination in quiet standing: Footwear and posture effects. Gait & Posture, 35, 511-516.

King AC, Wang Z, Newell KM (2012) Asymmetry of recurrent dynamics as a function of postural stance. Experimenral Brain Research, 220, 239250.

Ko JH, Challis JH, Newell KM (2014) Transition of COM-COP relative phase in a dynamic balance task. Hum Mov Sci 38:1-14.

Kouzaki M, Fukunaga T (2008) Frequency features of mechanomyographic signals of human soleus muscle during quiet standing. Journal of Neuroscience Methods, 173, 241248.

Kouzaki M, Masani K, Akima H, Shirasawa H, Fukuoka H, Kanehisa H, Fukunaga T (2007) Effects of 20-day bed rest with and without strength training on postural sway during quiet standing. Acta Physiologica, 189, 27992.

Kouzaki M, Masani K (2012) Postural sway during quiet standing is related to physiological tremor and muscle volume in young and elderly adults. Gait & Posture, 35, 117.

Kouzaki M, Shinohara M (2006) The frequency of alternate muscle activity is associated with the attenuation in muscle fatigue. J App Physiol 101: 715-720.

Kouzaki M, Shinohara M (2010) Steadiness in plantar flexor muscles and its relation to postural sway in young and elderly adults. Muscle & Nerve, 42, 7887.

Krishnan V, Aruin AS, Latash ML (2011) Two stages and three components of the postural preparation to action. Exp Brain Res 212:47-63.

Kuo AD, Speers RA, Peterka RJ, Horak FB (1998) Effect of altered sensory conditions on multivariate descriptors of human postural sway. Experimental Brain Research, 122, 185-195.

Kurabayashi J, Mochimaru M, Kouchi M (2003) Validation of the estimation methods for the hip joint center. Biomechanism 27(1): 29-36.

Lakie M, Caplan N, Loram ID (2003) Human balancing of an inverted pendulum with a compliant linkage: neural control by anticipatory intermittent bias. J Physiol 551: 357-370.

Lavoie BA, Cody FWJ, Capaday C (1995) Cortical control of human soleus muscle during volitional and postural activities studied using focal magnetic stimulation. Exp Brain Res 103: 97-107.

Lockhart DB, Ting LH (2007) Optimal sensorimotor transformations for balance. Nar Neurosci 10(10): 1329-1336.

Loram I, Lakie M (2002a) Direct measurement of human ankle stiffness during quiet standing: The intrinsic mechanical stiffness is insufficient for stability. J Physiol 545: 1041-1053.

Loram ID, Lakie M (2002b) Human balancing of an inverted pendulum: Position control by small, ballistic-like throw and catch movements. J Physiol 540(3): 1111-1124.

Loram ID, Maganaris CN, Lakie M (2005) Human postural sway results from frequent, ballistic bias impulses by soleus and gastrocnemius. J Physiol 564(1): 295-311.

Loram ID, Gollee H, Lakie M, Gawthrop PJ (2011) Human control of an inverted pendulum: Is continuous control necessary? Is intermittent control effective? Is intermittent control physiological? J Physiol 589(2): 307-324.

Loram ID van de Kamp C, Gollee H, Gawthrop PJ (2012) Identification of intermittent control in man and machine. J R Soc Interface 9(74): 2070-2084.

Maki B, Holliday P, Topper A (1994) A prospective study of postural balance and risk of falling in an ambulatory and independent elderly population. J Gerontol 49: M72-84.

Marr D (1982) Vision. A computational investigation into the human representation and processing of visual information. W.H. Freeman, San Francisco.

Marsden CD, Merton PA, Morton HB, Rothwell JC, Traub MM (1981) Reliability and efficacy of the long-latency stretch reflex in the human thumb. J Physiol 316(1): 47-60.

Marsden JF, Werhahn KJ, Ashby P, Rothwell J, Noachtar S, Brown P (2000) Organization of cortical activities related to movement in humans. J Neurosci 20:2307-2314.

Masani K, Popovic MR, Nakazawa K, Kouzaki M, Nozaki D (2003) Importance of body sway velocity information in controlling ankle

extensor activities during quiet stance. J Neurophysiol 90:3774-3782.

Mass N, Germn A, Rey F, Costa LL, Romero D, Guitart S (2004) Study of muscle activity during relev in first and sixth positions. J Dance Med Sci 8(4): 101-107.

Maurer C, Peterka R (2005) A new interpretation of spontaneous sway measures based on a simple model of human postural control. J Neurophysiol 93:189200.

Milton J, Townsend JL, King MA, Ohira T (2009) Balancing with positive feedback: The case for discontinuous control. Phil Trans R Soc A 367(1891): 1181-1193.

Mima T, Hallett M (1999) Corticomuscular coherence: a review. J Clin Neurophysiol 16:501511.

Mitchell SL, Collins JJ, De Luca CJ, Burrows A, Lipstz LA (1995) Open-loop and closed-loop postural control mechanisms in Parkinson's disease: increased mediolateral activity during quiet standing. Neurosci Lett, 197(2): 133-136.

Mitra S, Amazeen PG, Turvey MT (1998) Intermediate motor learning as decreasing active (dynamical) degrees of freedom. Hum Mov Sci 17:1765.

Mora I, Quinteiro-Blondin S, Prot C (2003) Electromechanical assessment of ankle stability. Eur J Appl Physiol 88: 558-564.

Morasso PG, Bottaro L, Capra R, Spada G (1999) Internal models in the control of posture. Neural Networks 12(7-8): 1173-1180.

Moritani T, Berry MJ, Bacharach DW, Nakamura E (1987) Gas exchange parameters, muscle blood flow and electromechanical properties of the plantar flexors. Eur J Appl Physiol 56: 30-37.

Moss CL (1991) Comparison of the histochemical and contractile properties of human gastrocnemius muscle. J Orthop Sports Phys Ther 13: 322-328.

Muro M, Nagata A (1985) The effects on electromechanical delay of muscle stretch of the human triceps surae. In Winter DA, Norman RW, Wells RP, Hayes KC, Patla AE (eds) Biomechanics IX-A. Human

Kinetics, Champaign, Ill., pp 86-90.

Myers LJ, Lowery M, O ' Malley M, Vaughan CL, Heneghan C, St Clair Gibson A, Harley YX, Sreenivasan R (2003) Rectification and non-linear pre-processing of EMG signals for cortico-muscular analysis. J Neurosci Methods 124:15765.

Navas F, Stark L (1968) Sampling or intermittency in hand control system dynamics. Biophys J 8(2): 252-302.

Nolan L, Kerrigan DC (2004) Postural control: toe-standing versus heel-toe standing. Gait Posture 19:11-15.

Nomura T, Nakamura T, Fukada K, Sakoda S (2007) Characterizing Postural Sway during Quiet Stance Based on the Intermittent Control Hypothesis. AIP Conference Proceedings, Noise and Fluctuations, 19th International Conference 922(1): 553.

Omlor W, Patino L, Hepp-Reymond MC, Kristeva R (2007) Gamma-range corticomuscular coherence during dynamic force output. Neuroimage 34:1191-1198.

Peterka R (2000) Postural control model interpretation of stabilogram diffusion analysis. Biol Cybern 82: 335-343.

Peterka RJ (2002) Sensorimotor integration in human postural control. J Neurophysiol 88: 1097-1118.

Pikovsky A, Rosenblum M, Kurths J (2001) Synchronization: A universal concept in nonlinear sciences. Cambridge, MA: Cambridge University Press.

Pinter IJ, van Swigchem R, van Soest AJK, Rozendaal LA (2008) The dynamics of postural sway cannot be captured using a one-segment inverted pendulum model: a PCA on segment rotations during unperturbed stance. Journal of Neurophysiology, 100, 3197-3208.

Pruszynki J, Scott S (2012) Optimal feedback control and the long-latency stretch response. Exp Brain Res 218: 341-359.

Redgrave P, Prescott TJ, Gurney K (1999) The basal ganglia: a vertebrate solution to the selection problem? Neuroscience 89(4): 1009-1023.

Rein S, Fabian T, Zwipp H, Rammelt S, Weindel S (2011) Postural control and functional ankle stability in professional and amateur dancers. Clinical Neurophysiology, 122, 16021610.

Riley MA, Clark S (2003) Recurrence analysis of human postural sway during the sensory organization test. Neuroscience Letters, 342, 45-48.

Rosenberg JR, Amjad AM, Breeze P, Brillinger DR, Halliday DM (1989) The Fourier approach to the identification of functional coupling between neuronal spike trains. Prog Biophys Molec Biol 53:1-31.

Rothwell JC (1994) Control of human voluntary movement. Chapman and Hall, London.

Saffer M, Kiemel T, Jeka J (2008) Coherence analysis of muscle activity during quiet stance. Exp Brain Res 185:215-226.

Sasagawa S, Ushiyama J, Kouzaki M, Kanehisa H (2009) Effect of the hip motion on the body kinematics in the sagittal plane during human quiet standing. Neurosci Lett 450:2731.

Sasagawa S, Ushiyama J, Masani K, Kouzaki M, Kanehisa H (2009) Balance control under different passive contributions of the ankle extensors: quiet standing on inclined surfaces. Exp Brain Res 196:537-544.

Sasagawa S, Shinya M, Nakazawa K (2014) Interjoint dynamic interaction during constrained human quiet standing examined by induced acceleration analysis. J Neurophysiol 111:313-322.

Schmit JM, Regis DI, Riley MA (2005) Dynamic patterns of postural sway in ballet dancers and track athletes. Experimental Brain Research, 63, 370-378.

Shadmehr R, Wise SP (2005) Computational neurobiology of reaching and pointing: a foundation for motor learning. MIT Press, Cambrigde.

Sherrington CS (1947) The integrative action of the nervous system. Cambridge University Press, Cambridge.

Sozzi S, Honeine J, Do M, Schieppati M (2013) Leg muscle activity during tandem stance and the control of body balance in the frontal plane. Clin Neurophysiol 124:1175-1186.

Stanley J, Miall RC (2009) Using predictive motor control processes in a cognitive task: behavioral and neuroanatomical perspectives. Adv Exp Med Biol 629: 337-354.

Steenbergen B, Marteniuk RG, Kalbfleisch LE (1995) Achieving coordination in prehension: Joint freezing and postural contributions. Journal of Motor Behavior, 27, 333-348.

Stephen DG, Mirman D (2010) Interactions dominate the dynamics of visual cognition. Cognition 115(1): 154-165.

Stpn G, Insperger T (2006) Stability of time-periodic and delayed systems A route to act-and-wait control. Annu Rev Control 30(2): 159-168.

Stins JF, Michielsen ME, Roerdink M, Beek PJ (2009) Sway regularity reflects attentional involvement in postural control: Effects of expertise, vision and cognition. Gait & Posture, 30, 106-109.

Suzuki Y, Nomura T, Casadio M, Morasso P (2012) Intermittent control with ankle, hip, and mixed strategies during quiet standing: A theoretical proposal based on a double inverted pendulum model. J Theor Biol 310:55-79.

Tanabe H, Fujii K, Kouzaki M (2012) Large postural fluctuations but unchanged postural sway dynamics during tiptoe standing compared to quiet standing. Journal of Electromyography and Kinesiology, 22, 975-982.

Tanabe H, Fujii K, Kouzaki M (2014) Inter- and intra- lower limb joint coordination of non-expert classical ballet dancers during tiptoe standing. Hum Mov Sci 34:41-56.

Telford CW (1931) The refractory phase of voluntary and associative responses. J Exp Psychol 14(1): 1-36.

Todorov E, Jordan MI (2002) Optimal feedback control as a theory of motor coordination. Nat Neurosci 5(11): 1226-1235.

Toiviainen P, Luck G, Thompson MR (2010) Embodied Meter: Hierarchical Eigenmodes in Music-Induced Movement. Music Perception, 28, 59-70.

Tresch MC, Salriel P, d'Avella A, Bizzi E (2002) Coordination and localization in spinal motor systems. Brain Res Rev 40:66-79.

Troje NF (2002) Decomposing biological motion: A framework for analysis and synthesis of human gait patterns. Journal of Vision, 2, 371-387.

Turvey MT, Schmidt RC, Rosenblum LG, Kugler PN (1988) On the time allometry of coordinated rhythmic movements. J Theor Biol 130:285-325.

Ushiyama J, Takahashi Y, Ushiba J (2010) Muscle dependency of cortiocomuscular coherence in upper and lower limb muscles and training-related alterations in ballet dancers and weightlifters. Journal of Applied Physiology, 109, 108695.

Ushiyama J (2013) Resonance between cortex and muscle: A determinant of motor precision? Clinical Neurophysiology, 124, 5-7.

van de Kamp C, Gawthrop PJ, Gollee H, Loram ID (2013) Refractoriness in sustained visuo-manual control: Is the refractory duration intrinsic or does it depend on external system properties? PLoS Computat Biol 9(1).

Van Der Kooij H, De Vlugt E (2007) Postural responses evoked by platform perturbations are dominated by continuous feedback. J Neurophysiol 98: 730-743.

Vette A, Masani K, Nakazawa K, Popovic M (2010) Neural-mechanical feedback control scheme generates physiological ankle torque fluctuation during quiet stance. IEEE Trance Neural Syst Rehabl Eng 18:86-95.

Vince MA (1948) The intermittency of control movements and the psychological refractory period. Br J Psychol Gen Sect 38(Pt 3): 149-157.

Wang Y, Asaka T, Zatsiorsky VM, Latash ML (2006) Muscle synergies during voluntary body sway: combining across-trial and within-a-trial analyses. Exp Brain Res 174:679-693.

Wang Z, Ko JH, Challis JH, Newell KM (2014) The Degrees of Freedom Problem in Human Standing Posture: Collective and Component Dynamics. PLoS One 9:e85414.

Warren GW (1989) Classical Ballet Technique. Florida, University Press of Florida.

Welch TDJ, Ting LH (2008) A feedback model reproduces muscle activity during human postual responses to support-surface translations. J Neurophysiol 99(2): 1032-1038.

Weyand PG, Smith BR, Sandell RF (2009) Assessing the metabolic cost of walking: The inuence of baseline subtractions. Proc 31st Annu Int Conf IEEE Eng Med and Biol Soc: Engineering the Future of Biomedicine, EMBC 2009(5333126): 6878-6881.

Winter DA (1990) Biomechanics and Motor Control of Human Movement. New York: Wiley.

Winter DA, Prince F, Frank JS, Powell C, Zabjek KF (1996) Unified theory regarding A/P and M/L balance in quiet stance. Journal of Neurophysiology, 75: 2334-2343.

Yasutake Y, Taniguchi S, Nomura T (2006) Pro. 28th IEEE EMBS Ann Intl Conf. New York City, USA 1189-1192.

Yoshitake Y, Shinohara M, Ue H, Moritani T (2002) Characteristics of surface mechanomyogram are dependent on development of fusion of motor units in humans. J Appl Physiol 93:174452.